Sensitivity of Ecosystem Net Primary Productivity Models to Remotely Sensed Leaf Area Index in a Montane Forest Environment

Diedre P. Davidson
B.Sc., University of Lethbridge, 1999

A Thesis
Submitted to the School of Graduate Studies
of The University of Lethbridge
in Partial Fulfillment of the
Requirements for the Degree

Master of Science

Lethbridge, Alberta, Canada
August, 2002

DEDICATION

To my family,

My mom, Laura and sister Kaurel without whose love, support and encouragement I couldn't have finished this. WE DID IT.

ABSTRACT

Net primary productivity (NPP) is a key ecological parameter that is important in estimating carbon stocks in large forested areas. NPP is estimated using models of which leaf area index (LAI) is a key input. This research computes a variety of ground-based and remote sensing LAI estimation approaches and examines the impact of these estimates on modeled NPP. A relative comparison of ground-based LAI estimates from optical and allometric techniques showed that the integrated LAI-2000 and TRAC method was preferred. Spectral mixture analysis (SMA), accounting for subpixel influences on reflectance, outperformed vegetation indices in LAI prediction from remote sensing. LAI was shown to be the most important variable in modeled NPP in the Kananaskis, Alberta region compared to soil water content (SWC) and climatic inputs. The variability in LAI and NPP estimates were not proportional, from which a threshold was suggested where first LAI is limiting than water availability.

ACKNOWLEDGEMENTS

There are many people I would like to thank for their support in this research as well as my master's program as a whole. First, I would like to thank Dr. Derek Peddle. Derek was the first to introduce me and excite me about remote sensing and provided the opportunity and environment to complete this research project. I would also like to thank Dr. Ron Hall who provided a wealth of guidance and encouragement in both forestry and remote sensing and gave to this research in both his time and research equipment. He also allowed my the opportunity to study at the Canadian Forest Service, Edmonton. I would also like to thank the members of my committee: Dr. Larry Flanagan, who provided insights and understanding into plant ecology, Dr. Bob Rogerson and Dr. Ivan Townsend for helping to maintain the big picture in geographic perspective. I would also like to acknowledge Dr. Olaf Niemann, external examiner from the University of Victoria whose insights and suggestion helped in the completion of the thesis.

This research was supported by NSERC, NRCAN, ULRF and Alberta Research Excellence Grants to Dr. Peddle. Additional support was also provided by Canadian Forest Service, Edmonton. I thank Gordon Frazer, Simon Fraser University, for providing the hemispherical camera system and software. Collaborating staff and students from the Universities of Lethbridge, Calgary, and Regina, are thanked for their contributions to the field program. Special thanks to Debra Klita, Kendra Gregory, and Dallas Russell who were all valuable members of the field research crews. You all made the field seasons memorable. Thank you to the staff at Kananaskis Field Stations namely Grace Lebel, Judy Buchannen-Mappin, Mike Mappin, and Ed Johnson, for the use of their GPS and

base station, logistical support, and endless help and advice about the study area. I would also like to thank the Department of Geography at the University of Lethbridge. The digital elevation model was provided by Craig Stewart from the Miistakis Institute of the Rockies. CASI image acquisition and preprocessing was performed through Itres Research. I would also like to thank Ryan Johnson for providing data and guidance for remote sensing and Dennis Shepard and Suzan Lapp for their computer help and friendship. I would like to extend a special thanks to Kathy Schrage who always seemed to know the answer to any question I asked.

Finally, I would like to thank my family and friends who stood by me through out the program. I would like to thank all the families the Lenek' s, the O'Shea' s and the Hamilton's, who provided me support and who welcomed me with open arms and cupboards when my home was so far away. To my friends (and you should know who you are, if I named you all and thanked you individually the acknowledgements would be as long as the thesis) thank you your support and encouragement. I am glad that I met all of you and thank you for lending an ear, shedding a tear or simply drinking a beer.

TABLE OF CONTENTS

LIST OF FIGURES

LIST OF EQUATIONS

LIST OF TABLES

LIST OF ABBREVIATIONS

Ω	Clumping index
ANOVA	Analysis of variance
ASD	Analytical spectral devices
ATP	Adenosine triphosphate
AVI	Alberta Vegetation Inventory
BA	Tree basal area
BEPS	Boreal Ecosystem Productivity Simulator
BIOME-BGC	BIOME Biogeochemical cycle model
C	Carbon
CASI	Compact Airborrne Spectrographic Imager
CO2	Carbon dioxide
CV	Coefficient of variation
CV_{LAI}	Coefficient of variation for leaf area index
CV_{NPP}	Coefficient of variation for net primary production
DBH	Diameter at breast height
DEM	Digital elevation model
DGPS	Differential global positioning system
DOB/DIB	Diameter outside bark/diameter inside bark
ELAI	Effective Leaf area index
FOREST-BGC	FOREST Biogeochemical cycle model
fPAR	Fraction of PAR
GEMI	Global Environment Monitoring Index

GLA	Gap Light Analyzer
GOMS	Geometric Optical Mutual Shadowing
GPP	Gross primary production
GPS	Global Positioning system
INS	Inertial navigation system
IPPC	Intergovernmental Panel on Climate Change
K	Extinction factor
LAI	Leaf area index
MIR	Miistakis Institute for the Rockies
MRSE	Root mean square error
MSR	Modified simple ratio
MSV	Multi-spectral video
MTCLIM	Mountain Microclimate Simulator Model
N	Nitrogen
NADPH	Nicotinamide adenide dinucleatide in it's reduced phase
NDVI	Normalized differences vegetation index
NIR	Near infrared reflectance
NLI	Non linear index
NPP	Net primary productivity
PAR	Photosynthetically active radiation
PPM	Parts per million
PVI	Perpendicular Vegetation Index
R	Red reflectance

Ra	Autotropic respiration
RDVI	Renormalized Difference Vegetation Index
RSR	Reduced simple ratio
SA	Sapwood basal area
SAVI	Soil adjusted vegetation index
SLA	Specific leaf area
SMA	Spectral mixture analysis
SMA_S	Spectral mixture analysis shadow fraction
S-N-K	Student-Newman-Keuls multiple mean comparison test
SR	Simple ratio
SWC	Soil water content
SWIR	Shortwave infrared
SZA	Solar zenith angles
TRAC	Tracing Radiant Architecture of Canopies Instrument
Ve	Needle to shoot ratio
VNIR	Visible near infrared
WDVI	Weighted difference vegetation index

CHAPTER I

1.0 Introduction

1.1 Introduction

Human activities are altering the earth's atmosphere, biosphere and hydrosphere at an accelerated pace, as manifested by ozone depletion, increases in atmospheric greenhouse gas emissions, pollution and changing patterns of landcover and natural resource use (IPPC, 2001; Myneni et al., 2000; Rizzo and Wiken, 1992). These activities are thought to be altering the global climate, beyond its natural variability, a process termed global change (CDIAC, 1999). The increase in atmospheric greenhouse gases such as carbon dioxide (CO_2) has been a major focus of recent research due to the considerable increase in levels of atmospheric CO_2 since the Industrial Revolution (Keeling et al., 1995). The terrestrial biosphere is the second largest reservoir for carbon with much of that being stored in forests. Canada's landmass consists of 417.6 million hectares of forested area or 10% of the world's terrestrial biosphere, therefore, the contributions from this land mass are significant at global scales to the world carbon sinks (CCFM, 1997; CFS, 1997).

One of the important descriptors of carbon storage is net primary productivity (NPP). NPP is the total amount of carbon fixed by photosynthesis less respiration, the carbon that is expended for the maintenance and growth of cells. It is therefore a quantitative measure of carbon and energy assimilation or absorption into a system (Chen et al., 1999; Melillo et al., 1993). Process-based simulation models have been developed

for the estimation of NPP. A process-based model simulates the functional mechanisms of an ecosystem. These process-based models are important to the study of ecosystems since they attempt to simulate or characterize the mechanisms that influence the functionality of an ecosystem without requiring vast amounts of data that are difficult or impossible to acquire (Waring and Running, 1998). These models have been shown to be the only feasible method to make spatially comprehensive estimates of NPP over large regions (Cramer and Field, 1999).

Physiological processes controlling NPP have been directly linked to leaf area index (LAI), an important measure of canopy structure (Waring and Schlesinger, 1985). LAI, has been defined as one half the total light intercepting area per unit ground surface area (Chen and Black, 1992), and is an objective measure of canopy structure without the complexities of leaf-age class distribution, angular distribution, or canopy geometry (Running and Hunt, 1993). It is influenced by site water balance, radiation regime, canopy architecture, specific leaf area, leaf nitrogen content and species and stand composition (Chen et al., 1997a; Pierce et al., 1994; Grier and Running, 1977). LAI has been recognized as being the most important variable for characterizing vegetation structure over large areas that can be obtained at broad spatial scales with satellite remote sensing data (Running and Coughlan, 1988). It was also found to correlate better with NPP than with other environmental gradients (Gholz, 1982). Accordingly, many process-based models (e.g. FOREST-BGC) use LAI as one of their main driving inputs, as it is related to vegetative biomass, carbon, and energy exchange (Running and Coughlan, 1988).

LAI can be estimated over large areas using remote sensing imagery or over small areas (e.g. field plots) using ground-based instruments. Accurate and consistent LAI estimation is of great importance as it will influence estimates derived from productivity models (Liu et al., 1997; Running and Coughlan, 1988). Thus, an assessment of LAI measures from various ground-based and remote sensing methods will aid validation of NPP modeling. Determining the variability in NPP estimates from the popular FOREST-BGC model in terms of output NPP from different LAI source inputs will provide insights into how the model uses the estimated LAI parameter within a given ecosystem particularly the montane. In western Canada, a large portion of forests are in high relief areas, thus variation in both ecological models, image processing, and field measurements must be explicitly accounted for, so that policy and informed decisions can be made for sustainable forest management.

In this research five different ground-based LAI estimation methods were evaluated: (1) hemispherical photography, (2) LAI-2000, (3) Tracing Radiation and Architecture of Canopies Instrument (TRAC), (4) the integrated LAI-2000 and TRAC and (5) sapwood area/leaf area allometrics for a mountainous study site in the Alberta Rockies. These tests were conducted for the four main species types in the area that included: lodgepole pine (*Pinus contorta* var. *latifolia* Dougl ex. Loud.), white spruce (*Picea glauca* (Moench) Voss), mixedwood and hardwood species including aspen (*Populus tremuloides* Michx.) and balsam poplar (*Populus balsamifera* L.). As well, different remote sensing LAI estimation methods were evaluated including a comparison of three different vegetation indices with Spectral Mixture Analysis (SMA) that were

identified from previous research as producing the highest correlation between remotely sensed and LAI estimates (Peddle et al., 1999a, 2001; Johnson, 2000; Chen, 1996a).

As a result, the three main objectives for this research are:

1. To determine the extent that five different ground-based methods for estimating LAI are similar over forest stands consisting of the four main species in the area.
2. To determine if there is a difference among LAI estimates derived from remote sensing using three vegetation indices and spectral mixture analysis.
3. To determine the sensitivity in NPP outputs from FOREST-BGC ecosystem model to different LAI inputs derived from both field and remote sensing methods as defined and analyzed in objectives 1 and 2.

1.2 Organization of Thesis

This thesis has been organized into five chapters. In this chapter the thesis has been introduced and research objectives defined.

In Chapter Two, a review of the literature and an overview of the broader contexts of the research are presented. The chapter begins with an overview of global climate change and carbon cycles to set the framework for this study. This material is followed by a description of process-based ecosystem models, with emphasis on the FOREST-BGC and BIOME-BGC models and including an in-depth discussion on model input parameters, which is pertinent in the estimation of carbon stocks. LAI estimation methods are introduced for both ground level and remote sensing techniques as a means for comparison and with reference to inputs to the ecosystem NPP models.

In Chapter Three, the research methods and experimental design are discussed. A description of the study area and ground-based measurements is first presented including forestry structural parameters and LAI estimation instrumentation and procedure is presented, followed by a description of the remote sensing imagery-based data sets. The various input parameters to the NPP model are then described. The experimental design for three analyzes are presented with a description and rationale for the statistical tests used for assessing the ground-based and remotely sensed LAI estimation methods, and the variability of the NPP model to those estimates.

In Chapter Four, the results of the LAI assessments and the NPP model sensitivity experiment are presented and discussed. A comparison of the results from the various ground-based LAI estimation methods is provided, to determine and understand the differences in ground-based LAI measurements by different species and then apply these to regional scales. This is followed by a comparison of results from the remote sensing LAI estimation techniques. Finally, to quantify the effects LAI has on NPP, the sensitivity of the NPP model to the various key input parameters is compared, and the variability of the modeled NPP is compared to the variability of the input LAI.

In Chapter Five, major conclusions from this thesis are presented. First, the results of the analysis are summarized, and then major conclusions from these results are drawn. Finally, the contributions to research from this thesis are outlined and areas for future research are identified.

CHAPTER II

2.0 Literature Review

2.1 Introduction

This chapter presents a review of ecological modeling of net primary productivity (NPP), and the inputs required for these models, with a particular emphasis on LAI. This chapter begins with a description of global change, carbon cycling, forest productivity modeling and remote sensing, to provide the broader context of this research. The modeling of ecological processes in the determination of NPP is described through an overview of the functionality and history of process-based models, specifically FOREST-BGC and BIOME-BGC. A perspective on the assumptions and deficiencies in LAI estimation techniques and the potential effect this has on modeled NPP is provided through a review of the ground-based and remote sensing LAI estimation techniques.

2.2 Climate Change, Productivity, and Forests

2.2.1 Global Climate Change

The Intergovernmental Panel on Climate Change (IPPC) has stated that most of the observed global warming over the last 50 years is likely due to anthropogenic increases in greenhouse gas concentrations (IPPC, 2001). Keeling et al. (1995) found that there is a proportional relationship between the rise in atmospheric concentrations of CO_2 and industrial CO_2 emissions based on historical atmospheric CO_2 data collected at Mauna Loa, Hawaii and the South Pole. In the last 40 years there has been a steady

increase in atmospheric CO_2 (Figure 2.1). If the emissions of these greenhouse gases continue at this rate, by 2100 CO_2 concentrations will be at 700 ppm, which is 2 ½ times the pre-industrial CO_2 concentration (IPPC, 2001). Keeling et al. (1996) observed that the amplitude of annual CO_2 was correlated with land surface temperatures, suggesting there is an influence on the global carbon cycle due to a changing climate. The projected range of global warming caused by increased greenhouse gas emissions has been simulated to be between a 1.4°C to 5.8°C increase in temperature over the 21st century (IPPC, 2001). This rise in CO_2 and subsequent global warming could have significant ecological, social and economic impacts on terrestrial ecosystems, such as shifts in precipitation patterns, potential shifts of the tree line to more northerly latitudes, progressive lengthening of the growing seasons, major shifts in ecological boundaries and changes in ecosystem structure and composition (Myneni et al., 2000; Gifford et al., 1996; Keeling et al., 1996; Baker and Allen, 1994; Rizzo and Wiken, 1992; Izrael, 1991). The observed increase in levels of atmospheric CO_2 is causing an increased focus on the processes that control CO_2 accumulation in the environment and the contributions to global CO_2 sources and sinks (Schimel, 1995).

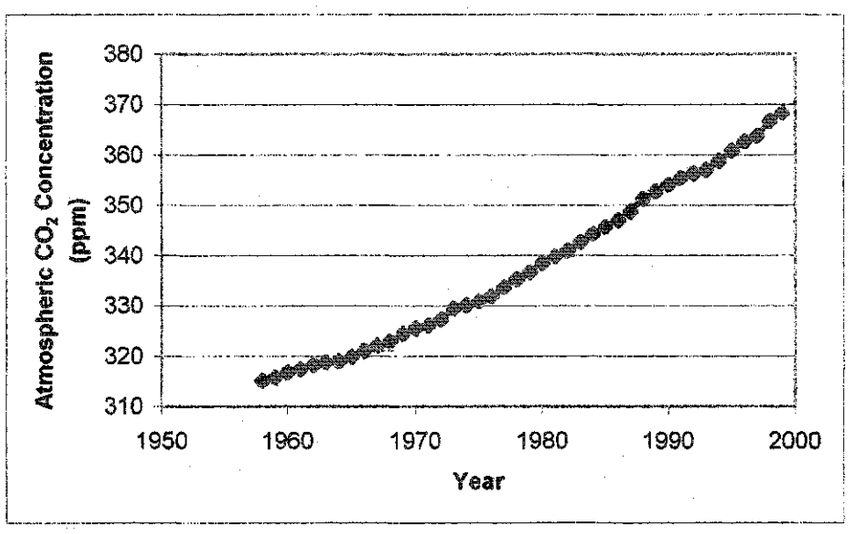

Figure 2-1 - Average annual atmospheric CO_2 concentrations measured in parts per million (ppm) derived from insitu air samples collected at Mauna Loa Observatory, Hawaii (20^0N, 156^0W). (Data source: Keeling et al., 2001)

The atmosphere is the main reservoir of carbon that is in constant exchange with the oceans and terrestrial biosphere (Tans and White, 1998). The increased emissions of fossil fuels, from vehicles, industry and other sources, into the atmosphere are placing greater demands on the ocean and terrestrial biosphere to maintain a balance with atmospheric carbon levels through the absorption of greater amounts of carbon (Schimel, 1995). Carbon storage by land ecosystems can play an important role in limiting the rate of atmospheric carbon increase (IGBP Terrestrial Carbon Working Group, 1998). Forested land accounts for approximately 90% of the terrestrial carbon storage in the world through sequestration of CO_2 from the atmosphere (Gates, 1990). Studies in Canada and Europe have suggested that the boreal forest may be a substantial sink of carbon (50-250Tg C yr^{-1}) (Breymeyer et al., 1996). Canada's landmass consists of 417.6 million hectares of forested area, or 10% of the world's terrestrial biosphere (CCFM, 1997; CFS, 1997). Therefore, Canadian forests play a major role in the world's carbon

budget by their contribution to, and regulation of global biogeochemical cycles (CCFM, 1997). Under Article 3 of the Kyoto Protocol, an international treaty signed by developed countries to limit net greenhouse gas emissions, countries must count both sequestrations and emissions of carbon from land use change and forestry activities towards meeting their Kyoto target commitments (Gov't of Canada, 2001). Thus, in accordance with the Kyoto Protocol, for Canada's greenhouse gas reduction target of 6% below 1990 levels by 2008-2012, anthropogenic disturbances of the terrestrial biosphere need to be monitored, and inventories or measurements of significant carbon sources and sinks in Canada's carbon cycles are imperative to direct international policies aimed at ensuring that the balance is maintained (Gov't of Canada, 2001).

2.2.2 Carbon Cycling in Forests

Carbon (C) is found in all terrestrial life forms; it is the currency that plants accumulate, store and use to build their structure and maintain their physiological processes (Waring and Schlesinger, 1985). It is introduced into plants by the assimilation of atmospheric CO_2 through photosynthesis into reduced sugar. Photosynthesis is an important phase in the biogeochemical global carbon cycle. Tree photosynthesis requires three main processes: light absorption, electron transport, and the carbon reduction (Calvin) cycle (Lambers et al., 1998). Light energy is harnessed from the sun by two photosystems containing chlorophyll, carotenoids and other pigments. Light energy is received between 400-700 nm or the photosynthetically active radiation (PAR) region. The electron transport chain produces energy in the form of adenosine triphosphate (ATP) and nicotinamide adenine dinucleotide in its reduced phase (NADPH) from the

light energy, which drives further reactions within the carbon reduction cycle. At the same time, atmospheric CO_2 is assimilated into the leaf as a result of a gradient between intercellular CO_2 to atmospheric CO_2. The carbon reduction cycle accepts the CO_2 and, using the energy from the electron transport chain, produces carbon in the form of sugar or starch. The initial carbon gain through photosynthesis is called gross primary production (GPP). Approximately half of the GPP is used as autotrophic respiration (Ra) by the plant for the maintenance and synthesis of living cells. During respiration, sugars are broken down and CO_2 is released (Waring and Running, 1988). The rate of photosynthesis and respiration is dependent upon site factors including CO_2 concentration in the atmosphere, surface temperature, nutrients, water availability and plant physiology (Waring and Schlesinger, 1985). Respiration is active all the time, while photosynthesis depends on light for the production of energy. The remaining carbon produced after respiration (GPP – Ra) goes into net primary production (NPP) as foliage, branches, stems, roots and plant reproductive organs (Waring and Running, 1998). NPP, therefore, quantifies the amount of large-scale carbon accumulation into an ecosystem (Figure 2.2). An ecosystem is defined as "an ecological system that consists of all the organisms (including plants) in an area and the physical environment with which they interact" (Lambers et al., 1998). Thus plant processes drive the input of carbon into the ecosystem, which is subsequently used by other organisms.

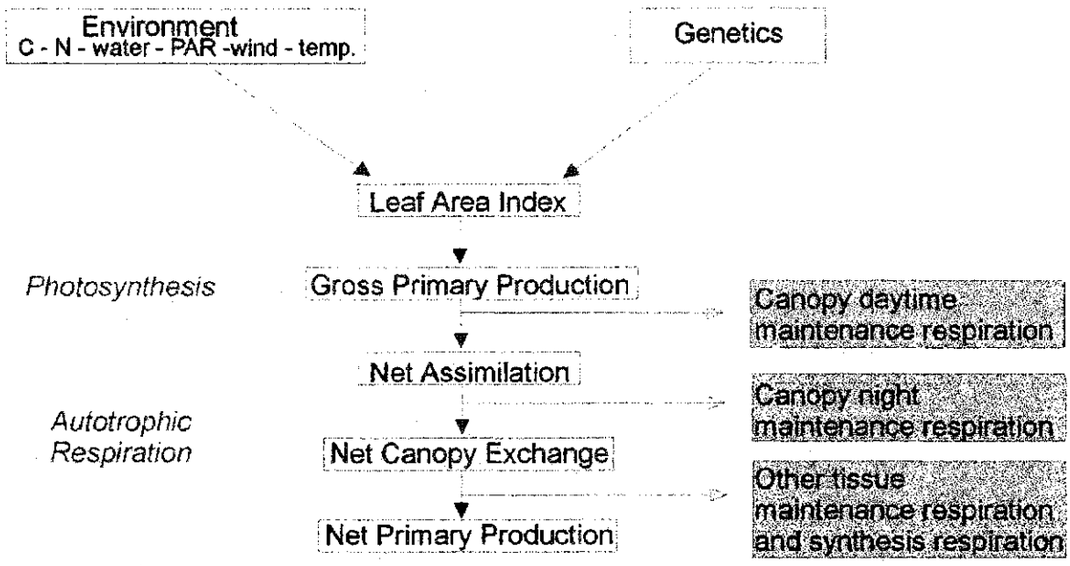

Figure 2-2 – Graphical representation of the processes involved in carbon accumulation (adapted from Waring and Running, 1998). Environmental inputs are carbon (C), nitrogen (N), water, photosynthetically active radiation (PAR), wind and temperature.

2.2.3 Remote Sensing of Forests and Forest Productivity

Much of today's understanding of large ecosystem functioning is extrapolated from smaller, intensively studied plots or sites, which may not adequately characterize the full spatial extent of large ecosystems without introducing bias or inaccuracies (Running et al., 1996). Remote sensing image analysis and modeling can provide spatially comprehensive information to help monitor ecosystem functioning at regional to global scales (Sellers and Schimel, 1993). In the forestry context, remote sensing has been used to provide estimates of forest cover and LAI that serve as inputs to ecological models (Peddle et al., 1999a; Liu et al., 1997). Many process-based NPP models such as FOREST-BGC, earlier versions of BIOME-BGC, and BEPS require input variables derived from remote sensing (Liu et al., 1997; Running and Hunt, 1993; Running and

Coughlan, 1988). Remote sensing can also aid in the validation of ecosystem model outputs, help refine model input parameters, and provide quantitative spatially continuous, timely, and synoptic information for model input (Roughgarden et al., 1991). Remote sensing, however, does not measure any forest structural or biophysical characteristics directly, rather, quantitative relationships must be established between fundamental ecological or stand structural variables (fraction of PAR (fPAR), evaporation, LAI, biomass, canopy chemistry) and remote sensing physical units (Peddle et al., 2001; Chen, 1996a; Running et al., 1986, 1989;, Wessman et al., 1988; Peterson et al., 1987;).

Hyperspectral remote sensing has advanced the development of these algorithms, as the electromagnetic spectrum has three main spectral regions that can describe the optical properties of leaves, within which detailed studies have been conducted (Guyot et al., 1989). There are three regions that characterize the intrinsic dimensionality of remote sensing imagery including, visible (400-700 nm), near infrared (NIR) (700 - 1300 nm), and shortwave infrared radiation (SWIR) (1300-2500 nm)(Figure 2-3) (Guyot et al., 1989). In the visible region, light is absorbed by chlorophyll a and b, and carotenoids with spectral absorption peaking at 450nm and 670nm for chlorophyll a and b, respectively. The NIR is dominated by the effects of leaf structure, characterized by mesophyll that results in a high degree of intra- and interleaf scattering in the plant canopies. Leaf reflectance in this region is increased by multiple layers of leaves, more heterogeneous cell shapes, more cell layers and intercellular spaces, and increased cell size (Running et al., 1986; Guyot et al., 1989). The shortwave infrared radiation (1300-2500 nm) characterizes leaf water content (Guyot et al., 1989). At 1400 and 1900 nm the

water in the leaves strongly absorb radiation thus dips in the spectral response pattern can be seen (Lillesand and Kieffer, 1994)(Figure 2-3). The leaf reflectance has been shown to be inversely related to the total amount of water present as a function of moisture content and the thickness of the leaf (Lillesand and Kieffer, 1994).

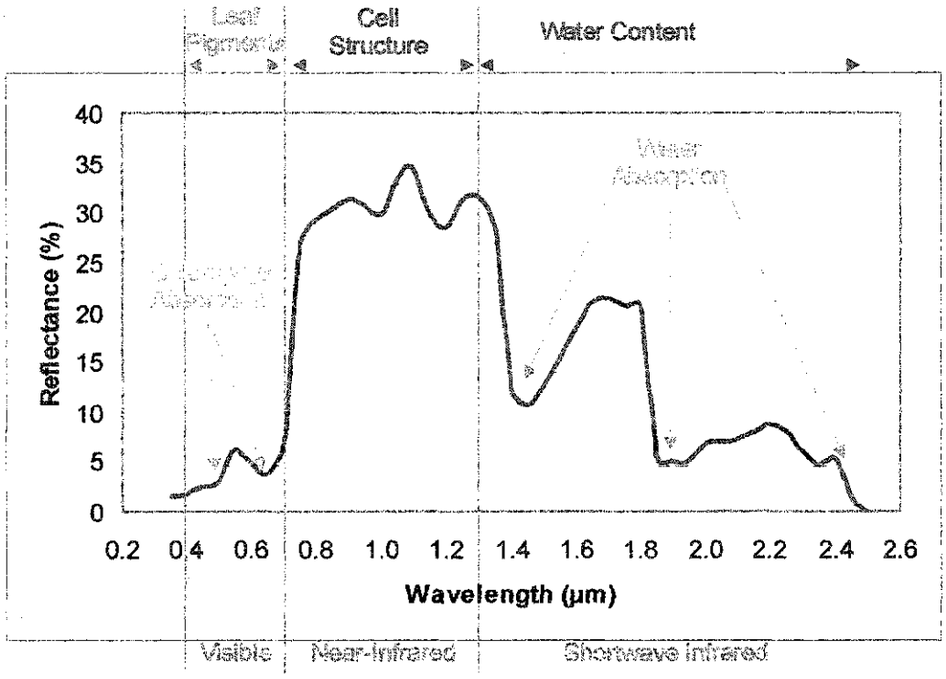

Figure 2-3 – Spectral response pattern for a white spruce tree characteristic of most green vegetation.

2.3 Process-based Ecosystem Models

2.3.1 Modeling Concepts

Smith (1990) defines a model as "*an abstraction or simplification of a natural phenomenon developed to predict a new phenomenon or to provide insight into existing ones.*" Computer models have been widely accepted for the translation of local scale ecological hypotheses to regional, continental or global scale ecosystem processes (Cramer and Field, 1999). There are three types of models generally used to estimate

ecological functions: (1) statistical, (2) parametric, and (3) process-based or simulation models (Liu et al., 1997). Statistical models use regression equations to predict ecological processes from other easily obtained ecosystem measurements. These models often consist of two or more variables from which a relationship is produced where one variable is a function of another. They are generally not very complex with a minimal number of variables. The second model type, parametric, uses efficiency concepts to derive ecological parameters. These models use a small number of important parameters that have the most significant impacts on what is being modeled. They are more complex than statistical models as relationships are weighted differently and combined as separate functions to develop the modeled parameters. Simulation or processed-based models attempt to simulate or characterize the mechanisms that control the functionality of an ecosystem (Waring and Running, 1998). They are not mutually exclusive from the parametric models, however, they tend to have a much higher level of interaction. Process-based models should be more reliable than the other types of models since their foundation is based on knowledge about ecosystems (Liu et al., 1997). Advantages of process-based models to ecosystem studies include providing a tool to extrapolate local scale phenomena to broader spatial and temporal scales, aiding the conceptualization of structure and function of an ecosystem, and facilitating the recognition of important spatial patterns and successional processes on vegetative structure (Lauenroth et al., 1998).

Since the late 1970s, emphasis has been placed on accurate calculation of a global carbon budget and the quantification of terrestrial vegetation activity (Running, 1990). The fundamental and critical ecological questions that need answers concern the rates and

controls of energy, carbon, water, and nutrient exchange at broader spatial scales (Running and Coughlan, 1988). To answer the ecological question at regional and global scales, Running (1990) suggested that a well-tested ecosystem process-based model would facilitate the extrapolation of information from local to broader scales. This simulation modeling can evaluate ecosystem activity at space and time scales greater than direct measurements by quantifying our understanding of fundamental mechanistic ecological processes of energy and mass fluxes (Waring and Running, 1998; Running, 1994). These models have been deemed the only feasible method to make spatially detailed estimates for large regions (Cramer and Field, 1999)

2.3.2 Review of Process-based Ecosystem Models

There are many types of ecosystem simulation models, such as biogeographical (geographical distribution of plant communities and biomes), successional (succession of plant species in an ecosystem over time), population dynamics (germination, birth, growth, and mortality in an ecosystem and interaction among members of a species and different species), soil-vegetation-atmosphere transfer (climate and land-surface relationships) and biogeochemical models (cycling of water, carbon and nutrients through an ecosystem) (Ford et al., 1994). For this study, only biogeochemical models are described as they are widely used in carbon studies and in quantifying carbon stocks. Biogeochemical models simulate the cycling of water, carbon and nutrients through an ecosystem. There are many models that attempt to simulate this cycle at different scales (from plant to globe) and for different ecosystems (e.g. grasslands, forests). Argen et al. (1991) did a comprehensive review of six local or regional scale biogeochemical models

including BACROS (deWit et al., 1978) for modeling crop growth; BIOMASS (McMurtrie et al., 1989) for modeling forest growth and water balance; FORGRO (Mohren et al., 1984) for modeling forest growth, water balance, nitrogen and phosphorus cycles; MAESTRO (Wang, 1988) for modeling forest canopy assimilation and transpiration; FOREST-BGC (Running and Coughlan, 1988) for modeling forest growth and water balance; and BLUE GRAMA (Detling et al., 1979) for modeling grass growth and water balance. Among these models they found many differences in the number and type of driving variables, the incorporation of canopy structure information, and ways in which each model dealt with photosynthesis, respiration, allocation, and litterfall. The models had different inputs and placed different weightings on the various input parameters, which reflected the objectives of the model and the geographic region being modeled. Because of the incorporation of different theories and inputs among the different models the estimation of the output ecological factors were different.

Another carbon model that was not discussed in Argen et al. (1991) is Boreal Ecosystems Productivity Simulator (BEPS). BEPS was developed by Liu et al. (1997) and is based on FOREST-BGC, however, it accounts for the effects of canopy architecture on radiation interception (Liu et al., 1997). The most important inputs for this model are LAI, available water content of the soil, and daily meteorological variables (short wave radiation, minimum and maximum temperature, humidity and precipitation) (Liu et al., 1997). BEPS has been further expanded through the Integrated Terrestrial Ecosystem Model (InTEC) (Chen, 2002). It has increased functionality with the addition of all atmospheric, climatic and biotic factors to decrease the uncertainty due to data limitations or simplistic assumptions (Chen, 2002)

A global terrestrial NPP model intercomparison was performed by the Potsdam Institute for Climate Impact Research to compare the NPP output from a variety of biogeochemical models (Cramer et al., 1999). They divided the models into three different types: satellite based models that use remote sensing data as the major input (CASA, GLO PEM, SDBM, SIB2, and TURC); models that simulate carbon flux based on vegetation structure (BIOME-BGC (newest model), CARAIB 2.1, CENTURY 4.0, FBM 2.2, HRBM 3.0, KGBM, PLAI 0.2, SILVAN 2.2, and TEM 4.0); and models that simulate both vegetation structure and carbon fluxes (BIOME3, DOLY, and HYBRID 3.0) (Cramer et al., 1999). The models differed widely in complexity and original purpose so differences in NPP values were expected. Formulation and parameter values used by the models introduce bias into the NPP estimates (Kicklighter et al., 1999). The study found that the broad global patterns and the relationships between major climatic variables and annual NPP coincided between the models. The differences that were found could not be attributed to the fundamental modeling strategies (Cramer et al., 1999). The high seasonal variations among the models indicated the specific deficiencies in the models. Most models estimated the lowest global NPP month in February, and the highest monthly global NPP during the northern summer (Cramer et al., 1999). The performance of an intercomparison of global NPP models is important to investigate the specific features of model behavior, including testing the underlying assumptions of each model. Global absolute measurements of NPP are impossible so no direct validation of global models could be done; therefore intercomparisons are an important technique to determine deficiencies and differences among the models (Cramer and Field, 1999). No one model was pinpointed as providing the best estimates of global NPP or providing the

best model construction due to the lack of validation NPP values, this exercise however, provided researchers with the means of identifying errors or inadequacies that can be corrected in subsequent models (Kicklighter et al., 1999). The study demonstrated the agreement between the present generation of models for broad features of behavior regardless of the different purposes and resources for the different models (Cramer et al., 1999)

Many ecological models have been built at various spatial and temporal scales, locations, and with different driving inputs and assumptions linking C, N, and water, representation of heterogeneity, detail of photosynthesis, allocation, and decomposition (Cramer et al., 1999; Argen et al., 1991). The ability of each model to reproduce current and forecasted conditions depends largely on how constrained the models are by the initial conditions (Breymeyer et al., 1996). General trends can be seen throughout all the models as they are generally produced using tested plant physiological laws and theories. Validation has been completed for some models, namely those built at local scales. For this study, FOREST-BGC (Running and Coughlan, 1988) will be used because it has been validated for forests in Montana, Florida, and Alaska, suggesting that this is a robust model that can be used in a multitude of environments in North America. This choice of model is discussed further in Section 3.5.1. In the next section, the FOREST-BGC and BIOME-BGC models are reviewed in more detail.

2.3.3 FOREST-BGC

FOREST – BGC originated as a water balance model, which emphasized canopy gas exchange processes and system water storage (Running and Milner, 1993; Running and Coughlan, 1988). The intent was to develop a "generic" process-based model to simulate

the cycling of carbon, water, and nitrogen through forest ecosystems (Waring and Running, 1998; Running and Coughlan, 1988). It was originally developed for coniferous physiology because it allowed efficient analysis of basic growth factors across a landscape, assuming no external perturbation (Running, 1994; Running and Miner, 1993). FOREST-BGC represents all essential ecosystem processes with minimal complexity, allowing the model to be applied at different temporal and spatial scales and locations (Running and Milner, 1993). To minimize the complexity and the ease of application in other locations, the model requires easily attainable data as its driving variables. The variables include standard meteorological information and the explicit definition of important site and vegetation characteristics such as soil water content and leaf area index (Nemani and Running, 1989). FOREST-BGC requires maximum and minimum temperatures and precipitation data that are routinely available from records at the nearest weather stations (Nemani and Running, 1989; Running and Coughlan, 1988). Soil water content (SWC) can be calculated as the water held between the field capacity and the permanent wilting point of the soil based on soil texture and depth (Nemani and Running, 1989). However, the key structural attribute defining vegetation characteristics is LAI, as it is the principal variable used to calculate CO_2 and water vapour exchange and can be estimated and assessed at regional scales through remote sensing technology (Waring and Running 1998; Running, 1994; Running and Gower, 1991; Running and Coughlan, 1988). LAI is a canopy structural variable that is useful in quantifying the energy and mass exchange characteristics directly involved in the functioning of all terrestrial ecosystems (Running, 1990; Nemani and Running, 1989). LAI reduces geometric complexities of the different tree canopies by treating the forest canopy as a

homogeneous three-dimensional leaf, with the depth being proportional to LAI (Waring and Running, 1998; Running and Coughlan, 1988). Running (1994) describes LAI using the analogy of it being a chlorophyll sponge blanketing the earth. LAI strongly affects this model because many processes are controlled by it, including snow melt, canopy interception and evaporation, transpiration, canopy light attenuation, photosynthesis, leaf maintenance respiration, litter fall, and leaf nitrogen turnover (Running, 1990).

To simplify reality, the model structure is based on a set of assumptions that define the system structure, basic linkages and constraints (Running, 1994). The most significant assumptions incorporated into FOREST-BGC are as follows (Waring and Running, 1998, Running and Milner, 1993; Running and Coughlan, 1988):

- Individual species are not explicitly defined, only general physiological attributes; however, physiological characteristics can be represented by the alteration of some key parameters (Table 2-1).
- Individual trees are not represented -- only carbon, water and nitrogen pools.
- No detail on internal physiology concerning water, carbon and nutrient transport is included.
- No individual canopy strata or structure, leaf age class or leaf angular distribution are defined -- only LAI.
- No belowground details on root distribution, variation in soil profile properties, rooting processes, root water or nutrient uptake are defined.
- Fluxes are defined in one dimension (vertical) so that horizontal homogeneity is assumed for the defined area.

These simplifications and assumptions have allowed this model to be applied at any temporal and spatial scale.

Running (1990, 1993) summarized the key processes that FOREST-BGC calculates for each of the hydrologic, carbon and nitrogen cycles:

Hydrologic

- precipitation, snow vs. rain partitioning
- snowmelt
- canopy/litter interception and evaporation
- surface runoff vs. soil storage
- transpiration
- physiological water stress and surface resistance
- subsurface outflow

Carbon

- photosynthesis
- maintenance respiration
- growth respiration
- carbon allocation (leaf, stem, root)
- net primary productivity
- litter fall
- decomposition

Nitrogen

- deposition uptake
- mineralization and leaching

The compartments storing C, N, and H_20 are not exclusive to a single process, many linkages occur between compartments (Figure 2-4). The model was developed to have a split or mixed time resolution so that each of the processes modeled will use its optimum time scale for adequate and efficient simulation. For example, hydrologic and canopy gas exchange are computed daily, while carbon and nitrogen cycles are computed annually (Running and Coughlan, 1988). The daily submodel calculates hydrologic balance and photosynthesis-respiration balance, and applies the carbon to the yearly submodel (Running and Coughlan, 1988). The yearly submodel controls the processes of carbon partitioning, growth respiration, litter fall and decomposition (Running and Coughlan, 1988).

Canopy photosynthesis is calculated by multiplying the CO_2 diffusion gradient by mesophyll CO_2 conductance and by the canopy water vapour conductance (Equation 2-1)(Running and Milner, 1993; Hunt et al., 1991; Running and Coughlan, 1988). Mesophyll CO_2 and canopy water vapour conductance are both controlled by daylight air temperature, average canopy absorbed radiation, maximum photosynthetic rate and daylength (Hunt et al., 1991; Running and Couglan, 1988). Canopy water conductance values are determined through leaf water potential (derived from soil water fraction based on precipitation and snowmelt and canopy interception or rain proportional to LAI) and absolute humidity deficit (Running and Coughlan, 1988).

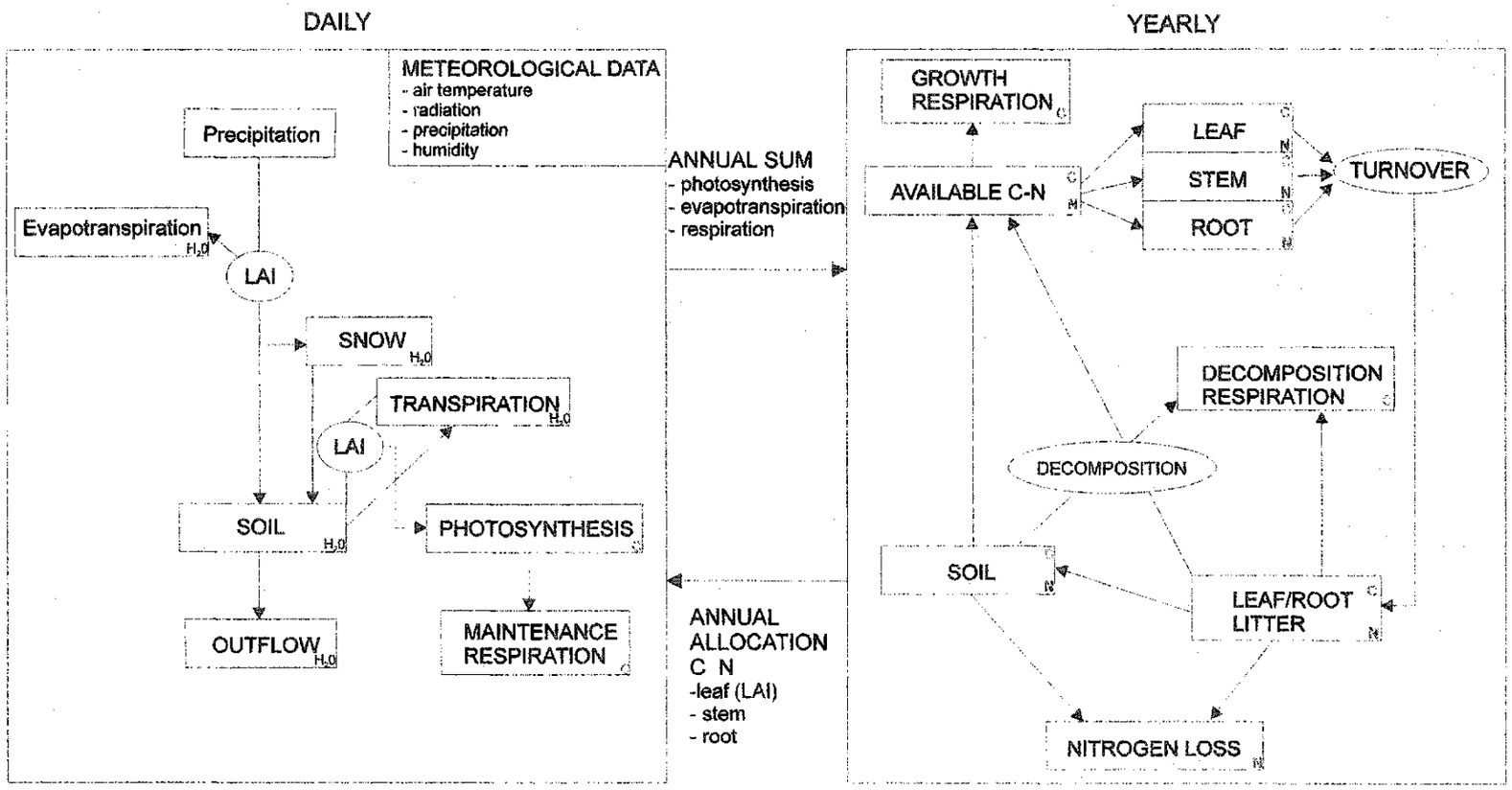

Figure 2-4 Compartment flow diagram of FOREST-BGC (adapted from Running and Gower, 1991

$$PSN = [(\Delta CO_2\ CC\ CM)/(CC + CM)]\ LAI\ \ DAYL$$

(Equation 2-1)

where:

PSN = canopy photosynthesis (kg CO_2 day^{-1})

Δ CO_2 = CO_2 diffusion gradient from leaf to air (kg m^{-3})

CC = canopy conductance (m s^{-1})

CM = mesophyll conductance (m s^{-1})

LAI = leaf area index

DAYL = day length

The carbon is then partitioned into compartments including maintenance respiration, growth respiration, leaf growth, root growth, and stem growth (Running and Gower, 1991). Maintenance respiration is calculated as an exponential function of air temperature where Q10 = 2.3. Q10 is the fractional change in rate of maintenance respiration with a $10^{o}C$ increase in temperature. Net photosynthesis is then calculated by subtracting the maintenance respiration from the canopy photosynthesis. Growth respiration is subtracted as a fixed function from the leaf, stem and root compartments. Net primary production is then calculated by the subtraction of growth respiration from net photosynthesis. The resulting carbon available to NPP is then partitioned into the leaf, stem and root growth compartments based on optimization logic which compares water, nitrogen, and photosynthate availability (Running and Milner, 1993).

Parameterization of an ecosystem model can be very difficult, as many of the processes are difficult, impractical or impossible to measure due to area, time, cost and other constraints (Running, 1994). Many aspects of FOREST-BGC have been tested and validated at different temporal and spatial scales and locations. Running and Coughlan (1988) showed that FOREST-BGC could determine the relative differences in ecosystem processes in variable climates and scales, without site or species-specific tuning. Ecological processes have also been validated including NPP estimates, water budgets, climate and soil control, and carbon allocation (Running and Gower, 1991; Nemani and Running, 198; Running and Coughlan, 1988).

2.3.4 BIOME-BGC

To apply FOREST-BGC to different biomes, a series of parameters were altered based on species-specific physiology (Running and Hunt, 1993). This was done to include other major landcover types (broadleaf forest, grasslands) in the creation of BIOME-BGC or an extension of FOREST-BGC. Many of the physiological parameters differ among ecosystems (Table 2-1). For example, leaf-on and leaf-off periods are very different in deciduous-dominant and coniferous-dominant forest biomes; conifers do not annually drop their needles, whereas deciduous trees shed and regenerate leaves seasonally. Other examples of physiological differences in the two biome types are specific leaf area, and leaf morphology and structure. To maintain the robustness of FOREST-BGC, Running and Hunt (1993) were able to reparameterize the model so that ecosystem function can also be simulated for either broadleaf forests or grasslands, in addition to coniferous biomes. In the alteration of some parameters to characterize the different biomes,

FOREST-BGC maintained its computational stability and the carbon and nitrogen remained balanced, thus leading to the development of BIOME-BGC. BIOME-BGC is a generic model that simulates a range of ecosystems.

Table 2-1 – Default parameter values used in creating BIOME-BGC by adding broadleaf and grasslands to FOREST-BGC (from Running and Hunt, 1993). The following is the suggested default values for model input.

Parameter	Conifer	Deciduous	Grassland
Maximum Leaf Area Index	10	6	3
Specific leaf area (m^2kg^{-1}drymass)	5	17	5
Specific leaf area (m^2kg^{-1}carbon)	25	75	25
Leaf ON date	0	120	120
Leaf OFF date	365	300	240
Maximum stomatal conductance (mm sec^{-1})	1.6	2.5	5.0
Boundary layer conductance (mm sec^{-1})	100	100	10
Maximum photosynthetic rate (umol m^{-2} sec^{-1})	5	5	10
Critical leaf water potential (MPa)	-2.0	-2.0	-3.5
Leaf maintenance respiration (g kg^{-1} day^{-1})	0.2	0.4	0.4
Stem maintenance respiration (g kg^{-1} day^{-1})	0.2	0.2	0.3
Root maintenance respiration (g kg^{-1} day^{-1})	0.4	1.1	0.6
Leaf turnover (% $year^{-1}$)	33	100	100
Stem turnover (% $year^{-1}$)	2	2	99
Root turnover (% $year^{-1}$)	80	80	40
Leaf lignin concentration (%)	25	18	17

2.3.5 The Effects of Environmental Factors on Modeled Productivity

Assessing the effects of individual variable on the ecosystem model is difficult as many of the variables are dependent on each other and are interwoven in the functionality of the ecosystem and how it is modeled. The important ecosystem input variables for BIOME-BGC are leaf area index (LAI), climatic information, available soil water content, and species composition. Generalizations about the variables are useful, however, the prediction of the composition and productivity of site vegetation based only on either soil moisture condition, climatic variables, species composition and LAI is inadequate for this characterization (Kimmins, 1997; Waring and Schlesinger, 1985). Interactions occur with all these variables to produce the structure of the vegetation. The recognition of the general functionality of each variable will provide a better understanding of the ecosystem. Climate sets the framework for much of the biotic potential of an environment. Temperature extremes and inadequate precipitation limit terrestrial NPP (Waring and Schlesinger, 1985). Climate is related to the amount of water present within the soil through both precipitation and evaporation, however, soils by themselves dictate the amount of water and nutrients available through porosity and parent material. Soils that have extremely low moisture storage or an excess of water are unsuitable for most forms of plant growth (Kimmins, 1997). However, soils that are well drained and maintain sufficient water availability throughout the growing season, generally support highly productive and lush vegetation (Kimmins, 1997). Species composition and LAI are largely based on the climatic variables. The influence of species composition and LAI on productivity and vegetation is dependent on competition,

efficiency of water and nutrient use, and successional stage. The amount of carbon produced and stored in a region is a function of both the LAI and species composition, which in turn, are a function of climate and soil.

2.4 Process-based Ecosystem Model Inputs

2.4.1 Ground Based Leaf Area Index (LAI) Estimation

LAI is an important parameter that characterizes a forest stand, as it is a controlling factor in both physical and biological processes of plant canopies (Daughtry, 1990). LAI has been related to site water balance in mature coniferous forests (Gholz, 1982; Grier and Running, 1977), specific leaf area and leaf nitrogen (Pierce et al., 1994), canopy interception, transpiration and net photosynthesis (Pierce and Running, 1988), and water, carbon and energy exchange (Gower and Norman, 1991). As well, functional relationships exist between LAI and net primary productivity, biomass (Gholz, 1982) and stem wood production (Schroeder et al., 1982). Waring (1985) also suggested that LAI may be useful in monitoring and detecting early symptoms of anthropogenic and natural stresses of forest ecosystems. Thus many large area ecosystem models have been developed to be sensitive to and driven by LAI (Liu et al., 1997; Running and Hunt, 1993; Running and Coughlan, 1988).

LAI was initially defined as the area of one side of green leaves (projected) per unit area of soil surface (Ross, 1981). This implies that the leaves receive light mainly in one direction. This definition is appropriate for most broadleaf plants and grasses but not for conifer species as the foliage elements are not flat (Daughtry, 1990). Conifer needles may be cylindrical or close to hemi-cylindrical, or have foliage clumps that may be

spherical, ellipsoidal or other shapes. Therefore, the meaning of one-sided area is not clear (Chen and Black, 1992). Chen and Black (1992) performed a theoretical study on radiation interception of conifer species and produced a more suitable definition of LAI for coniferous species or non-flat leaves, as "*half the total intercepting area per unit ground surface area.*" This definition is based on mathematical derivations and numerical calculations for mean projection coefficient of spheres, circular cylinders, hemicircular cylinders, bent plates, square bars and multi-sided bars with random angular distributions. They found that the mean projection coefficient for all the different shapes were all close to a constant of 0.5 based on the total intercepting area.

2.4.1.1 Absolute LAI Measurement

There are many approaches used to estimate LAI at the ground level. The most direct measurement technique requires destructive sampling (e.g. measuring the total area of all the leaves or needles removed from the canopy). Methods of direct measurement of LAI include leaf tracing methods, matching of standard leaf shapes and sizes, calculations based on linear measurements, leaf area to mass relationships, and optical planimetric methods (Daughtry, 1990). Leaf tracing methods incorporate the tracing of a leaf onto graph paper and the calculation of its area by counting the number of squares. This method has very high accuracy but determining the area of each leaf for a tree or many trees requires vast amounts of time. The matching of standard leaf shapes method is relatively efficient, simple to use and requires no special equipment. For this method a set of standard leaves with different shapes and sizes are assembled, and the area is calculated. Leaves of the test plants are then referenced to the set of standards, and the

standard that most closely matches the leaf is recorded. Accuracy of the matching standard leaf shape method is lower than the leaf tracing method (Daughtry, 1990). In the method of calculation based on linear measurements, the leaf is modeled as a simple geometric shape and the area is determined by linear measurements (i.e. length and width). This method is relatively easy to implement and is less time consuming than the leaf tracing method (Daughtry, 1990). The method of developing a leaf area to mass relationship is probably the most commonly used technique for direct absolute measurement of LAI in forestry research, as it is the most efficient technique for measuring a large amount of leaves at one time (Chen, 1996b; Daughtry, 1990). Leaf area and leaf mass are measured on a small subsample of leaves and a ratio is developed between leaf area and leaf mass. The remaining leaves are weighed and the ratio is applied to determine the leaf area for the entire plot. The final direct method of measuring leaf area is optical planimetric methods. These instruments employ planimetric principles and calculate the area as they are fed through an automated optical instrument (e.g. Licor LI-3100 Area Meter). All of these methods are useful in calculating leaf area index for small plants or in agricultural research; however, the use of these methods for forestry are not widely implemented due to cost, time and the irreversible, destructive removal of entire trees and vegetation.

An alternative to direct measurements that require destructive sampling, a variety of indirect methods have been developed to estimate LAI without the time and cost requirements associated with the direct absolute measurements. However, as with most indirect methods, additional error can be introduced in estimating LAI compared to direct measurement methods. In the next section, indirect methods for estimating LAI using

sampling methods (eg. Litterfall traps) and allometric techniques as well as optical measurements including hemispherical photography, LAI-2000 Plant Gap Analyzer, sunfleck ceptometers and Tracing Radiation and Architecture of Canopies (TRAC) instruments as well as the integration of two methods are reviewed.

2.4.1.2 Litterfall Traps

A litter trap is an apparatus that captures leaves, needles, branches and shoots that have been shed from trees within a stand. Hughes et al. (1987) defined the important features needed for a litter trap: (i) quickly and easily constructed from readily available, inexpensive materials, (ii) strong and durable and require minimum maintenance, (iii) stable and not easily tipped yet sufficiently lightweight so that large numbers of traps can be transported easily, (iv) easily positioned at any height or orientation even on steep, rocky slopes, (v) suited for use in stands of different successional age, (vi) easily emptied, (vii) rapidly drained following precipitation, and (viii) protected from seed predation from wildlife. There are a large range of sizes (0.18 – 1 m^2) and number of litter traps used for a stand, which is largely dependent on the plot area and structural variability of the stand (Cutini et al., 1998; Herbert and Jack, 1998; Voss and Allen, 1988; Hughes et al., 1987). Litterfall is then periodically collected within the year to ensure samples are preserved (Cutini et al., 1998). The litter is then sorted into components (leaves, needles, branches and seeds), dried, and weighed. To estimate LAI for the stand the total dry leaf mass collected per unit ground area (area of the trap) is multiplied by the weighted mean annual specific leaf area (SLA). SLA is the leaf area per unit of dry leaf mass. It can be determined by using a subsample of leaves where

both the leaf area and leaf dry weight are measured and a ratio is calculated. SLA is dependent upon species, site, season and year, therefore a SLA must be produced for each stand. To determine LAI for deciduous species the leaf fall is summed for the year (Cutini et al., 1998) whereas for coniferous species the needlefall must be summed for 2 or more years as the standard turnover rate for coniferous species is larger than the deciduous turnover rate (Voss and Allen, 1988; Hendry and Gholz, 1986).

2.4.1.3 Allometric Techniques

Allometric techniques are based on relationships of LAI to mensuration data such as sapwood area, basal area and crown closure (Buckley, 1999; Snell and Brown, 1978). Allometric equations relating species-specific cross-sectional sapwood area to individual tree leaf area have been developed for an array of species (White et al., 1997; Lavigne et al., 1996; Kaufmann and Troendle, 1981). For example, Marshall and Waring (1986) showed that the sapwood area was a better predictor of leaf area than tree diameter in conifer species. This method uses the pipe model theory, which states that for a given unit of leaves there must be a continuation of conducting tissue of constant cross-sectional area that services the above foliage (Waring et al., 1982). The sapwood is the most recently produced wood, which has open xylem conduits used for water transport (Lambers, 1998). Many studies have attempted to validate this theory (White et al., 1997; Lavigne et al., 1996; Gower et al., 1987; Waring et al., 1982; Kaufmann and Troendle, 1981; Snell and Brown, 1978), however, this allometric relationship has been found to be stand specific, dependent on season, age, stand density, tree crown size, canopy position, early stand growth and climatic differences (Mencuccini and Grace,

1995; Long and Smith, 1988; Hungerford, 1987; Dean and Long, 1986; Pearson et al., 1984; Gholz et al., 1976). Pearson et al. (1984) found the sapwood area to leaf area ranged from 0.20 to 0.57 m^2/cm^2 in lodgepole pine sites of different densities, ages and sites in Wyoming. White et al. (1997) combined cross-sectional sapwood area/leaf area values from a multitude of published allometrics obtained for the Rocky Mountain regions of North America, which were then compared to optical estimates from LAI-2000 and Ceptometer instruments to ground truth the estimates and provide a calibration for optical estimates.

2.4.1.4 Hemispherical Photography

When used for LAI estimation, a hemispherical photograph is a skywards photo taken under a forest canopy using an extreme wide-angle (180^{o}) or 'fish-eye' lens, which captures virtually the entire hemisphere above the camera plane (Figure 2-5). It captures the species, site and age-related differences in canopy architecture based on the light attenuation and contrast between features within the photo (sky vs. canopy) (Frazer et al., 1998). The position, size and shape of these openings or "gaps" in a forest canopy are captured and recorded (Frazer et al., 1998). Digital scanners and cameras are used to convert the hemispherical photos into digital bitmap files, which can then be analyzed using computer image analysis software (Frazer et al., 1999). The image processing involves the transformation of image pixels in which gaps in the forest cover (sky) are encoded as pixels with a value of 1 and obstruction to light rays caused by canopy components are encoded as pixels with a value of 0 (Frazer et al., 1999; Fournier and Mailly, 1999). This is used to supply canopy gap fraction or leaf angle distribution data for inversion models that calculate LAI (Norman and Campbell, 1989). The calculation

of LAI based solely on gap fraction has been termed effective LAI (eLAI) by Chen et al. (1997a), since it disregards the effects of gap size distribution and assumes a random leaf distribution. Effective LAI is calculated from the gap fraction using the following formula through the adoption of Miller's (1967) theorem:

$$eLAI = 2\int_0^{\pi/2} \ln\left[\frac{1}{P(\theta)}\right]\cos\theta\sin\theta d\theta \qquad \text{(Equation 2-2)}$$

where:

eLAI = effective LAI

$P(\theta)$ = gap fraction at view zenith angle (θ)

One operational consideration for hemispherical photography is that the ideal light condition for photographs is diffuse irradiance, or where the entire sky has a uniform irradiance field. This ensures that none of the photographs are over exposed due to the extreme brightness around the solar corolla, causing underestimation of LAI, and also to inhibit the direct reflections of the foliage from the sun (Fournier and Mailly, 1999). As well, the camera must be steady, immobile and leveled (Fournier and Mailly, 1999).

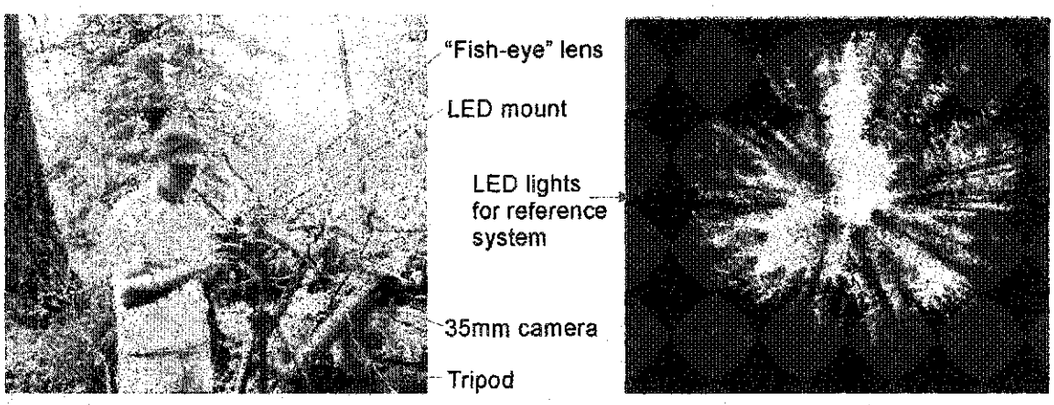

Figure 2-5 – Hemispherical camera set up (left) and example photo (right).

2.4.1.5 LAI-2000

The LAI-2000 has been regarded as a convenient hemispherical camera as it does not require any image processing (Chen et al., 1997a). The LAI-2000, like hemispherical photography, measures canopy gap fraction based on the amount of radiation transmitted through the canopy. It is an optical instrument that measures the light penetration through the canopy using five quantum detectors arranged in concentric rings at 0-13^{O}, 16-28^{O}, 32-43^{O}, 47-58^{O}, and 61-74^{O}, thereby capturing light attenuation at several angles from zenith (Li-cor Inc., 1990; Welles, 1990). The LAI-2000 follows four basic assumptions in its calculation of LAI (Li-cor Inc., 1990):

1. The foliage is black. No transmitted or reflected radiation by the canopy is included.
2. The foliage is randomly distributed.
3. The foliage elements are small.
4. The foliage is azimuthally randomly oriented.

The LAI measurement of the LAI-2000 uses only an estimate of canopy gap fraction and therefore, as with hemispherical photography, is termed effective LAI (eLAI) (Chen et al., 1997a). The lack of the gap size distribution measurement and the assumed random leaf distribution are suggested to be the cause of underestimation of LAI from the LAI-2000 for coniferous species (Chen et al., 1997a; Fassnacht et al., 1994; Gower and Norman, 1991).

There are three main operational considerations for the use of the LAI-2000 (Li-cor Inc., 1990). The first is that two measures of light are needed, a diffuse light measurement either outside or above the canopy, and a measure of diffuse radiation

below the canopy. Therefore, arrangements must be made for either two LAI-2000 instruments to be used (one above the canopy or outside the canopy in an open field, and one instrument within the canopy for field measurements), otherwise the field plots must be located near an open area where an outside measurement can be taken with the same instrument. The second main consideration is that the instrument is more accurate with diffuse light conditions; therefore measurements should be taken on cloudy days or near sunset or sunrise. The third consideration is that the field of view on the instrument is rather large; therefore the use of this instrument is more appropriate in larger stands where there is a homogeneous tree cover or minimal open areas. The field of view of the instrument can be altered with the inclusion of view caps, which can also be accounted for in processing.

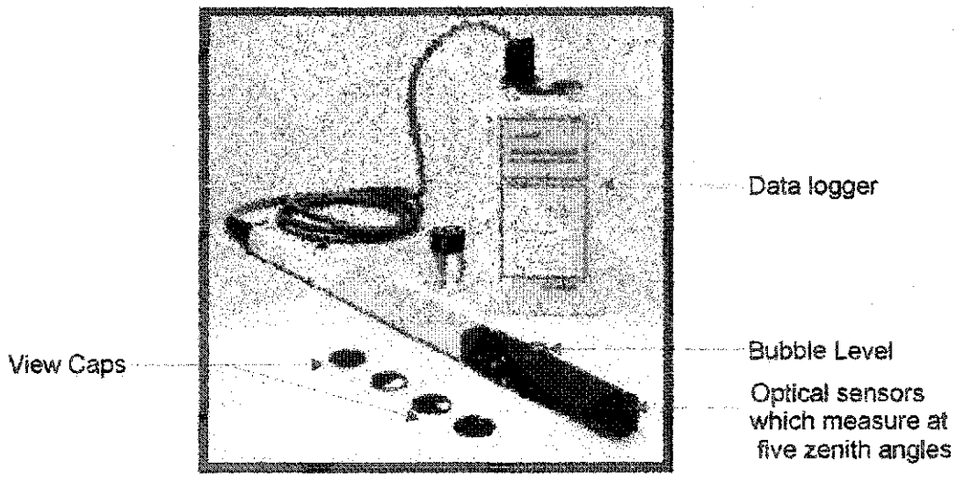

Figure 2-6 – The LAI-2000 instrument.

2.4.1.6 Ceptometer

The sunfleck ceptometer is another optical instrument used in the estimation of LAI. It is a 90 cm long wand consisting of 80 photodiodes at 1cm spacing that are sensitive to PAR wavebands (Decagon, 1994). It measures the average transmittance of

direct solar radiation, which is related to gap fraction at the solar zenith angle and with an assumed leaf angle distribution LAI can be estimated (Chen et al., 1997a). By using the exponential decay of light intensity through the canopy by taking the ratio of below canopy PAR to above canopy PAR, LAI can be estimated (Pierce and Running, 1988):

$$LAI = \ln(PAR_B/PAR_A)/-k$$

where: (Equation 2-3)

PAR_B is the below canopy estimate of PAR

PAR_A Is the above canopy PAR

k is a species-specific extinction factor

The extinction factor (k) corresponds to the portion of light intercepted by each successive layers of leaves. Values for this coefficient are 0.5 for deciduous and 0.6 for coniferous species but can range from 0.3 for vertically inclined leaves to 1.0 for horizontal leaf arrangements (Lambers et al., 1998; Noble and Schumann, 1992; Pierce and Running, 1988).

There are three main operational considerations for the use of a ceptometer. Like the LAI-2000 it requires a below canopy measurement of PAR and an above canopy or an open canopy measurement of PAR. Thus arrangements must be made for the field plots to be located near an open area. The ceptometer requires clear sky conditions with no cloud cover. Optimal measurement times should be taken an hour either side of solar noon to minimize the effects of changing solar zenith angle on PAR measurements.

2.4.1.7 TRAC

Chen and Cihlar (1995) took a further step with the development of the Tracing Radiation and Architecture of Canopies (TRAC) instrument, which accounts for not only canopy gap fraction but also canopy gap size distribution, thereby determining the leaf distribution or clumping index. The TRAC consists of three quantum sensors. Two sensors are oriented upwards to measure down-welling total diffuse PAR through the canopy, and one is oriented downwards to measure the reflected PAR off the ground (Figure 2-7). The TRAC measures sunfleck width (or the width of the light penetrating through the canopy to ground below) and relates this to gap size distribution, which is further related to information on canopy architecture (tree crowns, branches, and shoots) (Chen and Kwong, 1997). The addition of the gap size distribution provides another dimension to the gap fraction data. It quantifies the effect of foliage clumping at scales beyond that of shoots, thereby not relying on the assumption that there is a random spatial distribution of foliage in the canopy.

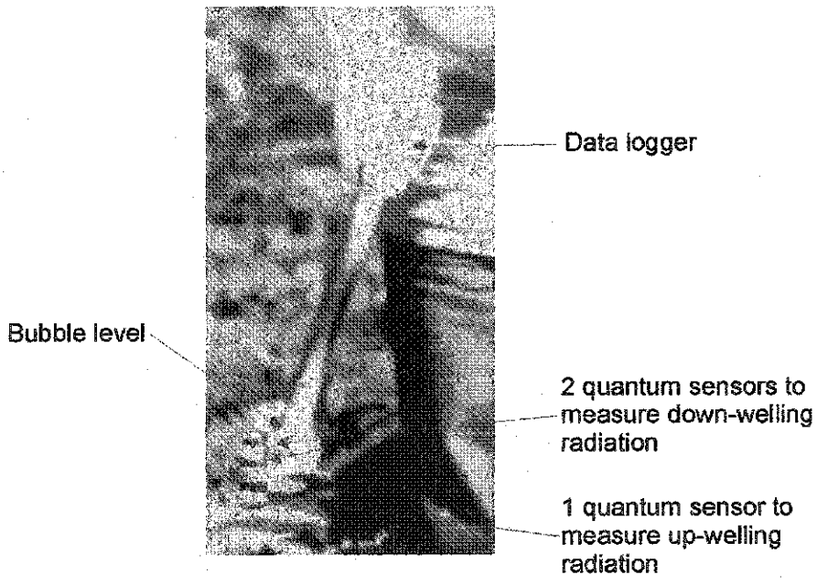

Figure 2-7 – The TRAC instrument

The TRAC calculates LAI by the following equation (Chen, 1996b):

$$LAI = (1- \alpha)*eLAI* \frac{Ve}{\Omega} \qquad \text{(Equation 2-4)}$$

where:

LAI = leaf area index

α = woody-to-shoot ratio

eLAI = effective leaf area index (from gap fraction)

Ve = needle-to-shoot ratio

Ω = clumping index

The woody-to-shoot ratio (α) converts plant area index (i.e. a ratio of total plant area including, leaves, branches and trunks, to ground area) into LAI, thereby removing the contributions of non-leafy material to the LAI estimate. Foliage, branches and tree trunks intercept incoming PAR, thus resulting in inflated LAI values. The TRAC quantifies the α parameter with respect to the clumping index (Ω), as it is assumed that the non-woody materials have a spatial distribution pattern similar to that of the leaves (Chen and Kwong, 1997). These woody-to-shoot ratios can also be calculated in the field by felling trees within the study area and determining the ratio between the needle area, and the tree trunk and branch area (Chen, 1996b). The needle-to-shoot ratio (Ve) is the ratio of half the total needle area in a shoot to half the total shoot area. This ratio is needed as the needles in the shoots of conifer forests are tightly grouped, making it difficult or impossible to infer the needle surface area from optical measurements (Chen,

1996b). Chen (1996b) determined that the average needle-to-shoot ratio is 1.4 for pure conifer stands and 1.0 for pure deciduous stands, but these values will vary for different species.

There are three main operational considerations for the use of the TRAC (Chen and Kwong, 1997). Firstly, transects must be walked perpendicular to the principal plane of the sun (i.e. the sun's azimuth should be perpendicular to the operator's shoulder) and parallel to the slope. Secondly, the optimal measurement times for the TRAC are within two hours of solar noon with solar zenith angles (SZA) between 35 ° and 60°, so that the trees do not cast long shadows. Thirdly, because the TRAC measures sunflecks, clear sky conditions with no cloud cover are required to ensure that the sunflecks are only affected by light penetration through the canopy.

2.4.1.8 Integrated LAI-2000 and TRAC

The TRAC, unlike the LAI-2000 or hemispherical photography, does not calculate an effective LAI by obtaining readings at several zenith angles, because it assumes the deviation from a random (spherical) leaf angle distribution is small, therefore readings are taken at a single zenith angle (Chen and Kwong, 1997). The LAI-2000 and hemispherical photography do not account for gap size distribution, while the TRAC does. Chen et al. (1997a) found that effective LAI estimated from the LAI-2000 were, on average, 15.3% less than those from the TRAC in conifer stands. Recognizing the different strengths and shortcomings of both instruments, Chen et al. (1997a) suggested that integrating the LAI-2000's effective LAI (eLAI) estimate with the TRAC's clumping index would provide a more accurate LAI estimate. This accounts for both gap angular

distributions at several angles from zenith, as well as the gap size distribution function. The integrated approach uses the same equation as the TRAC (Equation 2-3); however, rather than using the TRAC's effective LAI measurement (or gap fraction), it uses the eLAI estimate from the LAI-2000 or from hemispherical photography. This also allows the easy integration of ground based α into the equation, as the TRAC software calculates it based on Ω. Both Chen et al. (1997a) and Leblanc and Chen (1998) suggested that the combination of the LAI-2000's eLAI estimates with the clumping index of the TRAC should increase the accuracy of the LAI estimate. Chen (1995) found that the integrated approach out performed allometric techniques due to the magnification of error in the allometrics caused by the regression analysis. As well, the optical instruments were able to obtain measurements over a larger scale thus being more representative of the stand.

2.4.2 Remote Sensing of Forest Leaf Area

2.4.2.1 Vegetation Indices and Issues

The information contained in a single spectral band is generally insufficient for characterizing vegetation structure and status (i.e. canopy geometry, architecture, and health); therefore, vegetation indices and band ratios were developed to incorporate more information by combining two or more spectral bands from selected parts of the electromagnetic spectrum (Qi et al., 1994). Most vegetation indices utilize the red and near infrared (NIR) spectral bands (Baret and Guyot, 1991). Jordan (1969) theorized that, first of all, the intensity of red radiation reaching the canopy is approximately equal to the intensity of NIR radiation, but on the forest floor, the intensity of the NIR radiation is much greater, due to the absorption of red radiation by the chlorophyll in the leaves

(for photosynthesis). Since plants reflect less visible radiation, but more NIR radiation, the more leaves or the healthier the leaves that are present, the greater the difference will be between red and NIR radiation in vegetated surfaces. The intensities of red and NIR radiation can then be expressed as a ratio that can be associated with canopy characteristics and forest biophysical parameters. Different vegetation indices have been developed for retrieving vegetation information, each having different advantages and purposes (Chen, 1996a).

Bannari et al. (1995) summarized and discussed over forty vegetation indices that were developed from 1972 to 1995. They observed that vegetation indices do not have a standard universal value and are affected by atmosphere, sensor calibration, sensor viewing condition, solar illumination geometry, soil moisture, colour and brightness. They also remarked that each vegetation index is different and is dependent on the environmental characteristics it was developed for. Chen (1996a) identified the 10 most commonly used vegetation indices for forestry applications. He further split these vegetation indices into two main categories: those that are based on the slope of constant index lines in the NIR versus red reflectance plots, and indices that are based on the distance between vegetation and soil reflectance lines, assuming the lines are parallel to each other. The first type can be subdivided further into those that are expressed as a function of the simple ratio (SR) between red and NIR reflectance developed by Jordan (1969) and those that incorporate further mathematical equations. The vegetation indices that are derived from the simple ratio are Normalized Difference Vegetation Index (NDVI) (Rouse, 1973) and Modified Simple Ratio (MSR) (Chen, 1996a). The SR and its derivatives have red and NIR reflectance coordinates converging at the origin (0,0).

However, it has been shown that the converging point does not always occur at the origin (Huete, 1988). This led to the development of vegetation indices that attempt to account for the convergence point not at the origin. The Soil Adjusted Vegetation Index (SAVI) (Huete, 1988) introduced an L parameter, which is determined by the position of the convergence point. SAVI was further developed to allow the L parameter to vary with the surface conditions rather than being a constant value (SAVI1, SAVI2) (Qi et al., 1994). The Global Environment Monitoring Index (GEMI) is also based on the slope of a constant index; however, it attempts to reduce the atmospheric effects by using a curvilinear line between NIR and red reflectance (Pinty and Verstraete, 1992). The Non-linear Index (NLI) and Renormalized Difference Vegetation Index (RDVI) attempt to linearize their relationship between NIR and red reflectance with surface parameters (Goel and Qin, 1994; Roujean and Breon, 1995). The final type of vegetation indices includes the Weighted Difference Vegetation Index (WDVI) and Perpendicular Vegetation Index (PVI) that are based on the absolute differences between the vegetation NIR and red reflectance lines and the soil NIR and red reflectance lines (Clevers, 1989; Richardson and Weigand, 1977). The equations for all the vegetation indices described are presented in Table 2-2. Brown et al. (2000) developed a vegetation index, called the reduced simple ratio (RSR), which uses the shortwave infrared band to improve LAI retrieval. RSR is intended primarily for use with MODIS sensor data. RSR unifies deciduous and coniferous species so that a classification is not required prior to deriving the LAI estimation from regression models. This index has shown a 30% increase over the SR for LAI estimation (Brown et al., 2000).

For this thesis, three vegetation indices were chosen for comparison from each one of the three groups described by Chen (1996a). NDVI, SAVI1 and WDVI were chosen based on their performance for the prediction of forest biophysical parameters in studies that compared vegetation indices (Peddle et al., 2001; Chen, 1996a). The RSR was not used in this study because it uses the shortwave infrared band rather than the near infrared band, which is beyond the spectral resolution of the image data used in this study, and which is not always available in some of the other sensors available. The three vegetation indices chosen for this work are described further in the next section.

2.4.2.1.1 NDVI

NDVI was developed to normalize the difference between NIR and red reflectance, with the output values ranging between –1 (no vegetation) and 1 (high density of vegetation). Therefore, the brighter the pixel, the greater the amount of photosynthesizing vegetation present (Jensen, 1996). NDVI has been related to carbon dioxide, ecological parameters, photosynthesis, stomatal conductance, evaporation, net primary productivity and LAI (Carter, 1998; Chen, 1996a; Baret and Guyot, 1991; Cihlar et al., 1991; Running, 1990). It is limited at LAI values over approximately 3 because the ratio of red to near infrared reaches an asymptote (Wulder et al., 1998; Running et al., 1986). NDVI assumes that the NIR and red reflectance coordinates converge at the origin for a line with fixed NDVI values (Table 2-2).

Table 2-2 Vegetation index equations based on near infrared (NIR), red (R), and shortwave infrared (SWIR) reflectance (after Chen, 1996). SWIRmin is the reflectance from an open canopy and SWIRmax is the reflectance for a completely closed canopy (Brown et al, 2000)

Vegetation Index	Equation	Reference
NDVI: Normalized Difference Vegetation Index	$\frac{NIR - R}{NIR + R}$	Rouse et al., 1973
SR: Simple Ratio	$\frac{NIR}{R}$	Jordon, 1969
MSR: Modified Simple Ratio	$\frac{\frac{NIR}{R} - 1}{\sqrt{\frac{NIR}{R}} + 1}$	Chen, 1996
RDVI: Re-normalized Difference Vegetation Index	$\frac{NIR - R}{\sqrt{NIR + R}}$	Roujean and Breon, 1995
WDVI: Weighted Difference Vegetation Index	$NIR - a * R$ $\quad a = \frac{NIR, soil}{R, soil}$	Clevers, 1989
SAVI: Soil Adjusted Vegetation Index	$\frac{(NIR - R)(1+L)}{(NIR + R + L)}$ $\quad L = 0.5$	Huete, 1988
SAVI1: Soil Adjusted Vegetation Index 1	$\frac{(NIR - R)(1+L)}{(NIR + R + L)}$ $\quad L = 1 - 2.12 * NDVI * WDVI$	Qi et al., 1994
SAVI2: Soil Adjusted Vegetation Index 2	$NIR + 0.5 - \sqrt{(NIR+0.5)^2 - 2(NIR - R)}$	Qi et al., 1994
NLI: Non-Linear Index	$\frac{NIR^2 - R}{NIR^2 + R}$	Goel and Qin, 1994
GEMI: Global Environment Monitoring Index	$\frac{\eta(1 - 0.25*\eta) - (R - 0.125)}{1 - R}$ $\quad \eta = \frac{[2(NIR^2 - R^2) + 1.5*NIR + 0.5*R]}{(NIR + R + 0.5)}$	Pinty and Verstraete, 1992
RSR: Reduced Simple Ratio	$\frac{NIR}{R} * \left[1 - \frac{(SWIR - SWIRmin)}{(SWIRmax - SWIRmin)}\right]$	Brown et al., 2000

2.4.2.1.2 WDVI

Huete (1988) showed that the NIR and red converging point does not often occur at the origin; rather it occurs at a negative point on both NIR and red reflectance coordinates due to the effects of soil background. As a result, pixel reflectance values are comprised of subpixel scale reflectance components, including soil or background, vegetation and shadow (Richardson and Wiegand, 1977). Due to the complex soil-vegetation interactions within a single pixel, using vegetation indices it is difficult to remove or segregate the soil and vegetation reflection signals from the overall spectral response. This is important, since the soil reflectance has been shown to influence the relation between NIR reflectance and LAI (Clever, 1989). Thus, Clever (1989) derived WDVI for correcting the near-infrared reflectance of vegetation for the effects of soil background by subtracting the contribution of background or soil reflectance from the initial NIR reflectance (Table 2-2). The correction factor for the soil reflectance was obtained through a weighted difference between the measured near-infrared and red reflectance of the soil.

2.4.2.1.3 SAVI1

With the SAVI1 index, a soil adjustment factor L is defined which is intended to account for soil noise by minimizing the soil brightness influences and producing vegetation isolines more independent of the soil background (Table 2-2) (Qi et al., 1994; Baret and Guyot, 1991). The L constant should vary inversely with vegetation density. For intermediate densities, the best adjustment was shown to be 0.5 (SAVI). At low vegetation densities L is approximately 1; while at higher vegetation densities, the L

value is smaller (Huete, 1988). The ideal L factor does not remain constant because the soil-vegetation interaction varies with canopy closure. Qi et al. (1994) suggested that the L function could be optimized using the product of NDVI and WDVI, as both of these vary with soil brightness and with canopy density. At high vegetation densities, L approaches 0 and SAVI1 behaves similar to NDVI, while at lower vegetation densities, L approaches 1 and SAVI1 behaves similar to WDVI (Qi et al., 1994). Therefore SAVI1 raises the vegetation signal and lowers the soil-induced variation, allowing it to be a more sensitive indicator of vegetation amount. The L function allows SAVI1 isolines neither to converge at the origin nor to run parallel to the soil line. SAVI1 increases the vegetation dynamic response while further reducing the soil background influences, improving the vegetation sensitivity by a "vegetation signal" to "soil noise" ratio (Qi et al., 1994). Empirical evidence has shown that vegetation indices that attempt to minimize the soil background effects reduce the noise and are better predictors of forest biophysical parameters compared to other vegetation indices (Peddle et al., 2001; Baret and Guyot, 1991; Huete, 1988;).

2.4.2.1.4 Problems with Vegetation Indices

Chen et al. (1996) and Peddle et al. (2001) summarized several assumptions that vegetation indices make which may cause inaccuracies in deriving forest biophysical parameters. The first assumption is that for any given vegetated surface, NIR and red reflectance increase or decrease proportionally and simultaneously with each other. This assumption is often not met, causing inaccuracies in vegetation index values. A concern with vegetation indices is that they are based on measurements of entire pixels, thereby

not explicitly accounting for mixed pixels with non-vegetated components including shadows, background soil and understory vegetation (Hall et al., 1995; Peddle et al., 1999a, 2001). These non-vegetated mixtures complicate and diminish the ability to obtain meaningful information about the actual vegetation of interest (i.e. the trees). Furthermore, many vegetation indices are based on two spectral bands, and therefore do not incorporate or utilize other potentially useful information contained in other bands. Vegetation indices have also been shown to be less effective with canopies at higher leaf areas due to the saturation of band ratios at greater LAI. As a result, methods such as incorporating texture, performing spectral mixture analysis or reflectance modeling have been used to estimate LAI in attempts to provide improved results over vegetation indices by addressing some or all of these problems.

2.4.2.2 Texture

Texture can be characterized by the tonal properties and the spatial interrelationships found between them (Haralick, 1979). Image texture has been used to increase the accuracy of landcover classification and prediction of biophysical parameters such as LAI (Peddle et al., 1999a; Wulder et al., 1998; Wulder et al., 1996; Peddle and Franklin, 1991; Franklin and Peddle, 1989;). Wulder et al. (1996, 1998) showed that texture derivatives provide forest structural information that can be related to LAI. The inclusion of semivariance moment textures with NDVI has provided a more accurate estimate of LAI than NDVI alone in mixedwood stands in which the addition of texture increased the accuracy of the LAI prediction by 43% (Wulder et al., 1998). Peddle et al. (1999b) found texture alone (i.e. not using image pixel values, just the spatial texture)

had a stronger relationship with LAI ($r^2 = 0.29$) than NDVI ($r^2 = 0.01$) for lodgepole pine and aspen species. In both studies, texture provided a measure of additional structural information.

2.4.2.3 Spectral Mixture Analysis

Spectral mixture analysis (SMA) quantifies the abundance of subpixel scene components within an image (Adams et al., 1993). Subpixel scene components or endmembers are identified by the spectral properties of each material present within an image that are expected to contribute to the overall pixel level reflectance. SMA depends on accurate spectral characterization of endmembers by determining the purest (without the presence of other surface material) spectral response pattern of each scene component. The output from SMA is the fraction of each endmember over the pixel area. In the forestry context, three endmembers are often identified: sunlit canopy (C), sunlit background (B) and shadow (S). These endmember spectra can be estimated, measured or modeled (Peddle et al., 1999a). Reference endmember spectra can be measured in the field using a spectroradiometer. If endmembers are collected in this way, both the image and the endmember spectra must be calibrated to reflectance. Reference endmembers can sometimes be obtained from spectral library databases. Image endmembers are selected directly from the image from areas that contain homogeneous or near homogeneous samples of the endmember material. The spectral reflectance of each endmember (ρ_c, ρ_b, ρ_s) in each band is input to SMA and the overall pixel band reflectance values (ρ_y) to be unmixed (Peddle et al., 2000, 1999a; Hall et al., 1995)

$$\rho_y = C\rho_c + B\rho_b + S\rho_s$$

(Equation 2-5)

where:

ρ_y = overall pixel reflectance value
C = fraction of canopy
B = fraction of background
S = fraction of shadow
ρ_c = spectral reflectance of canopy
ρ_b = spectral reflectance of background
ρ_s = spectral reflectance of shadow

SMA expresses the amount of each material as a fraction of total pixel area; therefore the fraction components vary between 0 and 1. Fractions that are greater than 1 or less than 0 have not accurately characterized the material within the pixel, suggesting that the endmember selection did not account for some scene component or that one or more endmembers were not pure (Johnson, 2000; Adams et al., 1993).

SMA is a robust method for the extraction of forest biophysical information from remote sensing imagery, as different mixtures of scene components represent different forest structures. SMA has provided significant improvements over more traditional methods such as vegetation indices for obtaining biophysical estimates (Johnson, 2000; Peddle and Johnson, 2000; Peddle et al., 1999a; Hall et al., 1995, 1996). SMA accounts explicitly for the influence of background and shadows reflectance rather than using only the overall pixel level reflectance as with vegetation indices (Peddle et al., 2001). In

these studies, shadow fraction has been shown to be the best predictor of LAI and other biophysical parameters (Peddle et al., 1999a; Hall et al., 1995). The simplified physical explanation for this is that larger trees cast larger shadows, with the shadow fraction being more sensitive to tree size and structure compared to sunlit canopy fraction in the horizontal dimension (Peddle et al., 1999a). This suggests that shadow fraction may be a surrogate for stand characteristics and canopy dimension (Peddle et al., 1999a). Peddle et al. (2001) found SMA to provide a 40% improvement in the prediction of forest biophysical and structural information (biomass, NPP, LAI, and basal area) over 10 different vegetation indices.

Peddle et al. (1999b) evaluated multi-spectral LAI prediction using both texture and mixture analysis of airborne imagery in the Alberta, Rockies. In that study, a forest scale continuum was established with respect to sub-pixel scale mixture fraction, image tone (pixel values) and spatial texture derived from groups of pixels. SMA provided a better estimate of LAI compared to NDVI ($r^2 = 0.54$ vs. 0.01). The inclusion of texture with SMA shadow fraction increased the r^2 from 0.54 to 0.60 suggesting that the extraction of information over different scales has the potential to maximize the predictive capabilities of biophysical parameters (Peddle et al., 1999b).

2.4.2.4 Reflectance Modeling

Reflectance modeling has provided a powerful tool for the extraction of biophysical and structural characteristics of forest stands from remote sensing imagery. Goel (1989) provided a review of the canopy reflectance models, including geometric optical, turbid medium, a hybrid of geometric optical and turbid medium models, and

computer simulation. Li and Strahler (1986) suggested that geometric optical models are recommended for deriving forest related parameters from airborne and satellite imagery. For example, geometric optical models have been shown to provide improved estimates of important biophysical parameters such as LAI and biomass (Peddle et al., 1999a; Hall et al., 1997; Woodcock et al., 1993). These models treat vegetation canopies as a collection of individual, three-dimensional objects that cast shadows on a contrasting background (Li and Strahler, 1985,1986). For example in the Li and Strahler (1985) model, individual trees are modeled as cones. In forward mode the model predicts pixel brightness from the tree size, shape and density of the forest and the illumination angle, while in inverse mode the model estimates the mean height, shape and density of the canopy from pixel brightness obtained from the imagery. This model was further developed to produce the Geometric Optical Mutual Shadowing (GOMS) model (Li and Strahler,1992) to account for terrain variations, off-nadir view angle, a spheroid shape, and shadows falling on adjacent trees (Li and Strahler, 1992; Strahler and Jupp, 1990). This model requires spectral endmember values of each scene component and the viewing and solar illumination geometry of the image. This model has been used in "Multiple-Forward Mode" (Peddle et al., 1999a) and further expanded for mountainous terrain by Johnson (2000) to provide improved biophysical estimates.

2.4.3 Climatic Inputs to NPP Models

2.4.3.1 MTCLIM Model

FOREST-BGC requires climate data as an input, thus for site-specific measures of climate for incorporation into a montane ecoregion, the Mountain Microclimate

Simulator (MTCLIM) was used (Running and Coughlan, 1988). The primary function of the MTCLIM is the extrapolation of meteorological variables from an individual location where meteorological measurements are available (BASE) to another site where no meteorological data exists (SITE) (Hungerford et al., 1989). This model was developed due to the lack of available meteorological data in mountainous terrain, since most meteorological measurements are taken at city airports situated in flat, non-mountainous terrain. The extrapolation of climate data from the base station is completed by making vertical corrections to the base data for changes in terrain features, including elevation, slope and aspect. The accuracy of the extrapolation decreases with distance from the base station and the site due to the effects of air masses, cloud cover, precipitation and local scale phenomena (Hungerford et al., 1989).

Input requirements for MTCLIM are basic meteorological measurements, which are available from most weather stations, including daily maximum and minimum temperature and precipitation, as well as basic terrain features of the base station (Figure 2-8). Site information is also needed including physiographic features (elevation, slope, aspect, and east-west horizon angles) and initializing vegetation characteristics (LAI and albedo) (Figure 2-8). The input information is then used to predict daily minimum, maximum and average temperatures, precipitation, incoming solar radiation, and relative humidity for the site where meteorological data are not available (Figure 2-8).

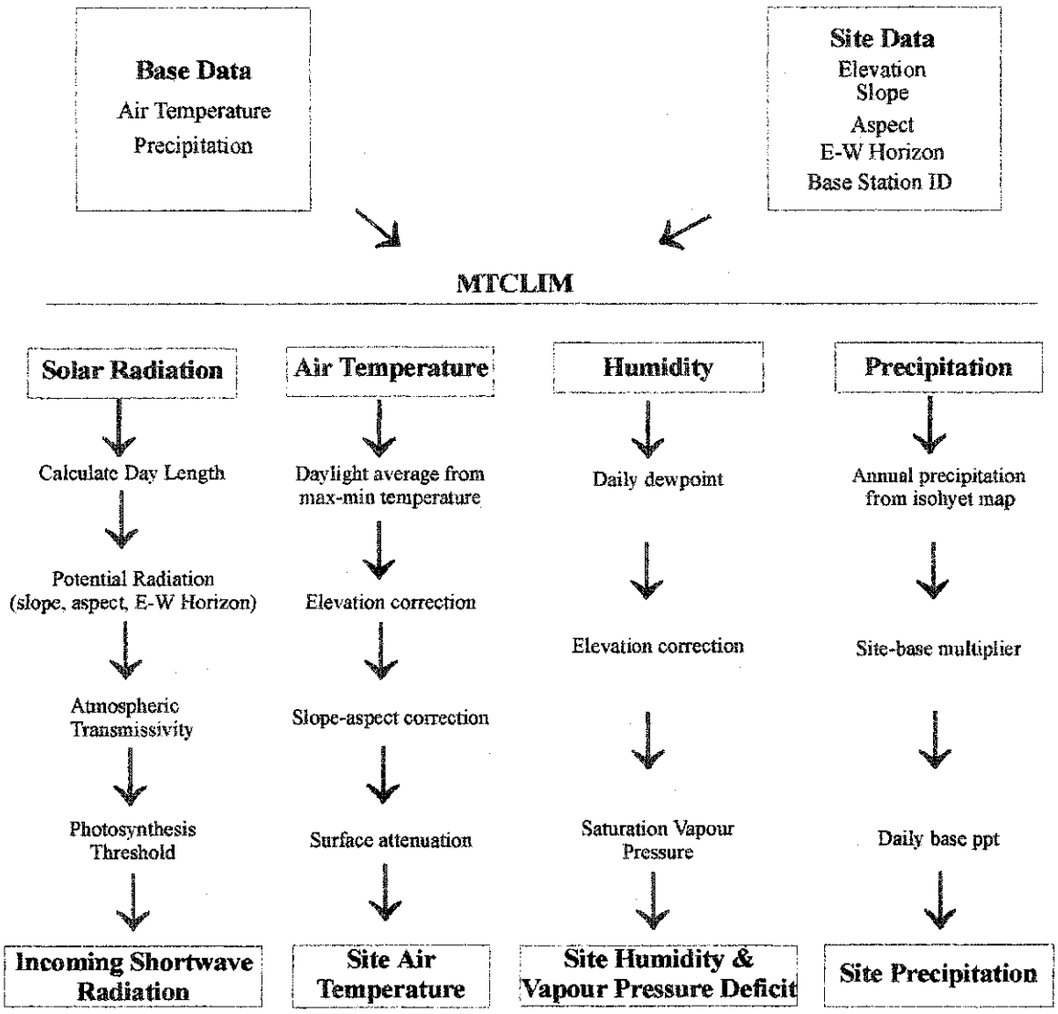

Figure 2-8 Flow chart of the Mountain Microclimate Simulator Model (MTCLIM) showing the transformation of climate data from a known base station to another location based on the physiographic information and climatic principles.

2.4.4 Soil Water Content (SWC)

Another input to the FOREST-BGC model is soil water content (SWC). Soil is the foundation of terrestrial communities and is an important vessel in nutrient and water cycles (Smith, 1990). The roots of trees occupy a considerable portion of the soil to anchor and support above ground biomass and to aid in the cycling of water, nutrients and oxygen needed by plants for growth and maintenance. Soil water is one of the major factors controlling plant growth. The amount of water stored within the soil is determined by the physical features of the soil, as well as climate and topography (Kimmins, 1997). The soil water available for extraction by plants is found between the field capacity, where the soil water has moved out of the macropores caused mostly by gravity and the remaining water is in the micropores, and the wilting coefficient, where plants are unable to extract sufficient water to meet their demands due to the lower water potential and conductivity in the soil (Figure 2-9). The soil water available for plant uptake depends on the relative abundance of different pore sizes, which in turn depends on soil texture, structure and depth. Soils are made up of various combinations of organic matter and mineral particles of various sizes defined as soil texture. Soil texture has three major size classes: sand (0.02 – 2.0 mm), silt (0.002 – 0.02 mm), and clay (<0.002 mm). As the fineness of texture increases (approaches clay), there is generally an increase in available moisture storage (Brady and Weil, 1999). In coarse textured soils (sand) the majority of the water is lost at field capacity due to gravitational water loss through the larger pore sizes (Kimmins, 1997). Fine textured soils (silts and clays) do not lose much water from gravity so the soil usually retains a higher saturated water content (Kimmins, 1997). The depth of the soil is also a determining factor for the

available water since, in general, the deeper the soil, the greater the amount available water (within the limits of the depths to which feeding plant roots can reach).

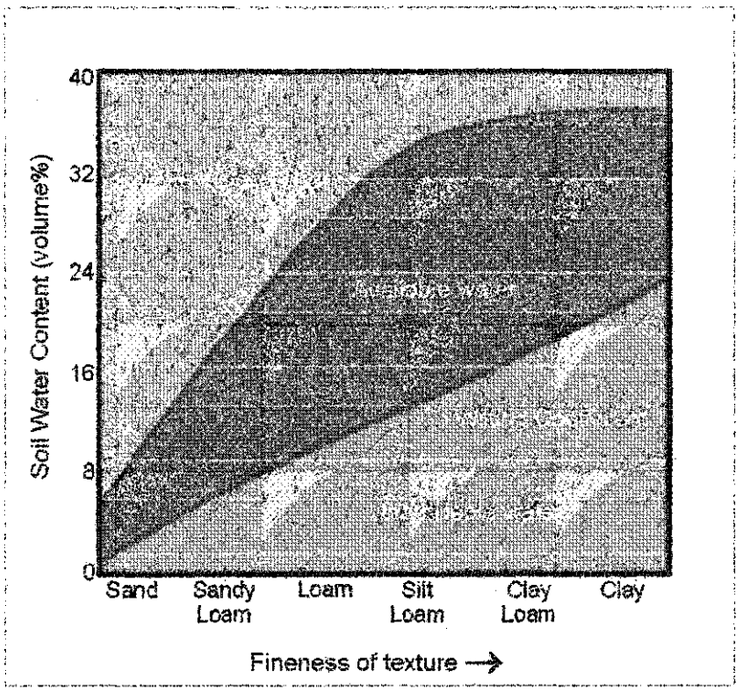

Figure 2-9 – Relationship between available water content and soil texture (derived from Brady and Weil, 1999).

2.4.5 Land Classification

The final input to the NPP model is species composition, which is usually generalized into life form groups (i.e. conifer, deciduous, grassland) as the physiological differences are more important among the physiological groups than among species within life forms (Bonan, 1993). Different biomes or sets of species have very different ecological and physiological properties; therefore, to characterize the functionality of each ecosystem accurately, the study area must be divided into separate, functionally similar units. For broad spatial scales this can be done with relative ease using multi-

spectral remote sensing land classification to characterize all the pixels in an image into landcover classes or themes. It does this by analyzing the set of spectral band values of each pixel and categorizing them based on similar spectral properties.

There are two general methods of land classification from remote sensing, supervised and unsupervised classification (Jensen, 1996). Supervised classification requires *a priori* knowledge about the study area for the collection of training sites (Jensen, 1996). Training sites are a collection of pixels which belong to the same class (e.g. conifer or deciduous forest), and which capture the spectral variability within each class. Unsupervised classification does not require *a priori* knowledge; rather it separates the image into classes based on statistically similar spectral groups (Jensen, 1996). These groups or spectral clusters are then labeled, however, the statistically similar spectral groups may not correspond to the classes of interest. Remote sensing image features can affect the classification accuracy of an area. The scale of the data affects the detail of the information classes and the boundary designation, while the spectral bands and the complexity of the environment affect the separability of the landcover classes (Wulder, 1998). Contextual neural networks (Jensen, 1996) and evidential reasoning classifiers (Peddle, 1995) have been developed to process more complex data sets, including hyper spectral imagery and spatial, terrain and multi-source spatial information.

2.4.6 Complexities of Terrain on NPP Modeling

From a modeling perspective, terrain increases the amount of complexity in estimating NPP or other forest biophysical parameters. Terrain variations affect ecosystem functionality including light and water regimes, soil types, forest structures,

and productivity. FOREST-BGC attempts to account for these effects through the inclusion of important variables. The incorporation of climate data, which has been derived from MTCLIM, account for changes in climate due to changes in terrain (elevation, slope, and aspect). As well it accounts for different soil types and the subsequently soil water content. Forest structure is adaptable in the model based on the inclusion of LAI. The accuracy of LAI estimation is also affected by terrain. Firstly at the ground level especially with optical instruments where terrain causes shadowing and affects the length of light penetration into the canopy thereby altering the solar zenith angles and the optimum times for data collection (i.e. TRAC). Secondly, from remote sensing where terrain influences the sun/surface/sensor geometry, which accounts for a significant difference in the spectral response of a forest stand. As well light will penetrate to different depths of the canopy, which will change the relative proportions of the canopy and background that would be presented to the sensor. Thus a study in mountainous terrain includes further complexities beyond that would be seen on flatter terrain.

2.5 Chapter Summary

Due to the increased focus on potential climate change impacts to sustainability, many countries are attempting to quantify their carbon stocks, for improved forest management and as part of international policy agreements. Net Primary Productivity (NPP) is one measure of this over large areas and this information can be obtained through ecosystem productivity models. One such model is FOREST-BGC, which was designed to be dependent upon LAI estimates, thus it follows that the accurate prediction

of LAI is important. The accuracy of the estimation of LAI is two fold with estimation for small areas using ground-based instruments and estimation of larger areas using remote sensing data. Many ground-based instruments and techniques have been developed for the estimation of LAI with varying assumptions and mechanisms. Some optical instruments estimate LAI based on the gap fraction of light penetration through the canopy (hemispherical photography and LAI-2000), while others go further with the inclusion of gap size distribution (TRAC and integrated approach). It is hypothesized that the inclusion of both gap fraction with gap size distribution provides a more accurate estimation of LAI. For large areas, vegetation indices have been widely implement in the estimation of LAI from remote sensing data. However, vegetation indices have been shown to be limited, as they do not adequately account for background reflectance, shadows and canopy geometry and are restricted to two spectral bands. Spectral mixture analysis (SMA) explicitly accounts for background reflectance, shadows and canopy geometry by quantifying the abundance of scene components at sub-pixel scales that contribute to the overall pixel level reflectance. The potential inaccuracies found in both ground-based and remotely sensed LAI estimates can subsequently produce errors or inaccuracies resulting in poor quantification of carbon and inadequate sustainable management practices.

CHAPTER III

3.0 Methods

3.1 Introduction

This chapter describes the experimental design and methods used to compare the ground-based and remote sensing estimates of LAI, and the influences these measures have on modeled NPP. It begins with a description of the Kananaskis study area and forest mensuration techniques to provide information about the composition and distribution of the forest stands. To quantify the differences in LAI estimation techniques from both the field and remote sensing data, a detailed description of the collection and processing of the ground-based and airborne LAI estimation techniques and the analytical and statistical approaches used to compare and evaluate the LAI estimation techniques are described. The NPP modeling is documented and justified, including how all ecosystem model inputs were obtained. The chapter concludes with the statistical and analytical methods used to determine the effects of LAI on modeled NPP, including both simulation modeling and analyzing the variability in both LAI and NPP results for this study area.

3.2 Study Area and Data Set

3.2.1 Kananaskis Study Area

The study area is centered at 115°4'20"W, 51°1'13"N straddling Barrier Lake within Bow Valley and Bow Valley Wildland Provincial Parks in Kananaskis Country, Alberta, Canada (Figure 3-1). It is situated in a montane region on the eastern slopes of the Canadian Rocky Mountains. This region covers approximately 77 km^2 with a full range of terrain aspects and slopes. The elevation of the study area ranges from 1400m (Barrier Lake) to 2000m (top of Prairie View). The study area lies within the Montane Natural Subregion of southwestern Alberta, which is characterized by patterns of open forests and grasslands with a very diverse understory vegetation (Archibald et al., 1996). Dominant softwood tree species in the area include lodgepole pine (*Pinus contorta* var. *latifolia* Dougl ex. Loud.), white spruce (*Picea glauca* (Moench) Voss), Engelmann spruce (*Picea engelmannii* Parry ex Engelm.), Douglas-fir (*Pseudotsuga menziesii* (Mirb.) Franco), and subalpine fir (*Abies lasiocarpa* (Hook) Nutl.). The dominant hardwood tree species include trembling aspen (*Populus tremuloides* Michx.), and balsam poplar (*Populus balsamifera* L.), with lesser amounts of white birch (*Betula papyrifera* Marsh.). The sampled areas consist of different stand structures and compositions, which range from pure softwoods and hardwoods to mixedwood stands (Figure 3-2). The spatial distribution of the dominant tree species is based largely on terrain and proximity to a water body (Figure 3-2). The LAI measurements taken within these stands typically ranged from 0.84 to 7.77.

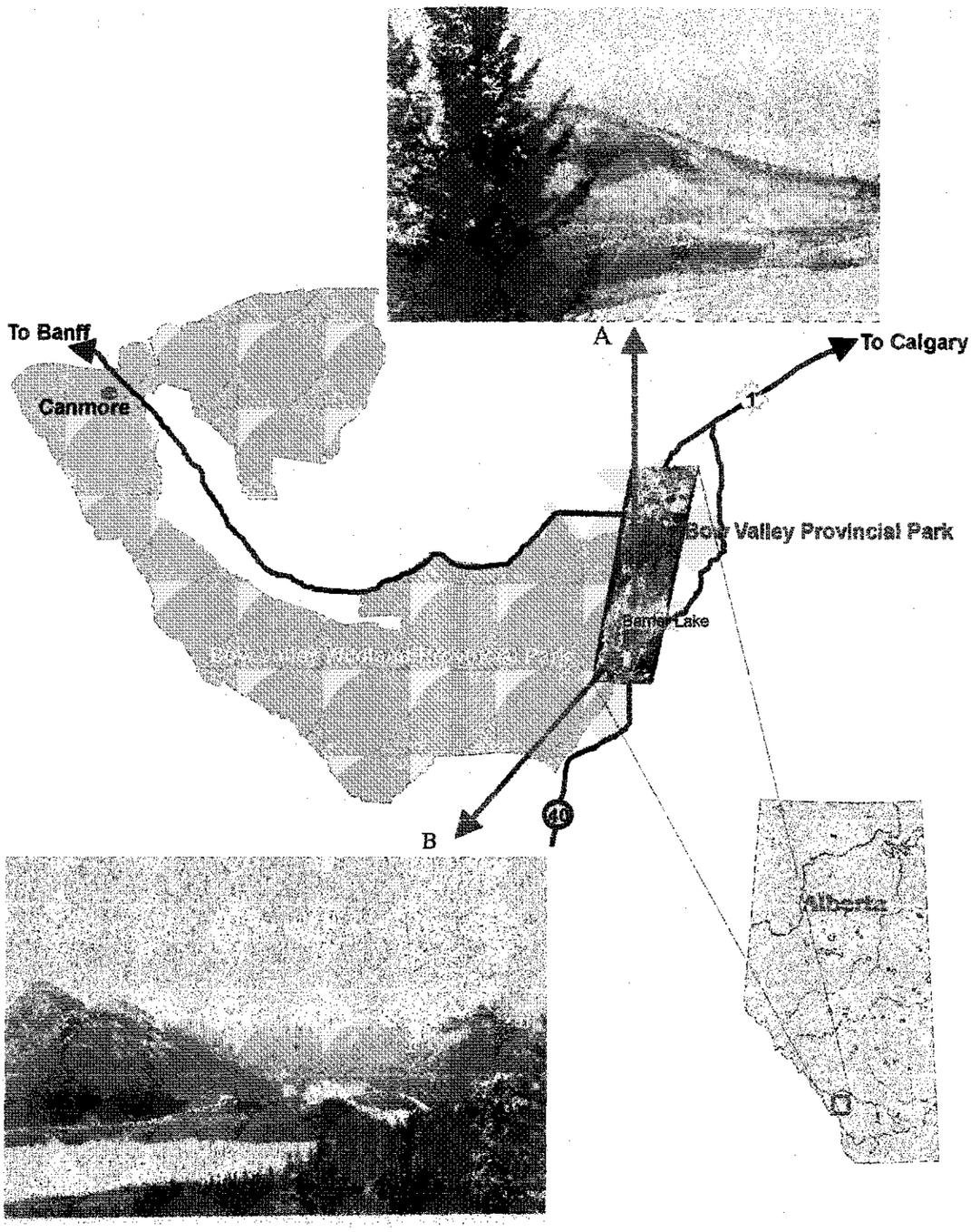

Figure 3-1 Study Area. The study area is located on the eastern slopes of the Canadian Rockies in Kananaskis Country, AB and is centered at 115 4'20"W, 51 1'13"N. Photo A is taken looking north across Barrier Lake from Highway 40. Photo B is taken from the CASI mounted aircraft looking south towards the end of Barrier Lake. Location of each photo is shown on the CASI image (see map inset).

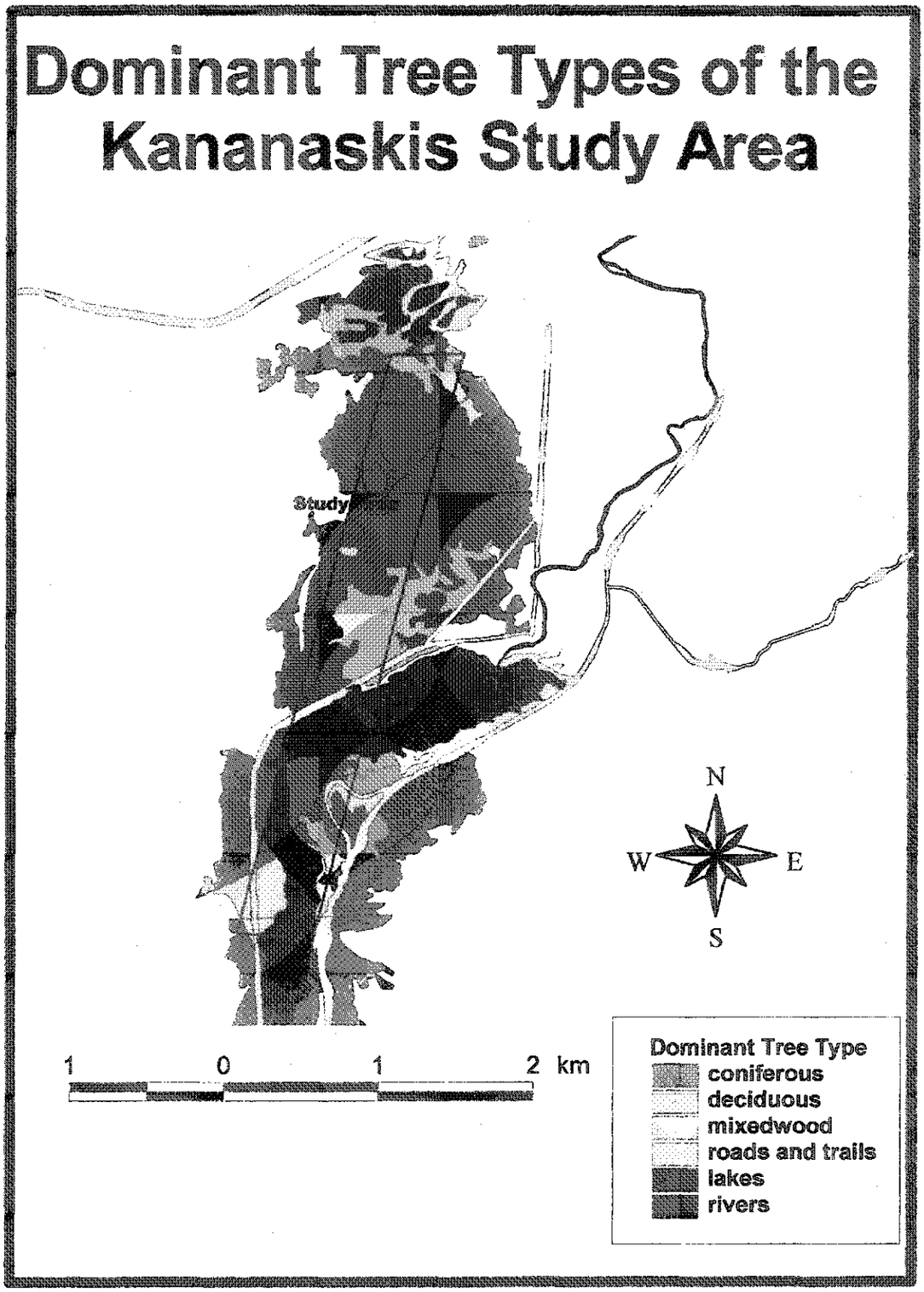

Figure 3-2 Dominant tree types in the Kananaskis study area based on classifications from the Alberta Vegetation Inventory (AVI).

3.2.1.1 Soil

Due to pronounced and complex changes in topographic and climatic conditions, the soil types within the Canadian Rockies are generally regarded as highly variable (Archibald et al., 1996; Crossley, 1952). Crossley (1952) studied the mountain soils of the Kananaskis Forest Experiment Station, which covers much of the same area as this study; however, the boundaries extended further east and south. Six soil classifications exist in the study area: alluvium, rendzina, brown and grey podzolic, brown forest and lithosolic (Figure 3-3). However, only brown and grey podzolic, brown forest and lithosolic soils are present within the field plots sampled. Brown podzolic soil has a light texture with only moderate leaching and usually supports coniferous forests. Grey podzolic soils generally exhibit a heavier texture due to parental materials and are more chemically fertile than the brown podzolic. Brown forest soil is generally more fertile than the other classes found within the study area. The main vegetation cover for the brown forest soil is aspen or balsam poplar. Lithosolic soils are stony shallow azonal soils frequently encountered on steep slopes and are characterized by stony thin brown podzols. This soil class is not conducive to tree growth; trees that do grow there have restricted room for the development of roots, resulting in an inadequate supply of soil nutrients. This soil also has a limited water storage capacity and may have excessive run-off. The location and depth of the various soils are dependent on both parental material and topographic location. Generally, steeper slopes have shallower soils due to wind erosion and runoff; thus many of the soils found on these slopes are lithosolic.

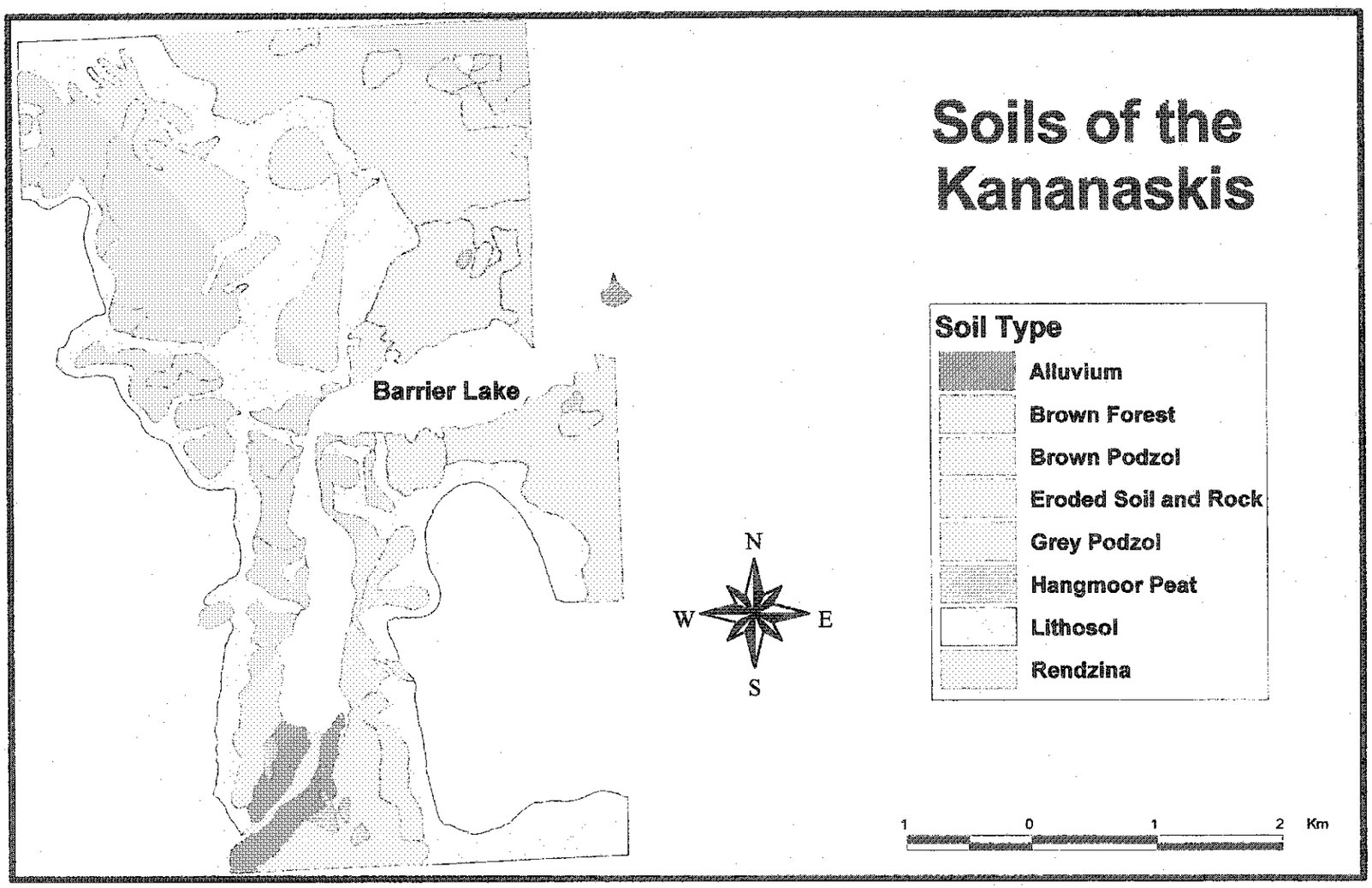

Figure 3-3 Soil Classification of the Kananaskis (taken from Crossley (1952))

3.2.1.2 Climate

The climate in this region is influenced by both the Cordilleran and Prairie climates. It has a mean summer temperature of 12°C and a mean winter temperature of -6°C based on data from 1939-1985 (Kirby, 1973; KCEED, 1995). Temperature extremes range from –45.6°C to 33.4°C. The average precipitation per year is 657.4 mm. Chinooks are common in this montane subregion with intermittent snow free periods during the winter (Archibald et al., 1996).

For this study, only the 1998 weather data were used corresponding to the year of image acquisition and fieldwork, and also since the study considered only annual increment of NPP. The weather data were obtained from the weather station situated at the University of Calgary, Kananaskis Field Station for the year 1998. The Kananaskis Field Station is located in a valley bottom at UTM coordinates 5654737.124 North and 637856.739 West with an elevation 1393.5 meters above sea level. Daily weather measurements were taken including maximum, minimum and average temperatures and precipitation. The weather conditions at the Kananaskis Field Station were similar to the norm in 1998 (Table 3-1). To be consistent with the nomenclature of the FOREST-BGC model the weather data for 1998 will be termed climate data it is however, acknowledged that climate refers to long term trends or patterns where as weather refers to more daily events.

Table 3-1 A summary of the 1998 weather data.

Weather Trend	Annual
Maximum Temperature (°C)	33
Minimum Temperature (°C)	-39
Mean Summer Temperature (°C)	14.8
Mean Winter Temperature (°C)	-6.3
Precipitation (mm)	875.6
Growing Season Precipitation (mm) (mid June – late August	603.0

3.2.2 Field Data Collection

3.2.2.1 Plot Location

Field plots were established to study and evaluate remote sensing information and ground-based forest biophysical parameters, and to develop ground truth information. Most of the plots were located along defined transects comprising three or more plots that coincided with the Compact Airborne Spectrographic Imager (CASI) airborne remote sensing flight lines (described later in this chapter). The middle of the surveyed transects (the middle of the flight line) were located approximately at the midpoints of each plot. Alberta Vegetation Inventory (AVI) maps and airphoto interpretation were used to assist in the location of transects and plots. The first plot of the transect was randomly selected to be greater than or equal to 3 times the stand height from the point of entry. To ensure an adequate spatial separation of plots the subsequent plot was located at 3 times the height of the present stand to ensure the LAI-2000 measurements were independent. The point of entry was generally from a trail or road. Each plot was also located to provide sufficient distance (approximately 3 times the height of the last plot) from the edge of the stand. Much of the fieldwork in 1998 was completed prior to the July 18 CASI image

acquisition date. In these cases the proposed center flight lines were used for the formation of transects (there was little deviation from this and the actual lines flown). Each plot was 10m x 10m, to be representative of the stand characteristics and to ensure that the number of pixels within each plot was adequate for each spatial resolution of CASI imagery (largest pixel =2m, resulting in a minimum of 25 pixels per plot). In total, 65 plots were established and oriented in a north-south direction to align the plot with the orientation of the north-south flight lines during image acquisition. The 1998 field season focused on the collection of pure and mixed conifer plots, while the 1999 field season focused on the collection of deciduous and mixedwood plots.

3.2.2.2 Field and Image Position

An important aspect to any remote sensing analysis is the ability to accurately locate field plots in an image for validation and testing purposes. A differential global positioning system (DGPS) was used in the field to obtain geographic position with a +/- 1 m accuracy. A Trimble Pathfinder Pro XL GPS was used to collect uncorrected GPS coordinates at each corner of the plots. These coordinates were then differentially corrected using the base station data collected simultaneously at the Kananaskis Field Station using Pathfinder Office 2.11 software. The corrected plot corner coordinates were overlaid on the CASI imagery and vectors were drawn to delineate plot area based on the 10mx10m plot size.

3.2.2.3 Forest Structural Data

The structural characterization of each stand was essential for studying the influence of LAI measures on process-based productivity estimates. Among the structural parameters measured were tree height, tree height distribution, diameter at breast height, stand density, and crown closure. Other variables collected at each plot, which aided in the characterization of the stands, were tree species, tree cores, slope and aspect, and descriptive plot maps of the location of each tree (stem maps). Tree heights were measured to the closest ½ or tenth of a metre using either a clinometer or a digital hypsometer, respectively. Diameter at breast height (cm) was measured at approximately 1.3m above the ground. The percentage of crown closure was estimated using both a spherical and GRS densitometer, and both measurements were averaged to produce a single plot estimate. Tree cores were collected from a representative number of trees within each plot. Two cores were extracted from breast height for each tree at right angles from each other. The number of trees cored was a function of the tree species present. Two cores were collected from the dominant species within the plot, and one core for each of the subordinate species. Stem maps were produced for each of the plots using locations determined relative to the marked corners. These maps were also used to aid in the identification of plot locations on the imagery. Forest structural data and plot characteristics are presented for each of the species in section 4.2.

3.2.2.4 Endmember Spectra Collection

A spectral library was built for the Kananaskis Region where the dominant canopy and understory species were identified. Spectra were collected using an Analytical Spectral Devices (ASD) spectroradiometer for each of the species with

illumination for both sunlit and shadow, using the portable field laboratory in Peddle (1998). The ASD spectroradiometer used in this research is a full range instrument (350-2500 nm), which takes spectra at 1nm spectral resolution. Samples were removed from the forest stands and measured in an open parking lot to avoid the influences of variable canopy shadowing and understory signals (Johnson, 2000). Tree canopy samples were arranged into optically thick stacks to ensure a pure measurement of a single species. To use the 1nm spectra with the imagery, endmember values were derived for the image bandwidths based on the spectral response function for each band of the CASI sensor. To create shadowed illumination, a sheet of plywood was used to block all direct sunlight onto the samples. All radiance measurements were corrected to reflectance using a coincident spectral measurement of irradiance from a calibrated Spectralon panel.

3.2.3 Ground-based LAI Estimation Techniques

3.2.3.1 Allometric Techniques

The transition zone between the sapwood and heartwood was marked on each increment cores in the field where visible. For each of the trees, sapwood widths were averaged and sapwood area was calculated as the difference between the stem area at breast height and heartwood area. Stem area at breast height was calculated based on the diameter of each tree inside the bark. The diameter inside bark was determined based on diameter outside bark/ diameter inside bark (DOB/DIB) models for each species in Provincial Natural Region 9, which encompassed this study area (Huang 1994). Since it was not possible to core all the trees in every plot, extrapolation was needed to determine sapwood area for the entire plot. Using the various tree data, regression models were

built to relate sapwood basal area to tree basal area for each species within the study area. Due to the small sample size of balsam poplar, the balsam poplar measurements were merged with the trembling aspen measurements in a composite deciduous group. The regression models were built and tested through the production of a fitting and a validation sample to allow the independent assessment of the regression models for predicting sapwood basal area. The validation sample set was chosen randomly from each species, with ¼ of the species data used to ensure an appropriate sample size for both the validation and fit data sets. The regression models were built from the fit data set. The regression models were chosen based on the magnitude of the coefficient of determination (r^2), root mean square error, the standardized residual plots and the statistical significance of each model. CurveExpert 1.3 software was used to determine the best line fit for each of the species ($r^2$and RMSE), and then the best models were incorporated into SAS software to determine further statistics (standardized residual plots and statistical significance) for the statistical models chosen. The results of this statistical analysis are presented in Section 4.3. The statistical models were then applied to the uncored trees within the plots to determine a plot level sapwood basal area estimate. Leaf area of each stand was estimated using allometric equations of sapwood basal area to leaf area for montane ecosystems in the Rocky Mountains (Gower et al., 1987; Waring et al., 1982; Kaufmann and Troendle, 1981) (Table 3-2). Absolute LAI measurements were not available since destructive sampling was illegal in the study area. Therefore, it was not possible to assess the published allometrics as they applied to this study area. Species sapwood basal area was summed for each plot and the coefficients related to the

separate species were applied. The summed leaf area was then divided by the plot ground area of 100 m^2 (10m x 10m) to determine LAI for each of the plots.

Table 3-2 – Literature cited for projected leaf area to cross-sectional sapwood area values. (Taken from White et al., 1997)

Species	**Common Name**	**Leaf area/sapwood area (m^2cm^{-2})**	**References**
Pinus contorta	Lodgepole pine	0.14	Gower et al., 1987
Picea engelmanni	White Spruce	0.34	Waring et al., 1982
Pseudotsuga menziesii	Douglas-fir	0.35	Gower et al., 1987
Populus tremuloides	Trembling Aspen	0.10	Kaufmann and Troendle, 1981

3.2.3.2 Hemispherical Photography

Hemispherical photos were taken at or near the centre of each plot. Five photos using 400 ASA Fuji NPH film were taken per plot with an aperture of F/8 at 5 shutter speeds (1/60s, 1/125s, 1/250s, 1/500s, and 1/1000s). From these bracketed exposures, the photos with the highest contrast between sky and canopy were digitally scanned using a HP 4C 600 dpi optical scanner. Plot LAI estimates from the digitized photos were obtained using the Gap Light Analyzer (GLA) software (Frazer et al., 1999), which includes terrain corrections based on local slope and aspect inputs.

3.2.3.3 LAI-2000

For each plot, overstory LAI was measured using the LAI-2000 at 8 locations within each plot. An outside canopy measure was also taken in an open field immediately prior to the measurements in the plot to simulate an above canopy measurement. Measurements were taken on overcast days or the operator shadowed the

sensor to prevent direct sunlight from reaching the sensor. The LAI-2000 values were post processed using manufacturer provided software to calculate LAI (Licor Inc., 1990). To minimize the effects of slope, either the last ring (61-74°) or the last two rings (61-74°, 47-58°) were removed during the calculation of effective LAI. The last two rings were manually scrutinized to determine if the PAR measurements fell between the ranges found in the earlier three rings. If this criterion was not met, the values were removed and LAI was recalculated.

3.2.3.4 TRAC

Using the TRAC, ten transects of 10m length each were established within each 10m x 10m plot at approximately 1m spacing and oriented perpendicular to the solar plane. Measurements were collected by walking at a rate of approximately 0.3 m/s. Measurements were taken on sunny days with no cloud cover. The TRAC values were post processed using manufacturer provided software to determine both clumping index and LAI (Chen and Kwong, 1997). A topographic normalization was completed by using a ratio between the depth of the canopy on flat ground to the depth of the canopy on sloped ground (Chen pers. comm., 1999). Canopy depth and slope were measured within each plot, and geometric principles were applied to determine canopy depth on sloped ground at the solar zenith angle measured by the TRAC. The ratio was then applied to the TRAC LAI estimates for each plot.

3.2.3.5 Integrated LAI-2000 and TRAC

The integrated approach was applied to each of the plots using the slope adjusted effective LAI estimates from the LAI-2000 and the clumping index from the TRAC (Equation 2-3) (Chen, 1996b). Woody-to-shoot ratios were not available for this region so instead ratios for the same or closely related species were obtained from the literature (Chen, 1996b). Ratios for jack pine were used for lodgepole pine, black spruce ratios were used for white spruce, and aspen ratios were used for trembling aspen and balsam poplar as measured from the BOREAS study area in Saskatchewan and Manitoba, using destructive sampling of entire trees. The needle-to-shoot ratio (Ve) is the ratio of half the total needle area in a shoot to half the total shoot area, to account for only the projected leaf area not total leaf area. This value was calculated in the field using the mean width and length of six randomly selected needles from each species. The clumping index (Ω) was obtained using the TRAC. No slope alterations were needed here as the incorporated LAI-2000 and TRAC data had already been adjusted for slope effects.

3.2.3.6 Summary of Ground-Based LAI Data

In total, 5 LAI estimation methods were evaluated for 4 species classes. All LAI measurements for a given plot were taken within a week of each other to ensure minimal effects from possible changes in phenology. No absolute measures of LAI were obtained in the field due to monetary, time and legal constraints. Thus a relative comparison of the ground-based LAI estimates was completed, as described later. Although, absolute measures of LAI from destructive sampling would be ideal for both comparison with the ground-based optical instruments and remote sensing validation, issues surround the

measurement of LAI for use with remote sensing. It should be noted that absolute measures of LAI coincident with the pixel spatial resolution of airborne or satellite sensors is difficult and often impractical or impossible. Often pixel resolution is beyond that of the achievable measurements of LAI, due to time or monetary constraints in destructive sampling. As well positional control issues arise for relating field measurements with the exact corresponding pixel within an image, especially where field sampling is performed prior or independent of the imagery acquisition. Even with absolute measurements of LAI for remote sensing validation relations between LAI and remote sensing are compromised by issues of spatial scale, positional accuracy and field sampling. The comparison of the plethora of optical instruments and allometrics attempt to balance the lack of absolutes with a large number of field methods for estimating LAI.

3.2.3.7 Ground-based LAI Estimation Experimental Design

Comparisons of some of the ground-based LAI estimation techniques has been completed, however, a comparison involving a multitude of optical and allometric techniques in a montane environment has not yet been attempted. By quantifying the differences in the ground-based LAI estimation techniques it will aid in the determination of the species-specific limitations of the various techniques and determine the viability of these techniques to this montane study area. Forty-two plots were chosen within the four stand compositions (lodgepole pine, white spruce, mixedwood, and composite hardwood). Within each of these plots, LAI or eLAI estimates were made using each of the optical instruments and allometric techniques described earlier. Slope normalization procedures were implemented during data collection and processing for each instrument. Although, the differences between eLAI and LAI has been acknowledged these terms

will be combined under the term LAI, as many studies refer to the estimates of the LAI-2000 and hemispherical photography as LAI (Fassnacht et al., 1994; Gower and Norman, 1991). Means and standard deviations were calculated for LAI estimates from each instrument and species. A statistical comparison for LAI by instrument and species was then performed, as described in section 3.6.

3.2.4 Remote Sensing Imagery

3.2.4.1 CASI Airborne Data

A multi-spectral Compact Airborne Spectrographic Imager (CASI) (Anger et al., 1991) from Itres Research Ltd. in Calgary, Alberta was used for the imaging of the study area from a fixed-wing aircraft. The CASI instrument is a visible-near infrared (VNIR) pushbroom imaging spectrometer with a spectral range between 400 nm and 1000 nm. The ground coverage and pixel size for the CASI imagery were determined by the altitude above the ground and the speed the aircraft was flying. The CASI was used in a modified spatial mode configuration, in which bandwidths and band locations are fully programmable, with a maximum of 19 non-overlapping bands set within the sensor's spectral range. Three spatial resolutions of imagery (60 cm, 1 m, and 2 m) were flown between 9:30 and 13:00 on July 18, 1998. The mission day was optimal as there were clear skies with only a light wind. The timing of the mission was based on weather, solar position, local terrain effects and image properties. The azimuth of the sun in the morning avoided large shadows cast by nearby mountains onto the study area. The larger solar zenith angles in the morning also increased canopy shadow, and reduced the effects of the background on the images. In mountainous terrain during favourable summer

weather, clear skies are generally more likely in the morning. The 2 m and 1 m data consisted of 18 bands, whereas the 60 cm had only 8 bands due to sensor integration time limitations. For this study, the 2 m imagery was used to reduce the processing time and to relate the LAI and the NPP modeling to a larger area. However, to facilitate the incorporation of SMA into this study, a validation of the spectral endmembers using the 60 cm data was required, therefore, the 2 m data needed to be reduced to the same bands available at the 60 cm (Johnson, 2000) (Table 3-3). This reduction of bands was completed using a weighted average of bands from the 18 bandset that matched the 8 bands presented in Table 3-3. Further image acquisition and flight planning information is available in Johnson (2000).

Table 3-3 – Reduced 2 m CASI image band set.

Band Number	Wavelength (nm)
1	450-500
2	540-560
3	610-640
4	640-680
5	690-715
6	730-755
7	790-810
8	850-875

3.2.4.2 Image Preprocessing

Itres Research Ltd. performed a geometric correction to account for distortions caused by aircraft orientation (e.g. pitch and roll) during image acquisition. Real-time altitude measurements were recorded on the aircraft using an Inertial Navigation System (INS) and locations were recorded using an onboard GPS system to facilitate the

geometric correction. Itres Research Ltd. also digitally resampled the image to remove the variation in pixel resolution across the mountainous terrain.

Empirical radiometric normalization was performed at the University of Lethbridge to account for atmospheric variations using 4 pseudo-invariant targets set up at a radiometric calibration site in a parking lot near Barrier Lake (Johnson, 2000). Ground-based reflectance values were determined for each of the pseudo-invariant targets and also for asphalt using an ASD field spectroradiometer and adjusted to the 8 CASI image bands using a linear spectral response function. A transformation function was computed between the CASI radiance data acquired over the radiometric calibration targets and the ground spectral reflectance measurements. This transformation function was then used to correct the CASI image to reflectance.

3.2.4.3 Terrain Normalization

An added dimension to the determination of LAI through remote sensing was the influence of mountainous terrain on the sun/sensor/surface geometry and therefore the spectral response patterns in the image. Both the slope and the aspect of a given pixel can cause radiometric distortion. Terrain correction methods have been derived to reduce the slope and aspect induced illumination variations within an image. Illumination is defined as a function of the cosine of the incident solar angle; thus this is dependent on the orientation of the pixel towards the sun's position (Meyer et al., 1993). There are four different illumination-based terrain normalization methods: Cosine Correction, Minnaert Correction, C-correction and Statistical Empirical Correction (Teillet et al., 1982). Johnson (2000) showed that terrain normalization can result in improvements to

the prediction of LAI. Meyer et al (1993) reported the C-correction provided the most increase in forest stand type classification accuracy compared to the other terrain normalization methods. Based on ease of implementation and the results of Meyer et al. (1993), the C-correction was selected for terrain normalization of the imagery and performed by Johnson (2000).

The C-correction uses a trigonometric approach that accounts for the proportion of direct illumination based on slope and aspect with an additional c parameter that emulates path irradiance (Teillet et al., 1982). The calculation of the c parameter is based on a linear regression between the original digital number collected by the sensor and the cosine of the solar incident angle in relation to a normal pixel (I). The equation is as follows:

$$LH = LT \frac{\cos(SZA) + c}{\cos(I) + c}$$

where: (Equation 3-1)

LH = radiance observed from a horizontal surface

LT = radiance recorded by the sensor

SZA = solar zenith angle

I = solar incident angle in relation to a normal pixel

c = correction parameter

c = b/m

m = slope of regression line

b = y intercept

3.2.5 Digital Elevation Data

The Miistakis Institute for the Rockies (MIR) supplied the digital elevation model (DEM). The initial DEM was from the Government of Alberta provincial database as compiled photogrammetrically from 1: 60 000 scale airphotos (Altalis, 1999). Further post processing was done by the MIR to remove or minimize data errors. The final spatial resolution of the DEM was 25 metres based on the original 1000m spacing. Although not ideal, the DEM was resampled to 2m to facilitate the required image preprocessing including image radiometric correction by Itres Research Ltd. and terrain normalization by Johnson (2000).

3.3 Remote Sensing LAI Estimation Comparison

3.3.1 Vegetation Indices

NDVI, WDVI and SAVI were computed from the 2 m image using the equations in Table 2-2. Since these indices require two bands (red and near infrared) the CASI data were first transformed using a weighted average of the bands that fell within the red and near infrared wavelengths. The soil or background spectral component reflectance value needed for WDVI and SAVI was the same as that used in the spectral mixture analysis described in section 3.4.2.2. Each vegetation index was computed for the entire study area. To obtain the same area of measurement as the ground-based LAI for each plot, the vegetation index values were aggregated to the plot scale by averaging the pixels over the 10m x 10m plot area. Linear relationships were produced between the aggregated vegetation index values, the different species types (coniferous, deciduous, and

mixedwood) and ground-based LAI instruments. Linear relationships, rather than more complex relationships, were developed to help simplify the remote sensing algorithms for application to regional scales (Chen, 1996a). More recently, however, Fernandes et al. (2001) showed that the use of linear relationships might not be appropriate. Regressions on transformed data including log and power transformation provided better results (Fernandes et al., 2001). However, for this research only the linear relationships will be use due to application ease and comparisons of these results with other studies.

3.3.2 Spectral Mixture Analysis

The three main scene components for this forestry study area are sunlit canopy, sunlit background and shadow. The endmembers were chosen from a spectral library of spectra measured in the field, using an ASD spectroradiometer including those from Johnson (2000). The sunlit canopy endmember was the spectra for either lodgepole pine, white spruce, or Douglas-fir depending on the species composition of the plot recorded in the field. Only conifer endmembers were tested and validated in this area for the use with spectral mixture analysis (SMA), therefore these results did not encompass the deciduous plots as the validation and testing of the endmembers was not available. The background endmember was obtained using spectroradiometer measurements of the aggregated background found on the forest floor including pine grass (*Calamagrostis rubescens* Buckl.), step moss (*Hylocomium splendens* (Hedw.) B.S.G.), and buffalo berry (*Shepherdia canadensis* (Nutt) L.). The shadow endmember was the darkest apparent reflectance of canopy or background within any of the field samples. The apparent reflectance (Peddle et al 2001; Miller et al 1997) of the canopy and background targets

was determined from spectral measurements of the targets in complete shadow, with respect to an illuminated and calibrated reference panel. In this study, the apparent reflectance of pine grass spectra was used as the shadow endmember reflectance. These estimates like the vegetation indices were aggregated to 10m x 10m so that linear regression equations could be built at the plot scale for SMA and ground-based LAI estimates.

3.4 Ecosystem NPP Model Parameterization

3.4.1 Model Inputs

FOREST-BGC/BIOME-BGC was chosen for this study as it has been validated for forests in Montana, Florida, and Alaska suggesting that this is a robust model that can be used in a multitude of environments. It can be used for both local and plot level estimates of NPP and also be expanded to regional scales. It was also one of the foremost models, upon which many other models were based such as BEPS (Liu et al, 1997) and Regional Hydro-Ecological Simulation System (RHESSys) (Nemani et al., 1993). FOREST-BGC continued to be improved through the validation and testing of each of its functions (Running and Gower, 1991; Nemani and Running, 1989; Running and Coughlan, 1988). It is relatively easy to parameterize and run. The four important parameters that drive the FOREST-BGC/BIOME-BGC NPP model are leaf area index, climate data, soil water content and species physiology (Running and Hunt, 1993; Running and Coughlan, 1988). All these measures can be determined in the field, calculated from existing field data, or obtained from the literature. These model input parameters will be discussed in each of the next four sections.

3.4.1.1 LAI

LAI was incorporated into the model as foliar carbon, which is calculated as a function of specific leaf area and LAI. Specific leaf area (SLA) is the amount of leaf area per unit leaf mass and can be attained from the literature (Running and Hunt, 1993). For coniferous species a SLA constant of 25 m/kg was used, for deciduous a SLA constant of 75 m/kg was used (Running and Hunt, 1993). Foliar carbon is calculated using the following formula (Kimball pers. com, 2000):

$$\text{Foliar carbon} = \frac{\text{LAI}}{\text{SLA}} \qquad \text{(Equation 3-2)}$$

Each of the ground-based LAI estimates were transformed into foliar carbon and the foliar carbon values for each plot were incorporated into the FOREST-BGC model. The equations for the statistically significant ($p<0.05$) regression models of the SMA and vegetation indices with ground-based LAI estimates where applied back to the aggregated 10 m image producing a remote sensing estimate of LAI for each plot. The remote sensing LAI values were then imported into BIOME-BGC as the transformed foliar carbon.

3.4.1.2 Climate

To produce plot specific climate data, the base station data from the Kananaskis Field Station were processed through the mountain microclimate simulator (MTCLIM) (Hungerford et al., 1989). Snowpack was calculated as the accumulation of snow water equivalent for an average of 10 years from 1989 to 1998 for the period between October

(or first day of snow) to April 1st as per Running and Nemani (1991). Site isohyet (precipitation contour) was based on the linear relationship developed by Shepard (1996) relating isohyet to elevation for the eastern slopes of the Canadian Rockies. East and west horizons were determined based on the DEM.

3.4.1.3 Species Physiology

Each plot was assigned a species type depending on the basal area of the trees found within each plot. To maintain the simplicity of BIOME-BGC it does not incorporate species-specific information. The model instead only requires a more general discrimination of the species into coniferous or deciduous stands (Table 2-1). For the mixedwood plots a first order NPP estimate was made by using a weighted estimate from the percentage of coniferous and deciduous species based on their respective basal area within each plot.

3.4.1.4 Soil Water Content

A soil classification is generally available for much of Canada, however, available soil water content is generally not measured. Therefore, to determine the soil water content for the region, estimates were made from the soil classes and the general soil water volumes for each soil texture taken from Brady and Weil (1999) (Table 3-4). Available water content was determined as the mid point between field capacity and wilting coefficient. Crossley (1952) describes in detail each layer of the soil classes including, a description and depth of each layer (Figure 3-5). The soil water content (m^3/ha) for each layer was calculated as the depth (cm) multiplied by the available soil

water (%). To determine the available soil water content for each of the plots, the soil water content for each layer was summed to a depth of 100 cm or the maximum rooting depth (Running, 1994; Running and Nemani, 1991).

Table 3-4 – The field capacity, wilting coefficients, and available soil water content, all in volume % for general soil types in North America.

Soil Type	Field Capacity	Wilting Coefficient	Available Water Content
Sand	9.2	2.5	5.85
Sandy loam	20.0	6.8	13.4
Loam	29.5	11.1	20.3
Silt loam	36	14.2	25.1
Clay loam	38.2	18.5	28.35
Clay	38.2	21.5	29.85

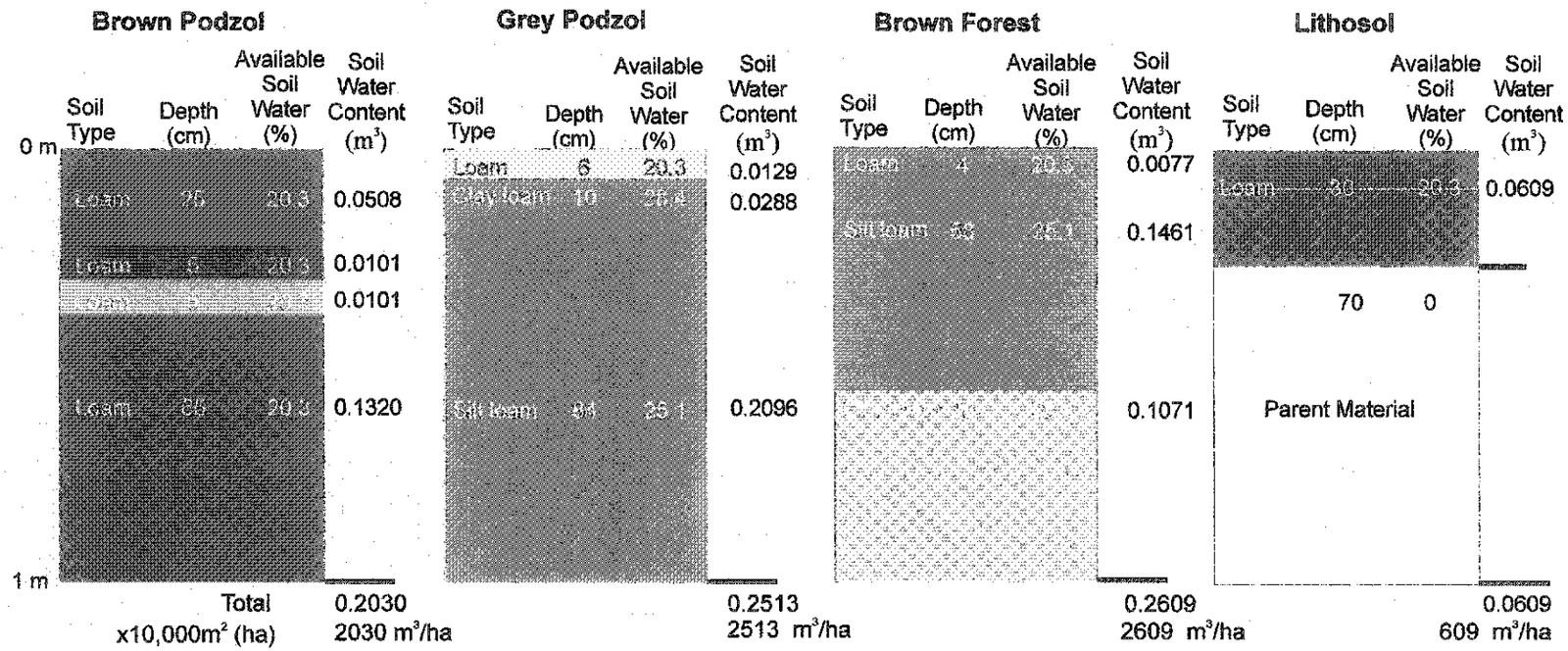

Figure 3-5 Description of each of the soil classes for the Kananaskis (from Crossley, 1952).

3.4.2 Plot Level NPP Model Sensitivity to LAI

To determine the effects of LAI, climate, soil water content, and vegetation changes on the estimation of NPP, values were simulated for each of these variables within the range measured for the study area and plotted using the same NPP axes on the graph, to allow direct visual comparison. Other model input variables were held constant with values used from a representative spruce plot, which was the dominant coniferous species type and had equivalent measurements to the mean LAI, tree height, and basal area of stands within the study area. Further comparisons of different species and plots were performed yielding similar results to the representative spruce plot, therefore only the spruce plot will be presented. The ranges of LAI obtained from each species and instrument were from a minimum of 0.5 to a maximum of 7.77. The soil water content ranged from 609.00 m^3/ha for a lithosolic soil to 2609.00 m^3/ha for a brown forest soil as defined in the section 3.5.1.4. The elevations tested were between 1375m and 1649m as the minimum and maximum plot elevations. Elevation was tested as it affects the microclimate of the study area, thus in essence a change in elevation can result in a change in microclimate. For example, as elevation increases, the temperature drops and precipitation may increase. The climate effects can be further broken down beyond elevation (i.e. precipitation, temperature, snowpack) however, for this study the climatic influences will be tested through elevation only to provide a generalized estimate of climate change over the study area.

By comparing the magnitude of variation in LAI and NPP, the importance of LAI in modeled NPP can be assessed. To determine if the variation in LAI measurement was similar to the NPP variation, two methods were used. The first was stack graphs of each

of the modeled NPP means and standard deviations for the different species, instrument and remote sensing types so that the patterns of NPP and LAI can be compared. In the second method, coefficients of variation were determined for each of the ground-based estimates and the remote sensing estimates of LAI and NPP, so that the variation in both could be standardized and compared. The coefficients of variation for LAI and NPP for the separate species and instruments were plotted together for visual assessment of the variation in each. Details of the statistical analysis are provided next.

3.5 Statistical Methods

For the comparison of ground-based LAI estimation techniques for species and by instrument, a factorial analysis of variance (ANOVA) was performed. An ANOVA is a comparison of two or more means to determine if there is a statistically significant difference among the various factors (Sall and Lehman, 1996). A factorial ANOVA is an analysis where there are many factors where, for each factor, there are different levels (Steel and Torrie, 1980). For example, in the case of the LAI comparisons, instrument and species are the factors and the levels within the factors are the different LAI instrument and different species types. Therefore, a factorial experiment is one that consists of all possible combinations of levels within a factor for the different factors (Steel and Torrie, 1980). The primary outcome obtained through using an ANOVA is to determine if the differences in response to the level of one factor are similar or different at different levels of another factor (Steel and Torrie, 1980). However, a cross effect or an interaction may occur between the factors, in that each factor affects the response differently depending on the level of the other factor within the model (Sall and Lehman,

1996). In that case, the response of the model is not only the sum of the separate factors but also a combination of the factors.

A two-way (two factors) factorial analysis of variance with interactions between LAI instrumentation and species type was conducted with SPSS software to determine if LAI values differed among estimation methods. Interaction terms were initially introduced into the model, however, if these terms were not statistically significant, they were removed and the model was run again without the interaction term to increase the degrees of freedom assigned to the residual error term. If a statistical difference is found by the ANOVA, further testing was pursued. To determine which levels among the factors were statistically different, a comparison of all the pairs was done using a Student-Newman-Keuls (S-N-K) multiple-mean comparison test. The S-N-K test compares the minimum and maximum means within the factor and if the range is not statistically significant further testing is not completed and the levels are regarded as homogeneous (Steel and Torrie, 1980). If the range is statistically significant, further testing is completed and levels that are statistically similar are categorized into groups. All statistical tests in this study were conducted at the 5% probability level.

The comparison of LAI prediction techniques was based on the linearity of each of the vegetation indices and the SMA fractions with respect to LAI. The comparison of models was based on the magnitude of the coefficient of determination (r^2), root mean square error, the standardized residual plots and the statistical significance of each model. The coefficient of determination (r^2) measures the proportion of the total variance explained by fitting the model. As the r^2 values approaches 1, a greater proportion of the variance is explained by the model, and similarly, as the r^2 values approaches 0, less

variance is explained. The root mean square error (RMSE) is defined as the positive square root of the residual mean square term. The smaller the RMSE, the better the model fit. The standardized residual plots are the residuals from the regression or the difference between actual and predicted values (Sall and Lehman, 1996). The residuals would be expected to be scattered randomly around the mean of zero if there is no bias in the model.

To determine if the variation in LAI is proportional to the variation in modeled NPP, a coefficient of variation was used for both LAI and NPP. The coefficient of variation (CV) is a quantity used to evaluate results from different experiments (Steel and Torrie, 1980). The CV is calculated as the standard deviation divided by the mean multiplied by 100. The CV is a relative measure of variation, unlike standard deviation where the units of standard deviation are the same as the observed measures. Thus the CV is a unitless measure that can be used to compare the variance from different experiments.

3.6 Chapter Summary

In this chapter, three separate tests were described for: (1) the comparison of ground-based LAI estimation techniques, (2) the comparison of remote sensing LAI estimation techniques and (3) to determine the effects of different LAI estimates on modeled NPP estimates. The first set of tests assess the variability of the ground-based estimates of LAI from different instruments or allometrics for different species types. This test was designed to quantify the differences and assumptions among the various ground-based instruments and the effects of species type on LAI output. The second set of tests were to

assess the remote sensing estimates of LAI for deciduous, coniferous and mixedwood tree types by comparing three vegetation indices with spectral mixture analysis in terms of the ability to predict LAI. The final set of tests were designed to assess the relative variability between LAI and NPP using two graphical techniques. This method was designed to characterize the relationship between LAI inputs and modeled NPP outputs, and to determine if their relationship was proportional.

CHAPTER IV

4.0 Results and Discussion

4.1 Introduction

In this chapter the results of the analysis from this research are presented and discussed. The chapter is organized according to the three thesis objectives (section 1.1). The first objective, the ground-based LAI estimate comparison, is intended to determine the relative differences in both the optical instruments and allometric techniques for each species types assessed through an analysis of variance. This analysis is directed at improving knowledge about the differences in LAI estimation techniques. The second objective involves estimation of LAI from remote sensing for deciduous, coniferous and mixedwood species based on linear regression analysis. This approach defines relationships between forest structural and spectral information for estimating LAI for input into regional scale NPP models. The third objective is to assess the effects of LAI variability on FOREST-BGC's NPP output, through model simulations of the key variables (LAI, soil water content, and climate). These are intended to determine the effects that each of the variables may have on the NPP output, and to determine if the variability in LAI was similar to the variability in modeled NPP. By quantifying the effects of LAI on NPP insights can be derived about how FOREST-BGC uses the estimated LAI parameter and what margins of error can be tolerated in LAI estimation from remote sensing.

4.2 Stand Mensuration Information

Since plots were chosen to incorporate representative stands of the four species types, the stands were first evaluated with descriptive statistics by species. White spruce had larger basal areas and tree heights while having smaller stem densities compared to the other species (Table 4-1). It would follow that larger basal areas and tree heights would inhibit the penetration of light to the forest floor. Those trees that are already established will out-compete other trees for light energy, thus reducing the stem densities within a stand due to lack of light for establishment and growth (Kimmins, 1997). Lodgepole pine stands were characterized by small basal areas, stem densities and tree heights (Table 4-1). Lodgepole pine species are highly adaptable and tolerant of low nutrient and moisture conditions (Johnson et al., 1995). However, the development in low nutrient conditions may inhibit growth, which may be the case in this study with small basal area, stem densities and tree heights. Both mixedwood and hardwood stands had highly variable crown closures with similar basal areas (Table 4-1). Mixedwood stands had the highest stem density and relatively taller trees that may be due, in part, to the composition of the mixedwoods being made largely of white spruce and deciduous species. The hardwood species had similar tree heights compared to the lodgepole pine, however, they also had larger stem densities and basal areas (Table 4-1). White spruce occurred on elevations that were higher than the other species. All species were represented at lower elevations, while at higher elevations not all species occurred. Hardwood species were the only one that did not occur on slopes greater than 15^{o}. Balsam poplar generally inhabited the valley bottom close to Barrier Lake, as these hardwood species thrive in moist/wet sites (Johnson et al., 1995). Aspen stands grow the

best in well drained moist loamy soils (Johnson et al., 1995). The hardwood trees had denser understory vegetation followed by mixedwood, lodgepole pine, and white spruce largely due to the light penetration through the canopy. Terrain, competition for light, the availability of water and nutrients, and plant-environment interactions all contributed to the structural development and characteristics of the various stands.

Table 4 -1 Summary of Descriptive Statistics for Field Plot Data by Cover Type.

	Lodgepole Pine	**White Spruce**	**Mixed-wood**	**Hardwood**
No. of plots	8	7	15	12
Min. Crown Closure (%)	25	46	29	26
Max. Crown closure (%)	52	66	80	75
Average stem density (stems/ha)	2200 (810)	1600 (510)	2900 (1100)	2600 (310)
Average tree height (m)	12 (1.38)	20 (1.60)	14 (5.42)	12 (3.10)
Average Basal area (m^2/ha)	30.07 (9.91)	51.79 (15.81)	37.31 (13.59)	38.23 (16.85)
Min. elevation (m)	1369	1315	1315	1374
Max. elevation (m)	1435	1642	1390	1552
Min. slope (degrees)	5.16	0.14	1.43	2.86
Max. slope(degrees)	36.16	33.46	40.5	14.95

4.3 Sapwood Extrapolation from DBH

An extrapolation of species-specific sapwood area from tree basal area was required based on a subsample from each plot because the measurement of sapwood area for each tree within the plot was prohibitively costly and time consuming. Two types of models were used: (i) a general linear model for Douglas-fir and (ii) a saturation growth

rate model for lodgepole pine, white spruce, and deciduous. The production of the model equations was based on the strongest model (highest r^2 and lowest RMSE) that characterized the patterns found within the data. All models were built from sample sizes greater than 40, had a coefficient of determination (r^2) greater than 0.83 and relatively small standard errors (Table 4 –2). These equations were applied to the validation data set for which a very strong relationship was observed (Appendix A).

Table 4-2 – Regression models for the prediction of species-specific sapwood basal area (SA) from tree basal area (BA) (cm^2) determined through area estimates from DBH.

Species	**Common Name**	**N**	**r^2**	**RMSE**	**Equation (cm^2)**
Pinus contorta	Lodgepole Pine	54	0.91	34.08	$SA = \frac{706.8689(BA)}{(986.6348 + BA)}$
Picea glauca	White Spruce	44	0.84	47.60	$SA = \frac{1742.1374(BA)}{(2559.8276 + BA)}$
Pseudotsuga menziesii	Douglas-fir	41	0.84	21.98	$SA = 0.8870 + 0.2993(BA)$
Deciduous (*Populus tremuloides* & *P. balsamifera*)	Deciduous (Aspen and Poplar)	64	0.83	40.87	$SA = \frac{-528.8743(BA)}{(-1266.7565 + BA)}$

4.4 Comparison of Ground-Based LAI Estimates

LAI estimates among the different species and instruments were different for each stand (Table 4 -3). White spruce had the highest LAI estimates of all the instruments used, followed by the mixedwood, hardwood and lodgepole pine, respectively (Table 4 - 3). The variation in LAI may be due, in part, to species type and stand structural attributes as well as the technique used to estimate LAI. The TRAC gave the highest

optical estimates of LAI for all species, followed by the integrated LAI-2000 and TRAC, LAI-2000, and hemispherical photography, respectively, however, the integrated approach produced lower estimates than the LAI-2000 in the hardwood stands (Table 4 - 3). Hemispherical photography and LAI-2000 produced the smallest estimates of LAI for all species, with the exception of the integrated estimates in the hardwood stands. Both the LAI-2000 and hemispherical photography do not account for gap size distribution (clumping index) thus a more conservative estimate of LAI would be provided by these instruments which is apparent in the lower estimates. It should be noted, however, that hemispherical photographs were taken only in the middle of each plot and may not be as representative of the stand as the LAI-2000. This may explain the empirical difference in LAI estimates between hemispherical photographs and LAI-2000. The TRAC produced the highest LAI estimates for the optical techniques (Table 4 –3), which may be due to using the clumping index and gap fraction as well as the measurement of gap fraction at a single zenith angle. For the optical instruments the TRAC exhibited the greatest variation around the mean for all species types (Figure 4–1). The clumping indices for all species showed relatively high values (Table 4–3, Figure 4 - 2). However, the clumping index values were larger in the white spruce stands followed by mixedwood, lodgepole pine and deciduous stands (Table 4 –3). Deciduous species are believed to have a random distribution of leaves, thus a clumping index value is not as important (Welles, 1990). However, in this study the deciduous species had a clumping index of 0.87, which is slightly smaller than the coniferous stands but still high enough to exhibit clumping within the canopy (Figure 4 –2). Other studies have also shown that a clumping index is also present in deciduous species (Chen et al., 1997b; Kucharik et al.,

1997). The integrated approach deflates the LAI estimate of the TRAC, while still incorporating both clumping index and gap fraction information at several zenith angles. The lower estimates of LAI calculated from the integrated approach as compared to the LAI-2000 for deciduous species may be due to the lower needle-to-shoot ratio (Ve) and clumping index (Ω) values.

Table 4 -3 LAI mean (and standard deviation) for each instrument or technique by species. The clumping index means (and standard deviation) from the TRAC are used in LAI estimates for the integrated approach and the TRAC.

	N	Hemi-spherical Photos	LAI-2000	TRAC	Integrated LAI-2000 and TRAC	Sapwood Area	Clumping Index
Lodgepole pine	8	1.22 (0.47)	1.53 (0.38)	2.62 (0.69)	1.75 (0.37)	2.54 (1.03)	0.89 (0.10)
White spruce	7	2.01 (0.61)	2.50 (1.03)	5.35 (2.03)	3.25 (1.32)	6.39 (1.49)	0.93 (0.07)
Mixedwood	15	1.85 (0.69)	2.39 (0.65)	4.86 (1.29)	2.67 (0.79)	3.74 (2.38)	0.90 (0.06)
Hardwood	12	1.66 (0.30)	1.75 (0.66)	3.51 (2.08)	1.69 (0.60)	2.29 (0.93)	0.87 (0.10)

The sapwood area/ leaf area gave the highest estimates of LAI for white spruce over the other optical instruments (Table 4 –3, Figure 4 –1). Sapwood area/leaf area estimates are lower than TRAC but greater than the other optical instruments for the lodgepole pine, mixedwood and deciduous species (Figure 4 –1). The sapwood area/leaf area estimates fall within the range of the optical instruments for all species except white spruce (LAI= 6.39 vs. LAI = 2.01-5.35) suggesting that this approach may provide first

order estimates of LAI if other techniques were unavailable. There is a large variation around the mean in sapwood area/ leaf area estimates for all species types (Figure 4 –1). The trends in these mean LAI estimates by instrument and species suggest that the differences in LAI estimation techniques and species type affects the resulting LAI estimates. This will be discussed further in section 4.4.1.

Chen et al. (1997a) found the mean LAI estimates from the LAI-2000 to be larger within black spruce (LAI=2.56) and mixedwood (LAI=2.60) sites than in aspen (LAI=2.19) and jack pine (LAI=2.12) within the BOREAS study area in Manitoba and Saskatchewan, Canada. This is similar to the results presented here, white spruce and mixedwood had greater LAI values than deciduous and lodgepole pine (Table 4 -3). White et al. (1997) reported coniferous (lodgepole pine, Douglas-Fir and western larch) and deciduous stands (aspen, paper birch and black cottonwood) within the mountainous terrain of Glacier National Park, Montana gave mean LAI-2000 estimates of 1.90 and 1.39 respectively. In this study area, coniferous stands (LAI = 3.25 for spruce and 1.75 for pine) generally had greater LAI-2000 values than deciduous stands (LAI = 1.69). From these comparisons, it was concluded that LAI values from this study area generally follow similar trends to that found in the literature for similar locations and species compositions reported in other studies in north central North America.

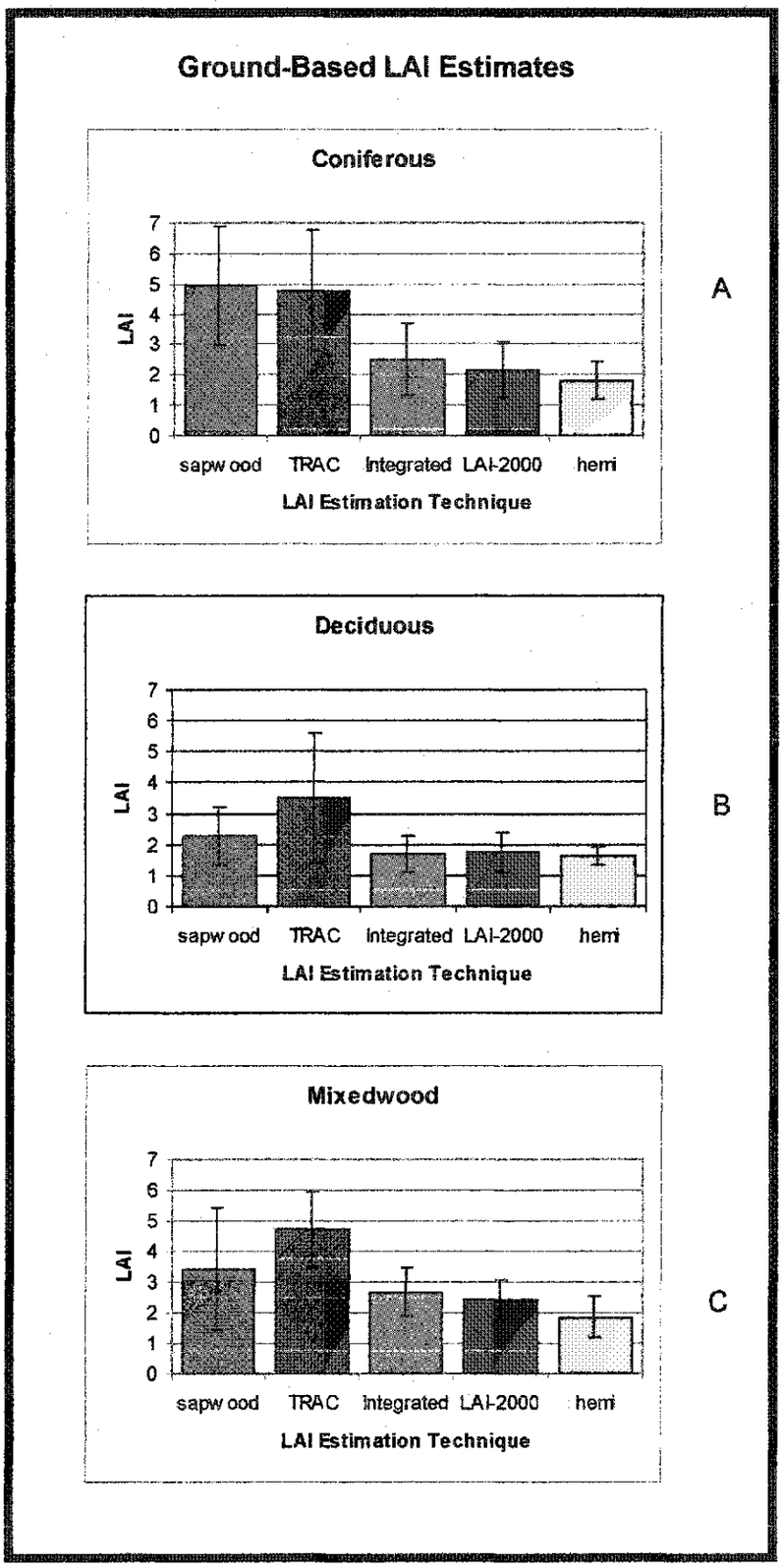

Figure 4-1 Mean LAI estimates and standard deviation from the sapwood area/leaf area, TRAC, integrated LAI-2000 and TRAC, LAI-2000, and hemispherical photography for coniferous (A), deciduous (B) and mixedwood (C) stand

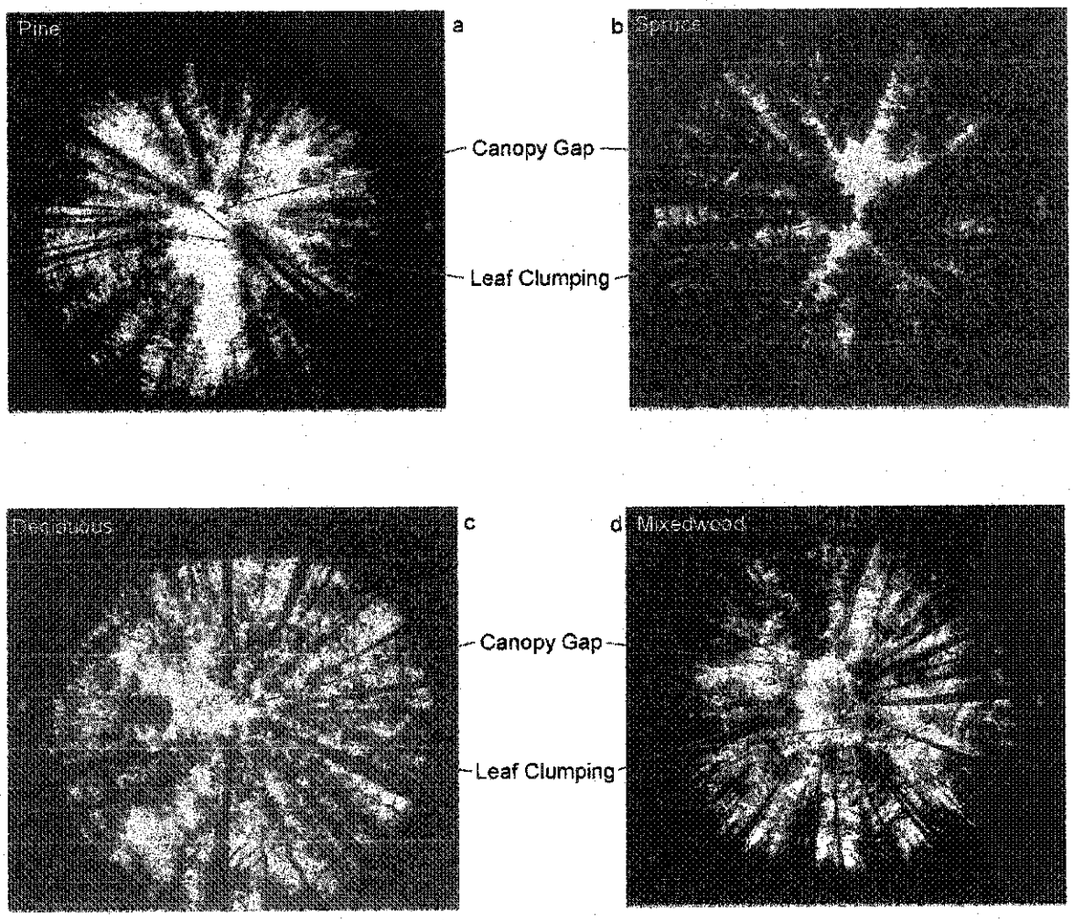

Figure 4-2 Hemispherical photographs depicting canopy gaps and leaf and needle clumping for (a) lodgepole pine, (b) white spruce, (c) deciduous and (d) mixedwood stands

4.4.1 Instrument and Species Comparison

4.4.1.1 Results

LAI estimates were significantly different among the different species and instrument factors (Table 4 -4). The S-N-K analysis distinguished which LAI estimation technique was statistically different from the others. The TRAC and sapwood area/leaf area estimates across all species were significantly higher than the other three approaches (Table 4 -5). Although not significantly different, the integrated approach gave larger mean LAI estimates than that from the LAI-2000 instrument (Table 4 –5). The LAI-2000 was statistically similar to both hemispherical photography and the integrated approach, however, according to the S-N-K results the integrated approach and hemispherical photography were significantly different (Table 4 -5). The instrument and species interaction factor was statistically significant, suggesting that LAI values varied with species and measurement technique (Table 4 -5).

Table 4 -4 Two-way factorial analysis of variance for species type, instrumentation and interactions.

	Df	**Mean square**	**F**	**p-value**
Instrument	4	34.43	28.01	.00*
Species	3	32.87	26.75	.00*
Instrument*Species	12	4.35	3.54	.00*

*statistically significant at $p<0.05$

Table 4 -5 Student-Newman-Keuls statistical test for LAI by instrument. Means with the same superscript are not significantly different from each other.

Instrument	N			
Hemi	37	1.67[a]		
LAI-2000	36	2.06[a]	2.06[b]	
Integrated	34		2.31[b]	
SA	42			3.42[c]
TRAC	39			3.88[c]

Note: numbers with the same superscript are not statistically different.

4.4.1.2 Discussion

The structural properties of a tree and its distribution within a stand have an important influence on the amount of light that penetrates to the forest floor. The differences in LAI among the species are attributed to the structural composition of the stand including canopy architecture and morphology, leaf orientation and distribution, stand structure, and foliar biomass. Thus a statistically significant difference in the LAI estimates between species was expected (Table 4-4).

The different assumptions built into the estimation of LAI from the different techniques affect the LAI estimations thus producing a statistically significant difference among them (Table 4-4). The LAI-2000 and hemispherical photographs do not account for gap size distribution but instead measures gap fraction at several zenith angles, therefore, no significant statistical difference was expected between them. The LAI-2000 has been described as a convenient version of hemispherical photography because image processing is not required (Chen et al., 1997a). In other studies, the LAI-2000 was found to underestimate LAI especially for coniferous forests whose foliage are typically clumped at the shoot and canopy levels (Fassnacht et al., 1994; Gower and Norman,

1991). Gower and Norman (1991) found that the predicted LAI-2000 values were 35-40% below direct LAI measurements for a red oak plantation in Wisconsin. This underestimation may be due in large part to the lack of gap size distribution information as well as the effects of blue light scattering within the canopy (Chen et al., 1997a).

The higher LAI estimates by the TRAC are attributed to the calculation of a clumping index, to determine gap size distribution, and the lower gap fraction estimate due to the optical measurement at one zenith angle (Leblanc and Chen, 1998; Chen and Cihlar, 1995). The clumping index calculation is more important in coniferous species where the assumption of a random distribution of leaves is not valid (Figure 4-2a and b) (Chen and Cihlar, 1995). However, in this study, clumping index may be as important in deciduous species as in coniferous ones because the clumping index for deciduous species was on average 0. 87. Therefore, the assumption of a random distribution of leaves in deciduous species may be invalid (Figure 4-2c). Chen et al. (1997b) suggested that the assumptions that foliage elements are randomly distributed within foliage clumps and foliage clumps are randomly distributed in space can not be substantiated for aspen stands. They calculated clumping index (Ω) values as 0.84, 0.75, and 0.70 for aspen stands within Prince Albert National Park, Saskatchewan, Canada. Kucharik et al. (1997) determined aspen and poplar stands within the BOREAS Study Area (Saskatchewan and Manitoba, Canada) to have clumping indices between 0.52 and 0.87. Thus, clumping is important to consider in both deciduous and coniferous stands (Figure 4-2).

The larger mean of the integrated approach over the effective LAI instruments (hemispherical photography and LAI-2000) suggests the importance of combining the effective LAI estimate of the LAI-2000 with the clumping index of the TRAC. Leblanc

and Chen (1998) reported that the integrated approach provided a more accurate estimate of LAI compared to TRAC or LAI-2000 alone. In this study, the integrated approach deflated the TRAC estimate by between 33% and 51%. The lower estimate of LAI by the integrated approach than by the TRAC suggests the importance of estimating eLAI at several zenith angles, otherwise estimates of eLAI my be inflated (Table 4 -3). Theoretically, this approach should provide a more accurate estimate of LAI since it includes gap size distribution (clumping index) as well as quantifying the effects of foliage distribution and gap angular distribution, measured as effective LAI at several angles from zenith (Chen et al., 1997a).

The sapwood area/leaf area LAI estimates were not significantly higher than the TRAC estimate, suggesting that the technique of sapwood area to leaf area ratios from other areas within the Rocky Mountains (White et al., 1997) may be viable for this study area if the optical instrumentation is not available (Table 4 -4). However, sapwood area/leaf area estimates for white spruce were much higher than all of the other optical measurements (Table 4 -3). Since the white spruce estimate exceeded the range in optical measurements this estimate may not be suitable for the Kananaskis study area. The use of the sapwood area/leaf area estimates in previous studies has shown to be stand specific, and dependent on season, age, stand density, tree crown size, and climatic differences (Mencuccini and Grace, 1995; Pearson et al., 1984; Gholz et al., 1976). For future work, further testing and validation should be pursued. Local sapwood area/leaf area relationships may be needed to generate LAI estimates that would be more appropriate for the species in this study area.

The interaction term between instrument and species was statistically significant suggesting that the instruments measure LAI differently for the different species. This is probably indicative of the assumptions built into the design of the instruments and the species-specific algorithms applied for sapwood area/leaf area estimates. The significant interaction term may be due to the coniferous species exhibiting a clumping effect on foliage distribution at different levels including branches, whirls and crowns, rather than shoots alone. Therefore estimating LAI for needles nested within clumps is complex (Chen and Cihlar, 1995). Instruments that only measure gap fraction (i.e. LAI-2000 and hemispherical photography) do not account for complex clumping of needles and assume a random distribution of leaves/needles. A clumping index was also found in deciduous stands (0.87) that was slightly smaller than the coniferous species, yet, still larger than a random distribution of leaves. Chen et al. (1997b) and Kucharick et al. (1997) also found that deciduous stands exhibit a clumping effect. Therefore in both deciduous and coniferous stands, where needle or leaf clumping is a factor, optical instruments that account for the clumping index are necessary and techniques that only use gap fraction may be inappropriate. However, to determine the importance of clumping index in both coniferous and deciduous species would require absolute measures of true LAI for validation and/or calibration.

4.5 Comparison of Remotely Sensed LAI Estimates

4.5.1 Results

SMA_S, NDVI and WDVI had a statistically significant relationship with LAI from both the LAI-2000 and integrated approach in coniferous stands (Table 4-6 and Appendix

B). However, the TRAC had no significant statistical relationship with any of the vegetation indices or SMA_S (Table 4-6). The SMA_S approach improved the coefficient of determination (r^2) by 0.35 (from 0.44 to 0.79) and reduced the root mean square error over the vegetation indices for the integrated approach (r^2= 0.79) and LAI-2000 (r^2= 0.75) for coniferous species (Table 4-6). NDVI performed better than the other vegetation indices for the integrated approach (r^2= 0.44) and LAI-2000 (r^2= 0.40) based on an increase in the coefficient of determination (r^2) and the lower root mean square error (Table 4 -6). A statistically significant relationship was also found between SMA_S and sapwood area/leaf area (r^2= 0.28), and SAVI and hemispherical photographs (r^2= 0.49) for coniferous species (Table 4 –6). Spectral mixture analysis produced the strongest relationships with LAI for coniferous species (r^2= 0.79), which may be indicative of the structural parameters that SMA models.

In deciduous stands a significant relationship was found between all the vegetation indices and ground-based LAI techniques, except for the TRAC (Table 4 –7, Appendix B). SMA_S was not completed for the deciduous species since appropriate endmembers where not available (Chapter 3). In deciduous stands, SAVI produced stronger relationships with the integrated approach (r^2= 0.61) and the LAI-2000 (r^2= 0.60), while WDVI had stronger relationships with hemispherical photograph estimates (r^2= 0.37) and NDVI had the strongest relationships with sapwood area/leaf area estimates (r^2= 0.39) (Table 4 -7). The integrated approach and LAI-2000 had the strongest relationship with all the vegetation indices for both the deciduous and coniferous species (Table 4 –7, Table 4 –6).

Mixedwood stands showed a statistically significant relationship ($p<0.05$) between SAVI and all the ground-based instruments (Table 4 -8). SAVI produced the strongest relationship with sapwood area/leaf area estimates ($r^2 = 0.78$) followed by the integrated approach ($r^2 = 0.58$) (Table 4-8). Both NDVI and WDVI did not have statistically significant relationships with any of the ground-based instruments for the mixedwoods (Table 4-8). It should also be noted that due to the smaller sample size an independent validation sample set was not produced for all stands. The entire usable sample was required for the regression model, and therefore it was not possible to have an independent mutually exclusive validation sub-sample. The model strength is presented based on their coefficient of determination and RMSE and not on the application of the data to a validation data set.

Differences were seen in both the mean and standard deviation of the ground-based LAI estimates compared to remote sensing LAI estimates (Figures 4 –3 through 4 –5). In both the coniferous and deciduous stands, the stronger the statistical model (higher coefficient of determination (r^2) and lower root mean square error) the closer the remote sensing modeled mean would be to the ground-based means (Figure 4 –3 through Figure 4 -5). For all stands, the variability around the mean for the SMA_S and the vegetation indices were smaller than the ground-based estimates (Figure 4-3 through Figure 4 –5). In general, the remote sensing estimates follow the same trends as the ground-based LAI estimates, but they were less variable.

Table 4 -6 – Coefficient of determination (r^2), standard error, and significance ($p<0.05$) for modeled estimates for each LAI estimation technique and using the remotely sensed vegetation indices and SMA shadow fraction for conifer species. The equations are provided in Appendix C.

Instrument	N	NDVI			WDVI			SAVI			SMA Shadow Fraction		
		r^2	SE	P<0.05	r^2	SE	P<0.05	r^2	SE	P<0.05	r^2	SE	P<0.05
TRAC	27	0.05	1.95	0.26	0.05	1.97	0.27	0.06	1.94	0.21	0.06	1.88	0.23
LAI-2000	22	0.40	0.60	0.00	0.32	0.64	0.01	0.00	0.77	0.93	0.75	0.47	0.00
Hemi	21	0.00	0.67	0.99	0.01	0.66	0.76	0.49	0.48	0.00	0.01	0.66	0.72
Integrated	22	0.44	0.65	0.00	0.35	0.70	0.00	0.00	0.87	0.89	0.79	0.51	0.00
Sapwood area	27	0.05	1.90	0.29	0.06	1.89	0.23	0.11	1.84	0.10	0.28	1.88	0.01

Table 4 -7 – Coefficient of determination (r^2), standard error, and significance ($p<0.05$) for modeled estimates for each LAI estimation technique and using the remotely sensed vegetation indices and SMA shadow fraction for deciduous species. The equations are provided in Appendix C.

Instrument	N	NDVI			WDVI			SAVI		
		r^2	SE	P<0.05	r^2	SE	P<0.05	r^2	SE	P<0.05
TRAC	10	0.00	1.86	0.87	0.03	1.84	0.65	0.07	1.80	0.48
LAI-2000	9	0.39	0.55	0.05	0.42	0.54	0.04	0.60	0.45	0.00
Hemi	11	0.31	0.23	0.05	0.37	0.22	0.03	0.23	0.24	0.05
Integrated	9	0.41	0.49	0.04	0.42	0.49	0.04	0.61	0.40	0.00
Sapwood area	11	0.39	0.99	0.03	0.30	1.06	0.05	0.33	1.04	0.04

Table 4 -8 – Coefficient of determination (r^2), standard error, and significance ($p<0.05$) for modeled estimates for each LAI estimation technique and using the remotely sensed vegetation indices and SMA shadow fraction for mixedwood species. The equations are provided in Appendix C.

Instrument	N	NDVI			WDVI			SAVI		
		r^2	SE	P<0.05	r^2	SE	P<0.05	r^2	SE	P<0.05
TRAC	10	0.12	1.15	0.33	0.28	1.04	0.11	0.39	0.96	0.05
LAI-2000	11	0.00	0.71	0.92	0.03	0.70	0.59	0.47	0.52	0.02
Hemi	10	0.00	0.84	0.99	0.04	0.82	0.58	0.58	0.54	0.01
Integrated	11	0.06	0.71	0.47	0.00	0.73	0.90	0.35	0.59	0.05
Sapwood area	11	0.01	2.18	0.81	0.08	2.12	0.41	0.78	1.03	0.00

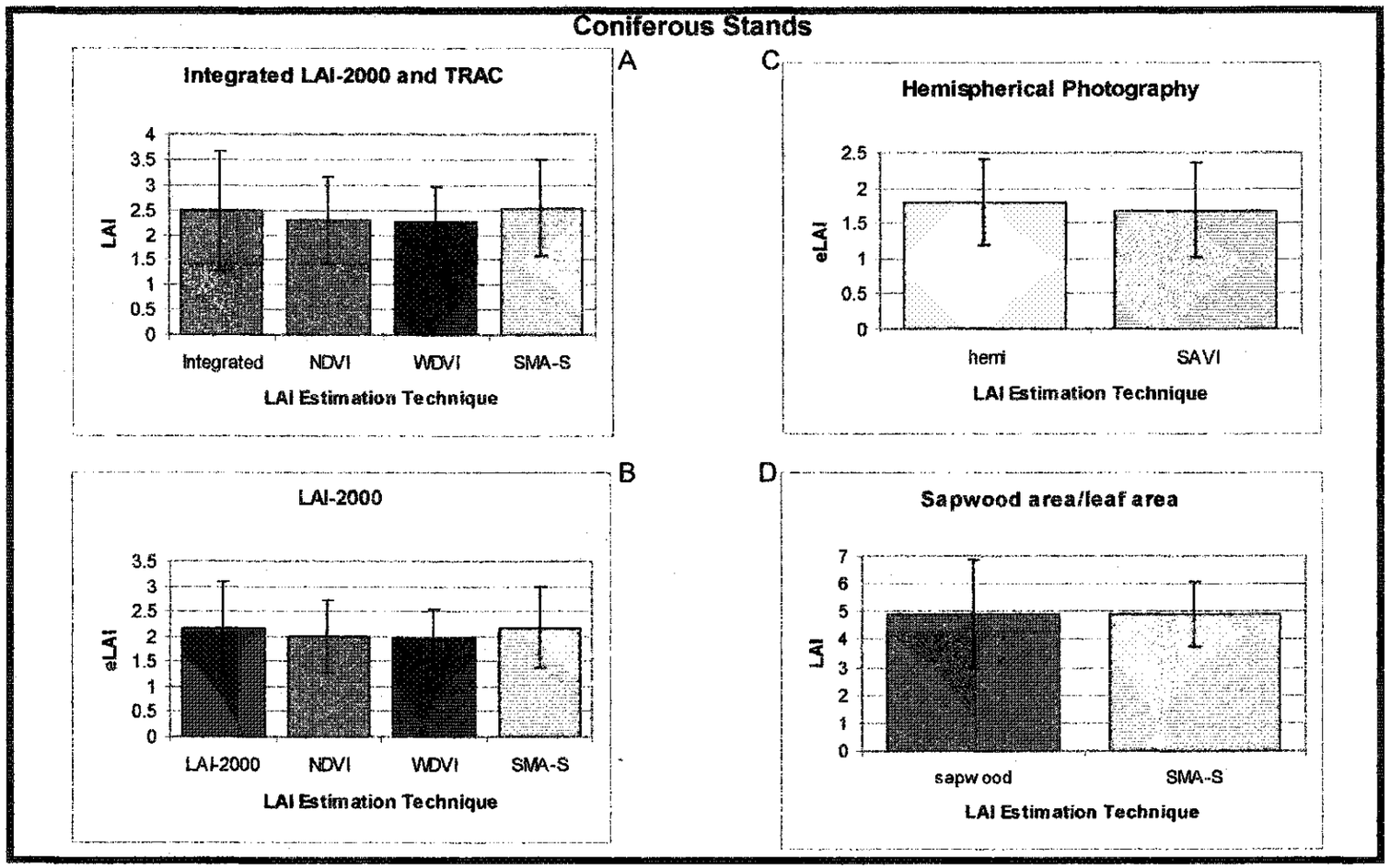

Figure 4-3 A comparison between ground-based and remote sensing LAI estimates. Mean LAI estimates and standard deviation (shown as line bar) from integrated LAI-2000 and TRAC (A), LAI-2000 (B), hemispherical photography (C), and sapwood area/leaf area (D) from ground-based and remote sensing techniques for all coniferous stands. Results that were not statistically significant are not shown.

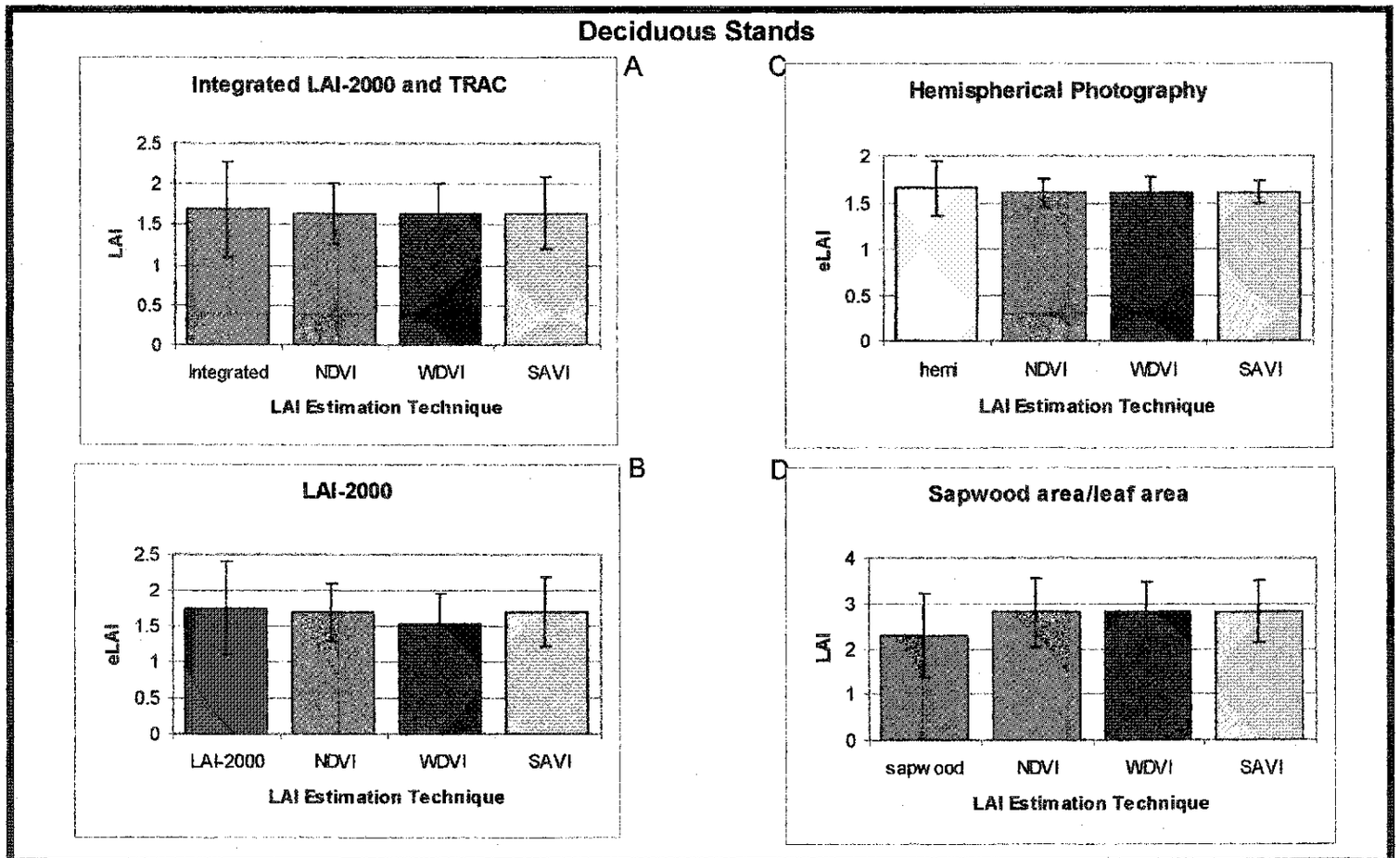

Figure 4-4 A comparison between ground-based and remote sensing LAI estimates. Mean LAI estimates and standard deviation (shown as line bars) from integrated LAI-2000 and TRAC (A), LAI-2000 (B), hemispherical photography (C), and sapwood area/leaf area (D) from ground-based and remote sensing techniques for all deciduous stands. Results that were not statistically significant are not shown.

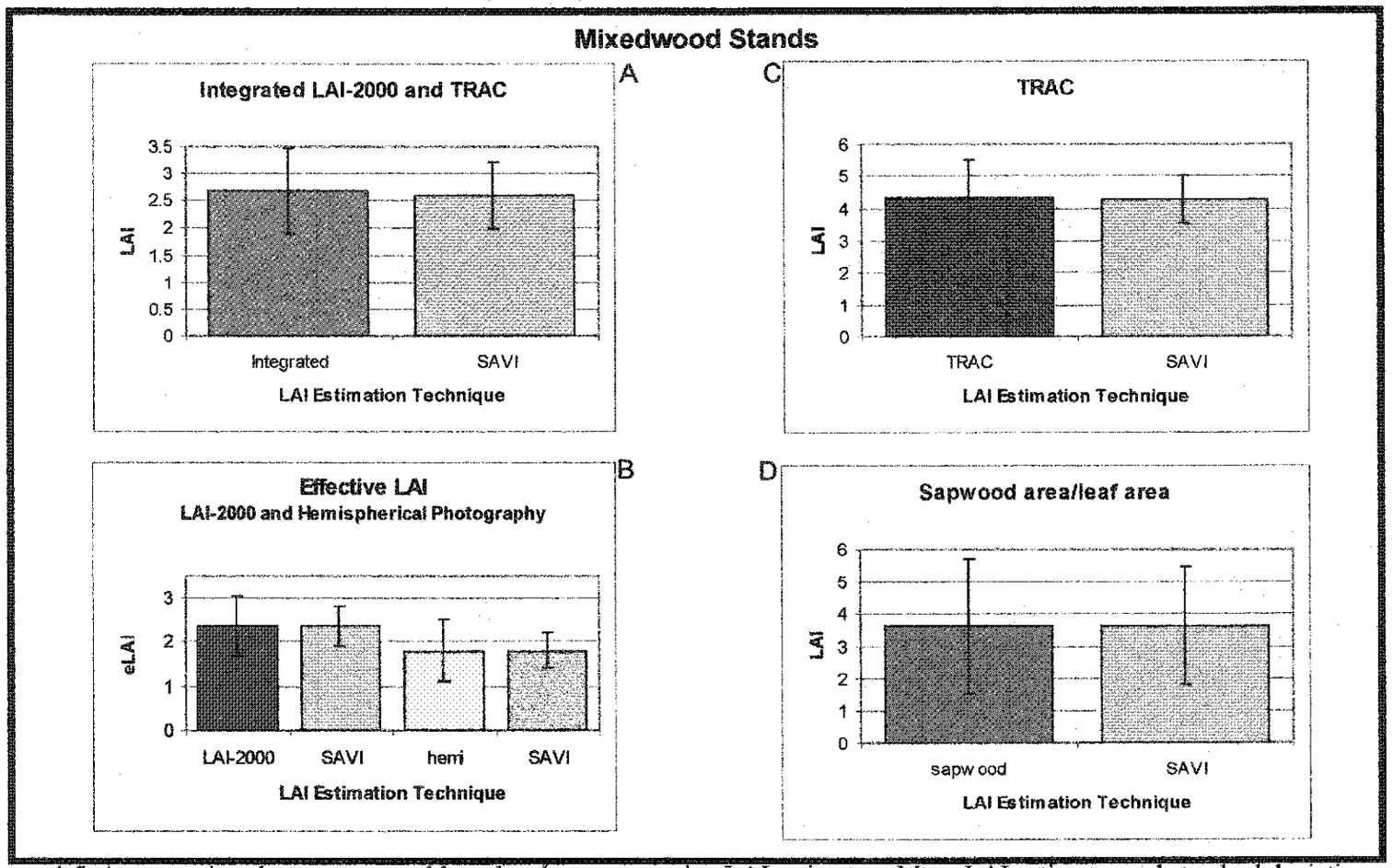

Figure 4-5 A comparison between ground-based and remote sensing LAI estimates. Mean LAI estimates and standard deviation (shown as line bars) from integrated LAI-2000 and TRAC (A), effective LAI instruments (LAI-2000 and hemispherical photography) (B), TRAC (C) and sapwood area/leaf area (D) from ground-based and remote sensing techniques for mixedwood stands. Results that were not statistically significant are not shown

4.5.2 Discussion

Shadow fraction from SMA produced the "best" regression results based on the coefficient of determination and RMSE for conifer species, compared to the vegetation indices (Table 4 –6, Appendix B). SMA has been shown to provide better estimates of forest biophysical parameters than vegetation indices in other studies (Peddle et al., 1999a, 2001; Peddle and Johnson, 2000; Johnson, 2000). Peddle et al. (2001) reported an average 40% improvement using SMA compared with 10 vegetation indices in the prediction of biomass, NPP, and LAI in a black spruce forest in Minnesota, USA. Peddle and Johnson (2000) found SMA shadow fraction improved LAI estimates by an average of 20% compared to NDVI for Multi-Spectral Video (MSV) data of trembling aspen and lodgepole pine stands in Kananaskis. In this study, SMA shadow fraction improved the r^2 by 0.35 and reduced the RMSE compared to any of the vegetation indices for the LAI-2000 and integrated approach (Table 4-6).

Of the vegetation indices, in conifer stands, NDVI produced improved regression results with higher r^2 values and reduced the RMSE over both WDVI and SAVI. In general, most of the conifer plots were comprised of white spruce stands with larger tree heights and basal areas which inhibit more light penetration to the soil or background, possibly reducing the effects that background has on the remote sensing signals. Chen et al. (1996a) found that simple ratios such as NDVI performed better than other vegetation indices that attempt to minimize soil background effects in predicting LAI and fPAR as the signal noise is proportional in both the red and infrared bands, thereby canceling out signal noise in jack pine and black spruce stands in Manitoba, Canada. Chen et al. (1996a) hypothesized that signal noise can be retained or amplified through the

mathematical equations in SAVI and WDVI. However, Peddle et al. (2001) found that vegetation indices that incorporated background effects were better predictors of forest biophysical parameters including biomass, NPP, LAI, DBH, stem density and basal area fraction for black spruce stands in Minnesota, USA. Black spruce and jack pine species generally have smaller crown sizes and smaller branches than that of white spruce or lodgepole pine species respectively (Johnson et al., 1995). By segregating the general conifer species into lodgepole pine and white spruce, the results may coincide with the results presented by Peddle et al. (2001) and Chen et al. (1996a), however, due to the relatively small sample size, this was not possible.

For the deciduous stands, SAVI showed the best relationship to LAI for both the integrated approach and LAI-2000. Deciduous canopies in this area have lower tree heights and mid-range basal areas (38 m^2/ha). This may result in a greater amount of canopy gaps and therefore the light penetration to the understory would increase and may have a greater background effect on the remote sensing signal. For both coniferous and deciduous species, except for SAVI in coniferous stands, the integrated approach produced higher coefficient of determination values than the other ground based estimates suggesting that the integrated approach may indeed be a more accurate LAI estimation technique than the other measures.

The same rationale for the deciduous species can also be applied to the mixedwood stands where there was a stronger relationship with SAVI than the other vegetation indices, likely because mixedwood stands have a relatively small basal area and the tree heights are lower than the white spruce. The sapwood area/leaf area estimate had a

strong relationship with SAVI. The integrated approach did, however, perform the best of the optical ground-based LAI estimates.

The similarity of the remote sensing mean LAI estimates to the ground-based mean LAI estimates is indicated by the magnitude of the coefficient of determination. The higher the coefficient of determination and the lower the root mean square error the more similar the remote sensing estimates were to the ground-based estimates. The decreased variability in the remotely sensed LAI estimates compared to the ground-based LAI estimates was quantified using the linear regression model. A linear model was fit to produce the remote sensing equations by using a line of best fit for which the extremes are not accounted for and the deviation will be less. Therefore, in the application of the remote sensing equations to the same plots, the estimates should be similar to the ground-based estimates used to build the equation, however the variation should be less, which was seen in this study.

4.6 NPP Model Sensitivity to LAI

4.6.1 Results

4.6.1.1 NPP General Simulations

Several NPP model simulations were completed where only one variable was altered to test the impacts of each variable, for the ranges found in the study area. LAI appears to have had a positive linear relationship with NPP (Figure 4 –6a). A range in LAI between 1-8 produced a range of NPP estimates from 1496-14035 kg_C/ha/yr. Soil water content and elevation had very little variation over the ranges of each variable tested (Figure 4 –6 b, c). The SWC ranged between 500-3000m^2 resulted in a range of

NPP estimates from 2909 to 2953 kg_C/ha/yr. A gain in elevation from 1389m to 1649m resulted in a decrease in NPP from 3034 kg_C/ha/yr to 2455 kg_C/ha/yr. For LAI, species also affected the NPP output, with deciduous species having a greater NPP than coniferous species at higher LAI values (Figure 4 –6a). The simulation results suggest that LAI is the main driving variable for FOREST-BGC in this region at this scale.

4.6.1.2 NPP Output From Field and Remotely Sensed LAI Inputs

The modeled NPP estimates produced similar patterns among the ground-based and remote sensing techniques to that seen in the LAI estimates. The NPP estimates were larger for the ground-based TRAC (NPP =6889-10474 kg_C/ha/yr) and sapwood area/leaf area (NPP = 6072-8572 kg_C/ha/yr) LAI inputs in all species, followed by integrated (NPP = 3903-5411 kg_C/ha/yr), LAI-2000 (NPP = 3664-4863 kg_C/ha/yr) and hemispherical photographs (NPP = 3009-3643 kg_C/ha/yr) (Figure 4 -8). Sapwood area/leaf area NPP estimates (NPP = 8572 kg_C/ha/yr) were only larger for the coniferous stands, while TRAC NPP estimates were higher in both the deciduous (NPP = 6889 kg_C/ha/yr) and mixedwood stands (NPP = 10474 kg_C/ha/yr) which was consistent with the patterns for ground-based LAI estimation (Figure 4 –8, Figure 4 –1). The same relationship was seen in the remote sensing techniques, where the patterns of NPP and LAI were similar (Figures 4-9 through 4-11, Figures 4 –3 through 4 -5). The similar trends between modeled NPP estimates and LAI estimates are consistent with the emphasis placed on LAI by the model.

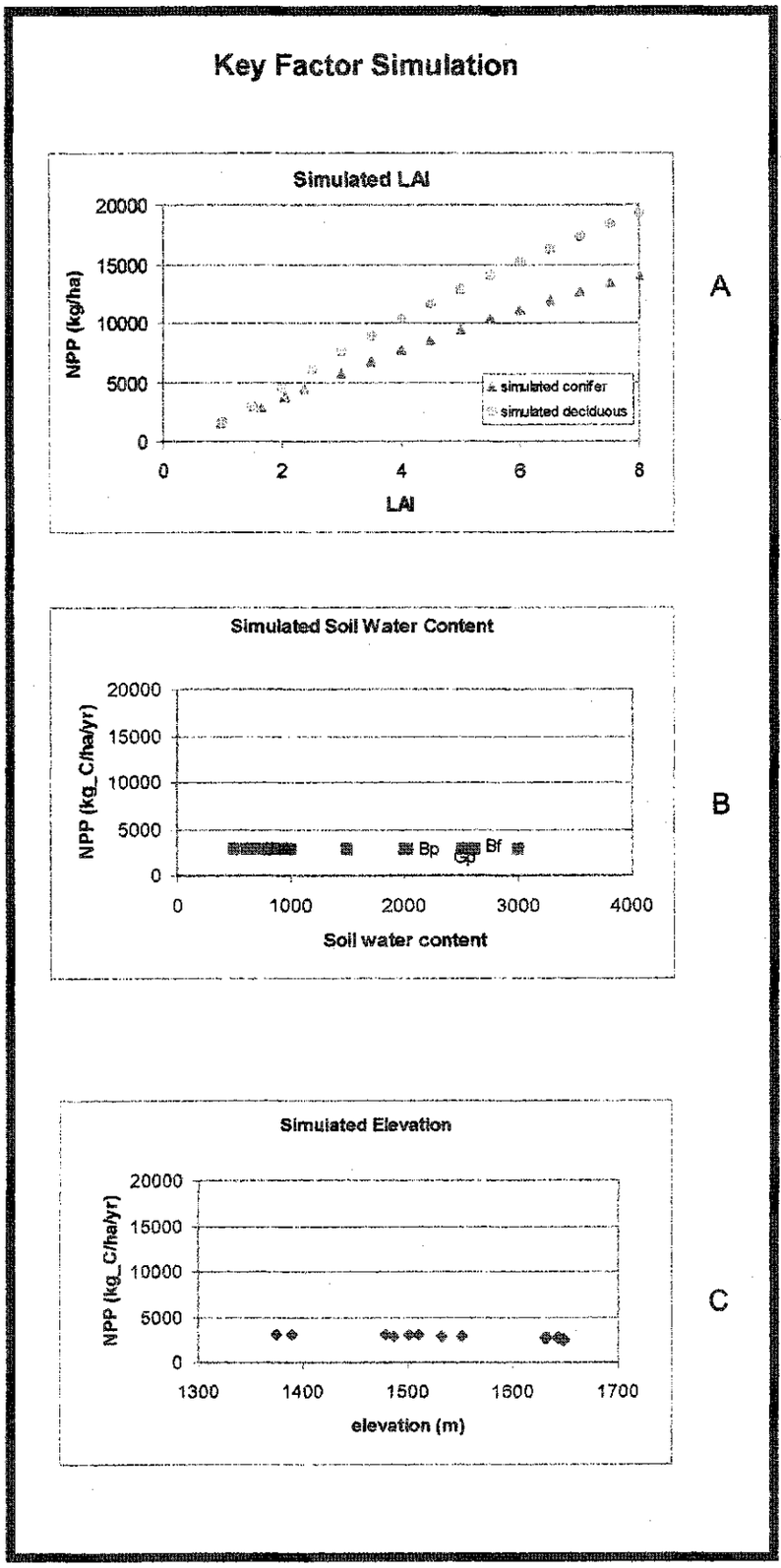

Figure 4-6 The effects of the key factors dictating FOREST-BGC NPP output including LAI (A), soil water content (B), and elevation (C). The key factors were altered based on the ranges of each found within the study area. For each of the factors being tested, all other variables were held constant. Elevation is a contributing factor to microclimatic changes.

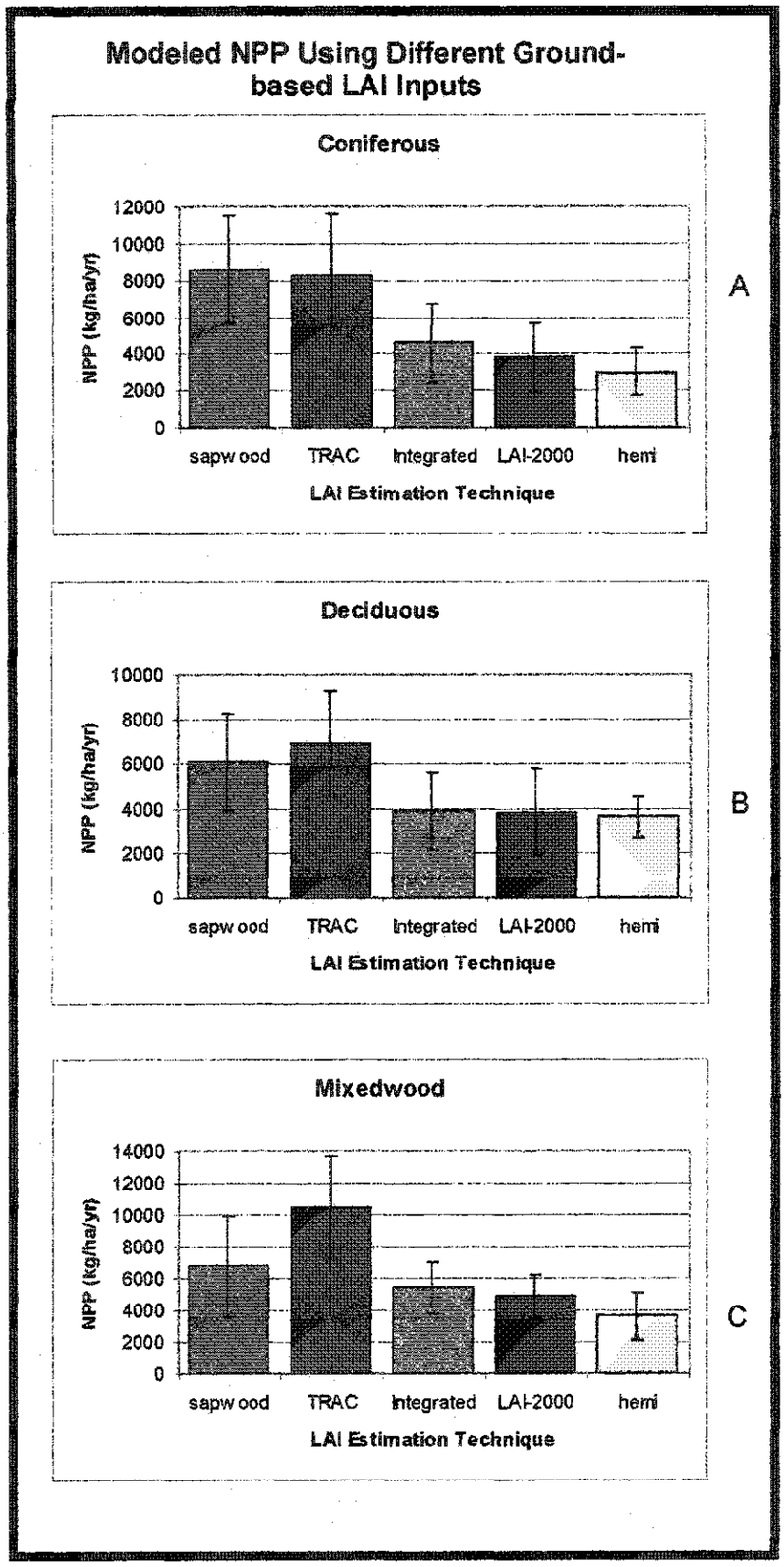

Figure 4-7 Mean NPP estimates and standard deviation (shown as line bars) from FOREST-BGC using LAI inputs from the sapwood area/leaf area, TRAC, integrated LAI-2000 and TRAC, LAI-2000, and hemispherical photography for coniferous (A), deciduous (B) and mixedwood (C) stands.

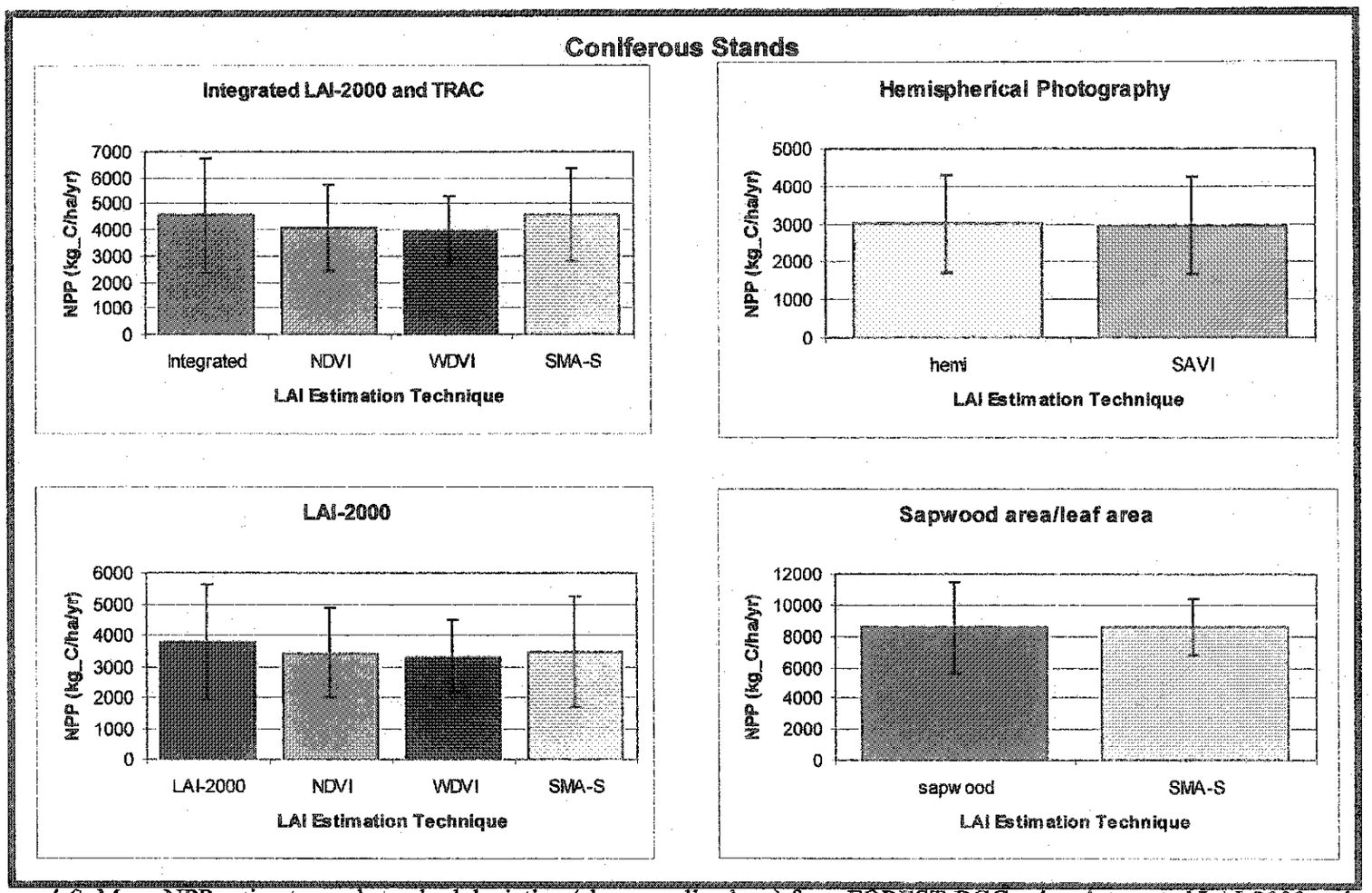

Figure 4-8 Mean NPP estimates and standard deviation (shown as line bars) from FOREST-BGC using integrated LAI-2000 and TRAC (A), LAI-2000 (B), hemispherical photography (C), and sapwood area/leaf area (D) from ground-based and remote sensing techniques for coniferous stands. Results that were not statistically significant for the LAI inputs are not shown.

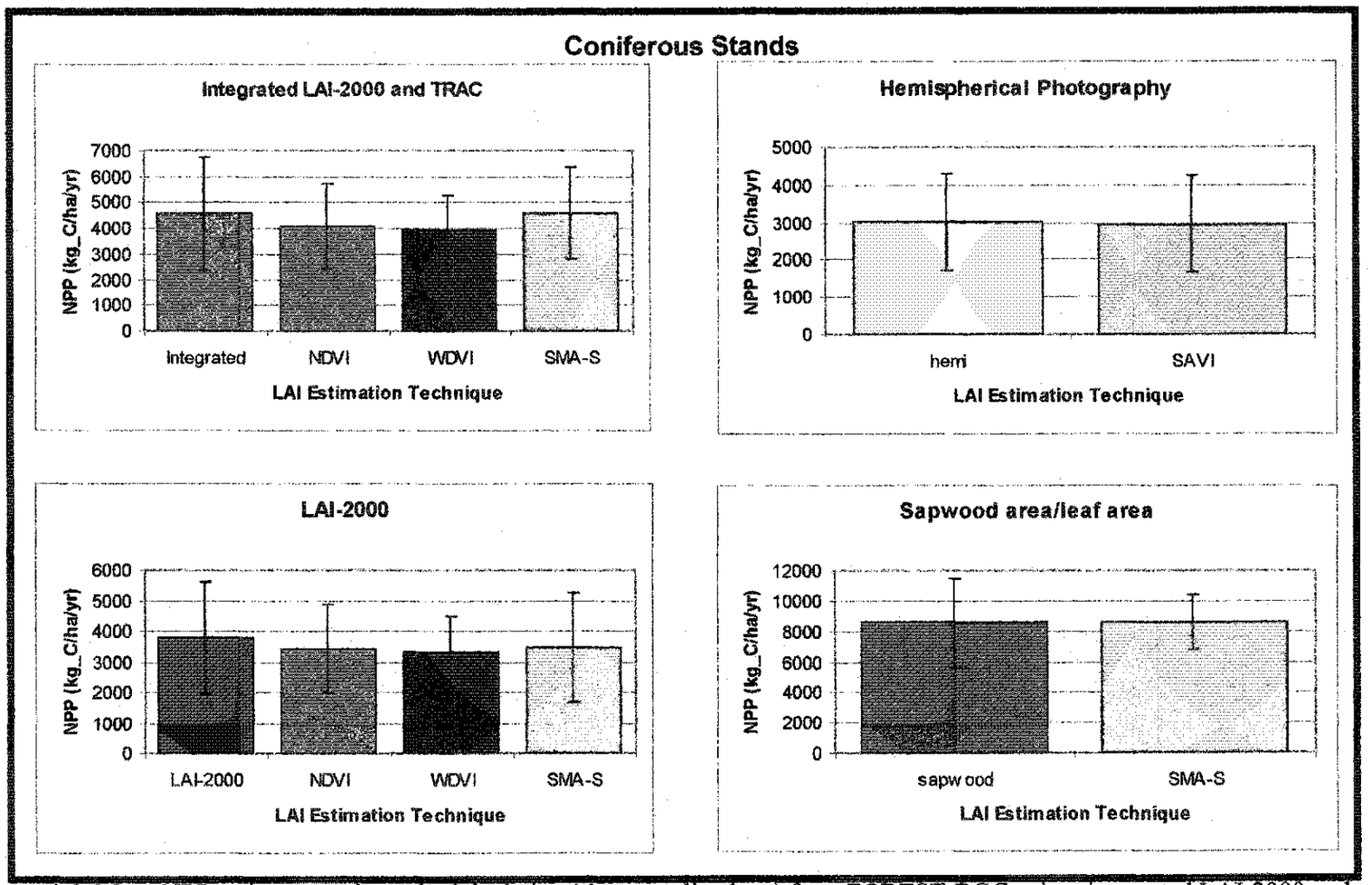

Figure 4-8 Mean NPP estimates and standard deviation (shown as line bars) from FOREST-BGC using integrated LAI-2000 and TRAC (A), LAI-2000 (B), hemispherical photography (C), and sapwood area/leaf area (D) from ground-based and remote sensing techniques for coniferous stands. Results that were not statistically significant for the LAI inputs are not shown.

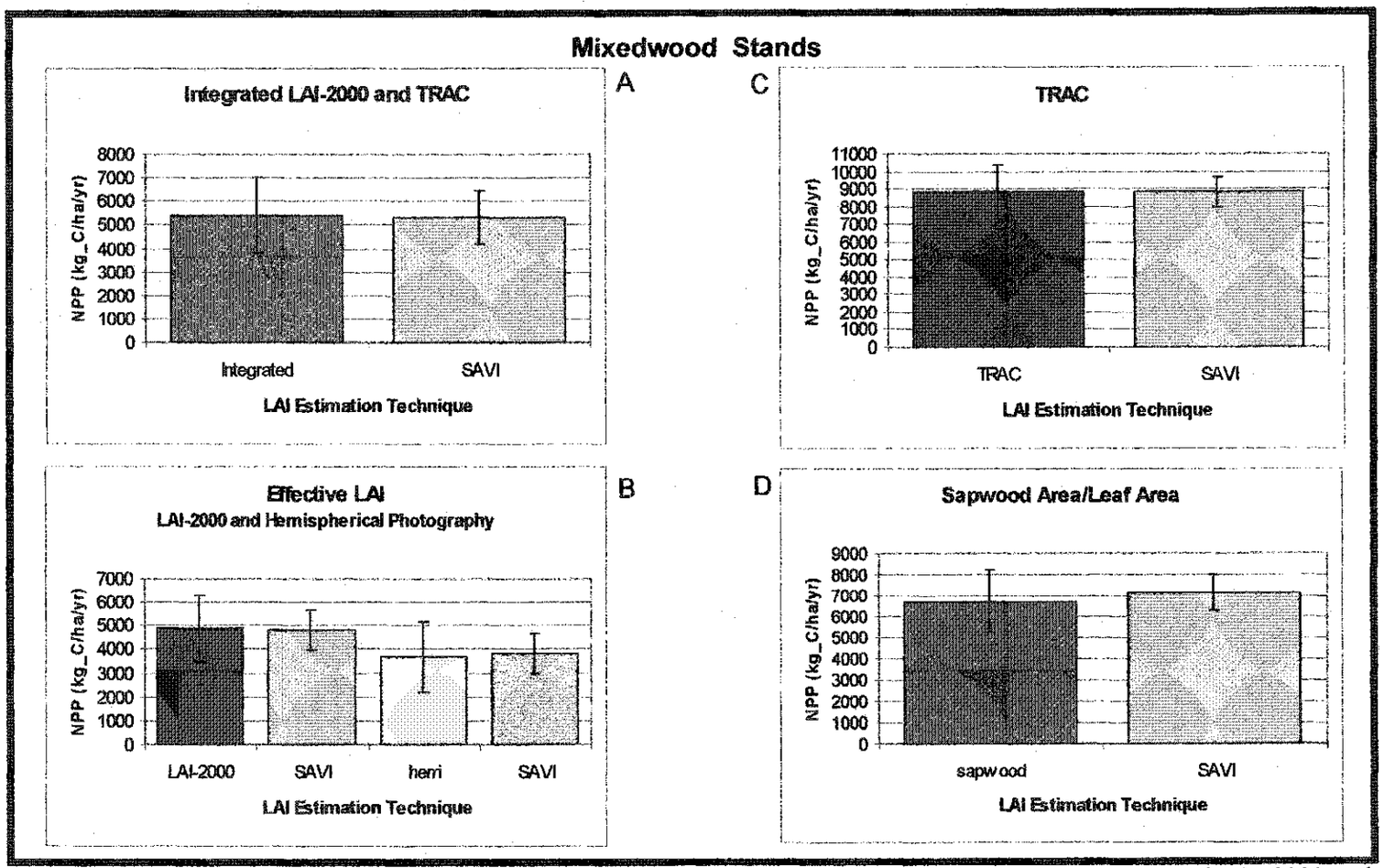

Figure 4-10 Mean NPP estimates and standard deviation (shown as line bars) from FOREST-BGC using integrated LAI-2000 and TRAC (A), effective LAI instruments (LAI-2000 and hemispherical photography) (B), TRAC (C) and sapwood area/leaf area (D) from ground-based and remote sensing techniques for deciduous stands. Results that were not statistically significant for the LAI inputs are not shown. SMA was not performed for mixedwood stands.

4.6.1.3 Comparison of Variability Between LAI and Modeled NPP

Variation around the mean is observable in both LAI and NPP estimates for each stand. Determining the coefficient of variation for each of the estimates enabled the direct comparison of variation among the different measures. In this section, the coefficient of variation for LAI will be designated as CV_{LAI} and the coefficient of variation for NPP will be CV_{NPP}. The greater the coefficient of variation the more variable either the NPP or LAI estimates were. The variability found within the NPP estimates was not proportional to the variability in LAI estimates (Figure 4 -12). In general, larger LAI estimates (i.e. TRAC and sapwood area/leaf area estimates), had a larger CV_{LAI} than CV_{NPP}, however for smaller LAI estimates (i.e. LAI-2000 and hemispherical photography) the CV_{LAI} were smaller than the CV_{NPP} (Figure 4 –12). The larger ground-based estimates of LAI produced by the sapwood area/leaf area and TRAC had smaller variability in NPP compared to the variability in LAI in all the stands ($CV_{LAI} > CV_{NPP}$), with the exception of the TRAC in the mixedwood stands ($CV_{LAI} < CV_{NPP}$) (Figure 4 –12). The smaller ground-based estimates of LAI from the LAI-2000 and hemispherical photographs had greater variability in NPP than in LAI ($CV_{LAI} < CV_{NPP}$) for all species (Figure 4 -12). While the variability in the NPP and LAI estimates for the integrated approach appeared similar ($CV_{LAI} \cong CV_{NPP}$) in the coniferous ($CV_{LAI} = 48.4$, $CV_{NPP} = 48.3$) and mixedwood stands ($CV_{LAI} = 29.5$, $CV_{NPP} = 29.7$), the variability is greater in the NPP estimate ($CV_{LAI} < CV_{NPP}$) in deciduous stands ($CV_{NPP} = 44.4$, $CV_{LAI} = 35.5$) (Figure 4-12). A threshold is suggested where the coefficient of variation is equal for both NPP and LAI, above which LAI has a larger variation, and below which NPP has a larger variation. The threshold value for conifer and mixedwood stands were close

to the integrated estimate of LAI (conifer LAI= 2.48, mixedwood LAI= 2.67, and for deciduous stands the threshold was between the sapwood area/leaf area (LAI=2.29) and integrated LAI estimate (LAI =1.69) (Figure 4-12).

In all stands, both CV_{LAI} and CV_{NPP} were lower for the remote sensing than the ground-based estimates (Figure 4 –13 through 4-15). Based on the smaller standard deviations for the mean remote sensing LAI estimates over the ground-based LAI estimates (Figures 4-9 through 4-11), the coefficient of variation for the remote sensing LAI and NPP estimates should be lower than the ground-based LAI and NPP estimates. The coefficients of variation for both NPP and LAI for the remote sensing estimates have similar patterns to the ground-based estimates. In both coniferous and deciduous stands, the smaller LAI estimates of hemispherical photographs, LAI-2000, and the integrated approach for both ground-based and remote sensing techniques had less variable LAI estimates than NPP ($CV_{LAI} < CV_{NPP}$), except the ground-based integrated approach in coniferous stands where LAI was slightly more variable ($CV_{LAI} > CV_{NPP}$) (Figure 4 –13 and 4 -14). The mixedwood and conifer stands had a greater variation in LAI than NPP ($CV_{LAI} > CV_{NPP}$) for sapwood area/leaf area estimates for both the ground-based and remotely sensed results (Figure 4 –13 and 4-15). Also, in mixedwood stands there was greater variability in LAI over NPP ($CV_{LAI} > CV_{NPP}$) for both TRAC ground-based and remote sensing estimates (Figure 4 –15). In deciduous stands, LAI had greater variability over NPP ($CV_{LAI} > CV_{NPP}$) for ground-based sapwood area/leaf area estimates, however remote sensing sapwood area/leaf area estimates had more variable NPP estimates ($CV_{LAI} < CV_{NPP}$). The variability in remote sensing techniques show similar patterns to the variability in ground-based estimates with threshold values of equal coefficient of

variation for both NPP and LAI, however, the coefficient of variation for both the NPP and LAI from remote sensing are lower than the ground-based estimates.

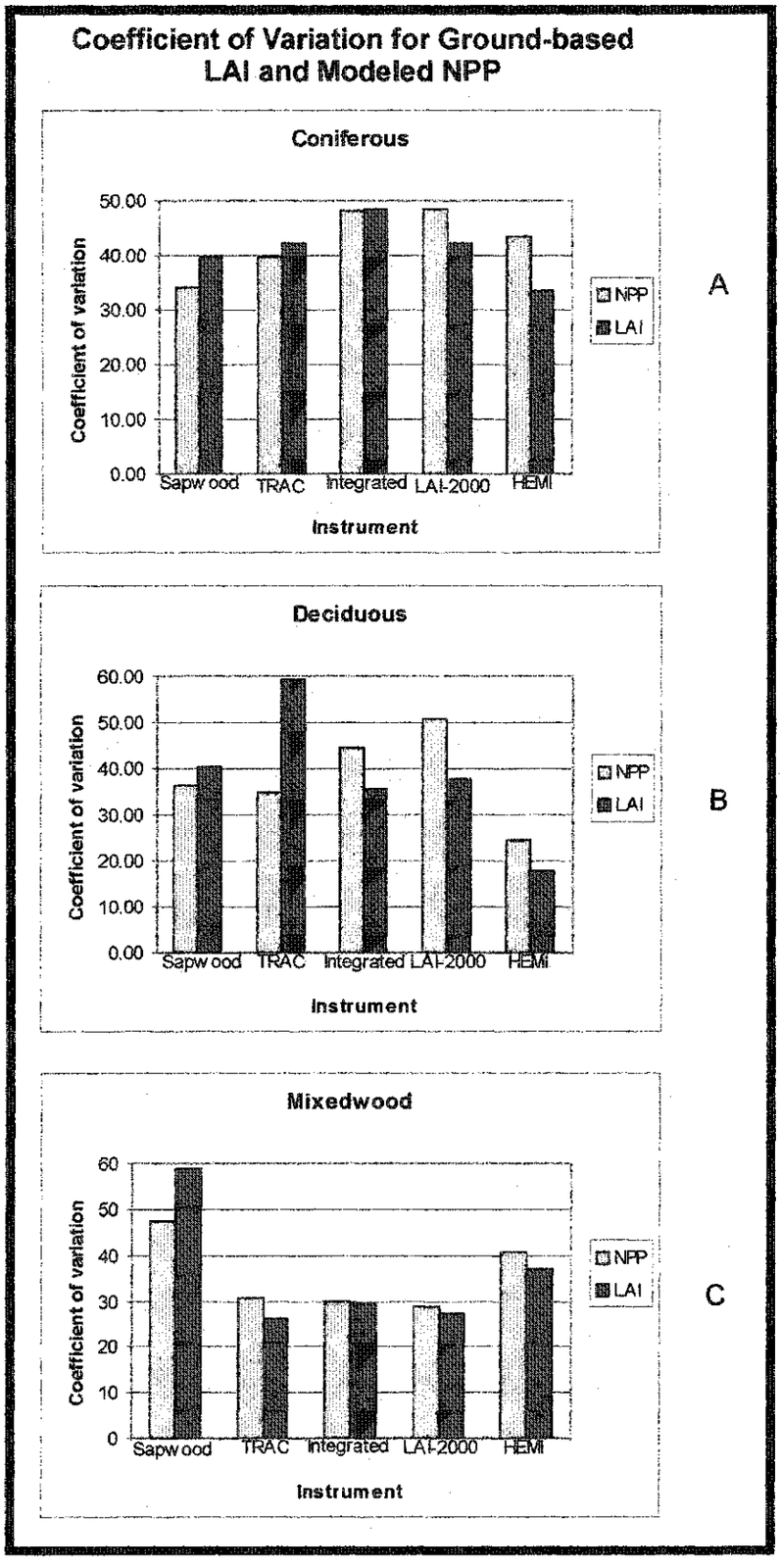

Figure 4-11
Coefficient of variation for both LAI and modeled NPP from ground-based LAI estimates for coniferous (A), deciduous (B) and mixedwood (C) stands.

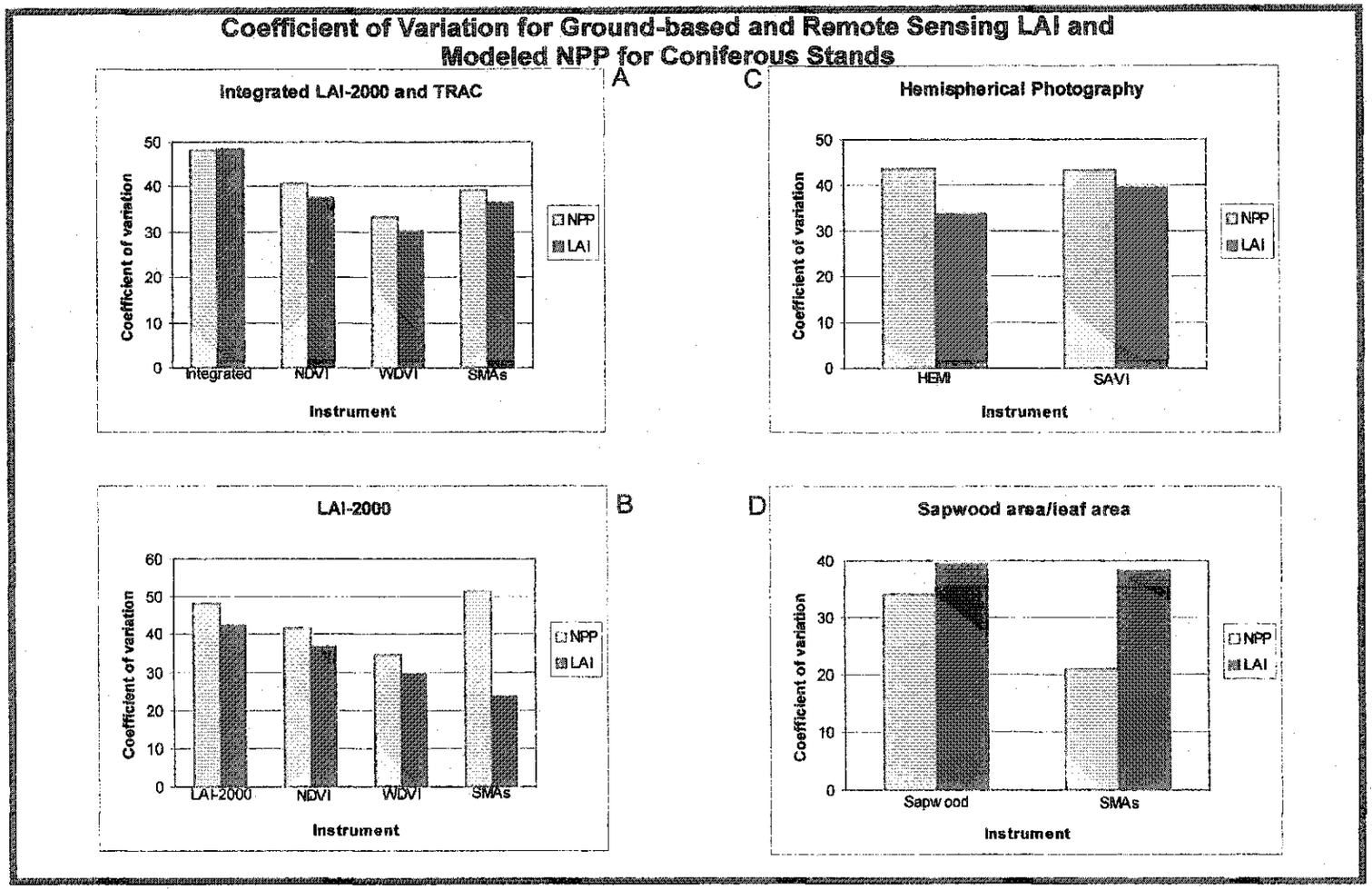

Figure 4-12 Coefficient of variation for both LAI and modeled NPP from integrated LAI-2000 and TRAC (A), LAI-2000 (B), hemispherical photography (C), and sapwood area/leaf area (D) from ground-based and remote sensing estimates for coniferous stands. Results that were not statistically significant for the LAI inputs are not shown.

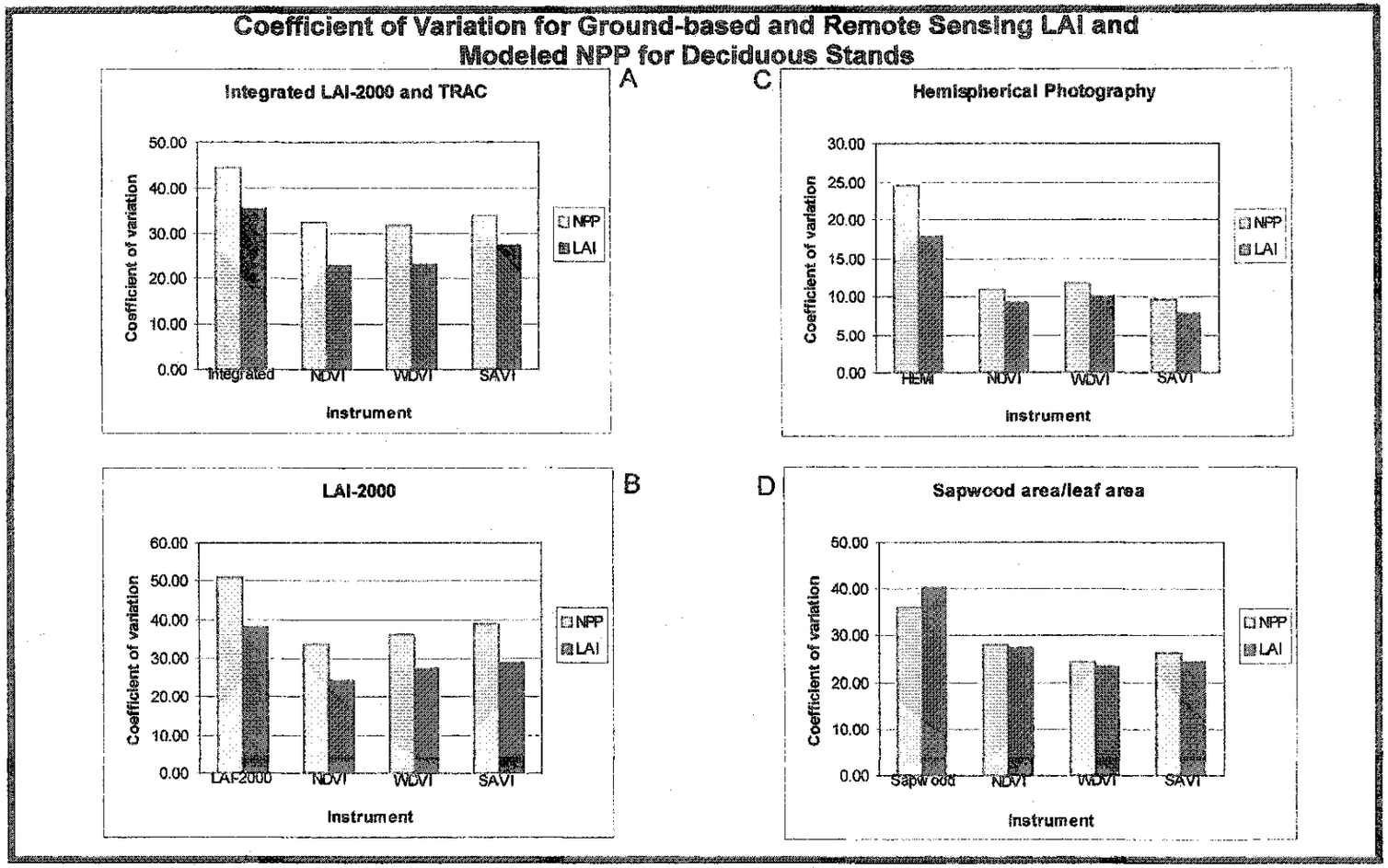

Figure 4-13 Coefficient of variation for both LAI and modeled NPP from integrated LAI-2000 and TRAC (A), LAI-2000 (B), hemispherical photography (C), and sapwood area/leaf area (D) from ground-based and remote sensing estimates for deciduous stands. Results that were not statistically significant for the LAI inputs are not shown. SMA was not performed for deciduous stands.

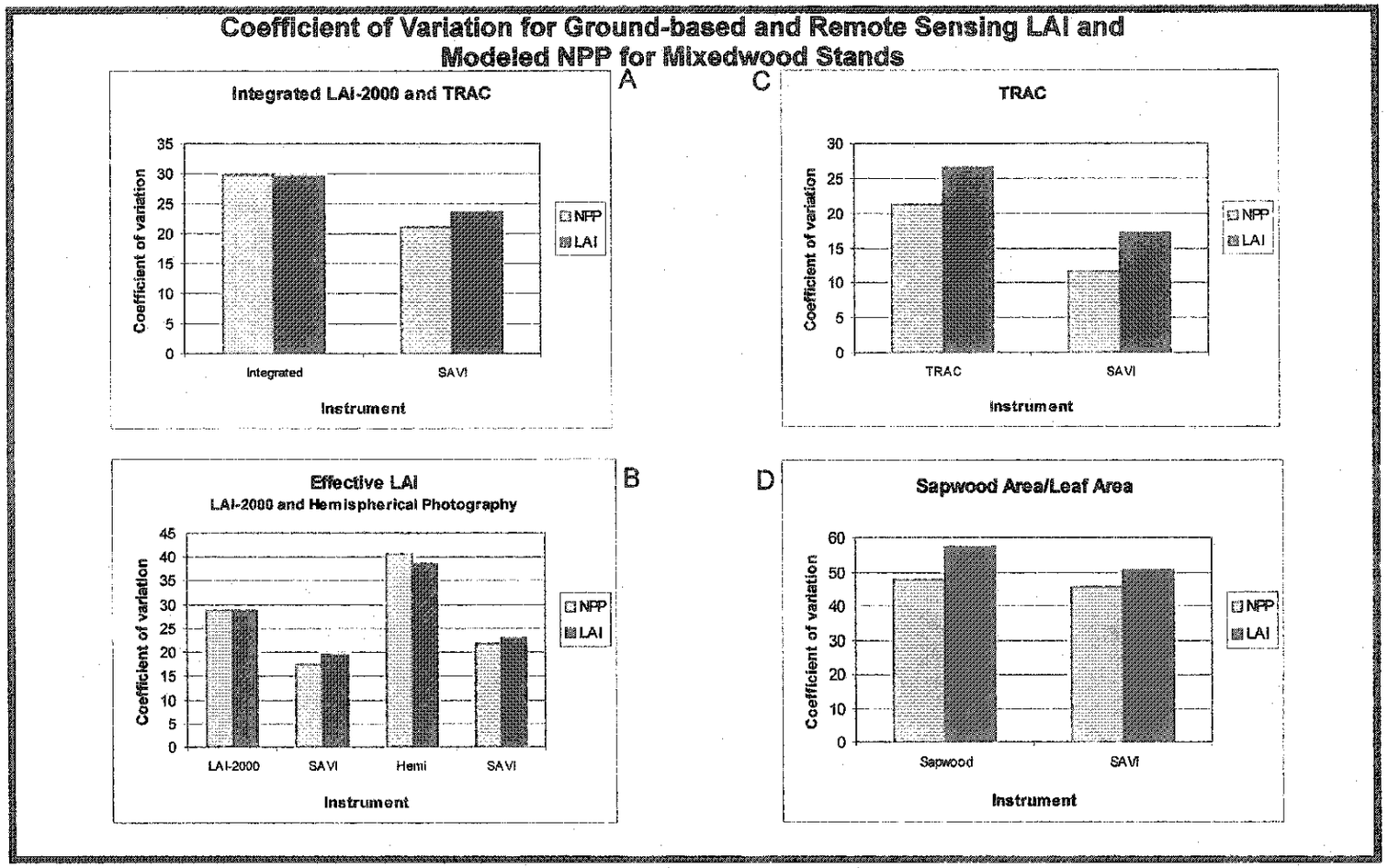

Figure 4-14 Coefficient of variation for both LAI and modeled NPP from integrated LAI-2000 and TRAC (A), effective LAI instruments (LAI-2000 and hemispherical photography) (B), TRAC (C) and sapwood area/leaf area (D) from ground-based and remote sensing techniques for deciduous stands. Results that were not statistically significant for the LAI inputs are not shown. SMA was not performed for mixedwood stands.

4.6.2 Discussion

The magnitude of NPP change with altered LAI in comparison to the altered soil water content and elevation illustrates the importance the FOREST-BGC model places on LAI inputs over the other variables (Figure 4 –6). Thus accurate and consistent LAI estimates are imperative in the modeling of NPP. Species also influences NPP model output due to basic physiological differences that are characterized by maximum LAI, specific leaf area, leaf on/off dates, respiration and conductance rates among species (Figure 4 –7) (Running and Hunt, 1993).

Running and Coughlan (1988) modeled NPP estimates for a hypothetical coniferous forest stand using FOREST-BGC in Missoula, Montana for variable LAI values of 3, 6 and 9 and produced NPP estimates of 4.1 tonnes of carbon/hectare/year (t/ha/yr), 4.9 t/ha/yr, and 4.9 t/ha/yr, respectively. Prescott et al. (1989) determined NPP in the Kananaskis region for lodgepole pine, white spruce and Douglas-fir stands to be 4.57 t/ha/yr, 4.32 t/ha/yr, and 3.83 t/ha/yr, respectively. In this study the average NPP estimate for coniferous stands (including lodgepole pine, white spruce and mixed conifer where the latter consisted of lodgepole pine, white spruce and Douglas fir) using the integrated approach (theorized to be the most accurate) was 4.56 t/ha/yr. These results are similar to both the Prescott et al. (1989) ground-based NPP estimates, and Running and Coughlan (1988) modeled results for NPP estimates of coniferous species on the eastern slopes of the Rocky Mountains. Since there are no other studies of deciduous NPP in montane ecozones a comparison with the same species in boreal stands was performed instead. Gower et al. (1997) measured annual NPP for aspen stands in a boreal ecozone in Saskatchewan to be 3.12 t/ha/yr and 3.52 t/ha/yr, and in Manitoba at 2.49

t/ha/yr and 3.49 t/ha/yr. In this study, the integrated LAI-2000 and TRAC, and LAI-2000 techniques produced NPP estimates of 3.9 t/ha/yr and 3.85 t/ha/yr for deciduous stands. The results for this study are slightly higher than the measurements taken in Saskatchewan and Manitoba. This is due to the more southerly location of the study area and the difference in ecozone (montane cordillera vs boreal forest) affecting climate, growing season, parental material, permafrost and soil (Johnson et al., 1995).

The mean NPP estimates and standard deviations for the ground-based and remote sensing techniques follow the same patterns of the mean LAI estimates (Figure 4-8 through 4-11). Large LAI estimates (sapwood area/leaf area and TRAC estimates) produce larger NPP estimates (sapwood NPP = 8.57 t_C/ha/yr and TRAC NPP = 8.30 t_C/ha/yr) compared to those of smaller LAI estimates (hemispherical photography and LAI-2000) (hemispherical NPP = 3.01 t_C/ha/yr and LAI-2000 NPP = 3.80 t_C/ha/yr). This again shows the influence of the LAI estimates on the modeled NPP output.

The variability of LAI and NPP was not proportional. A threshold value was suggested at the point where the variability of NPP and LAI were equal. For LAI estimates lower than the threshold, there is more variability with the NPP estimates than the LAI estimates. Alternatively, if the LAI estimates are greater than the threshold value, the NPP variability will be less than the variability in the LAI estimates. The threshold values for the coniferous stands were suggested to be approximately similar to the integrated LAI-2000 and TRAC approach. For deciduous stands, the threshold value was suggested to be between the LAI estimates of the LAI-2000 and sapwood area/leaf area, and for the mixedwood stands between the LAI-2000 and integrated approach. Beyond this LAI threshold, other environmental factors including climate and soil water

content may limit the increase in NPP, while below this threshold LAI may limit the increase of NPP (Nemani and Running, 1989; Running and Coughlan, 1988).

Photosynthesis, NPP and CO_2 uptake rely on the capture of PAR by trees (Bonan, 1993). The amount of PAR captured is largely dependent upon the surface area of leaves or LAI (Kimmins, 1997; Bonan, 1993). The leaf area is determined based on the availability of site resources including: water, nutrient and light (Kimmins, 1997). Stand leaf area is usually lower where water is limited (Nemani and Running, 1989). Both climate and soil play a significant role in determining the water availability of a site because the climate dictates the amount of available precipitation and evaporation for the site and the soil dictates the amount of water that is stored. As a result, equilibrium should exist between climate, soil and leaf area due to the supply-storage-demand interaction (Nemani and Running, 1989; Grier and Running, 1977). Equilibrium is met where photosynthesis is maximized and a suitable internal water status is maintained (Nemani and Running, 1989). By increasing tree leaf area, there is an increase in photosynthetic potential, however, increased leaf area will also cause an increase in transpiration loss. Therefore, to restrict water stress there is reduced stomatal aperture, which also causes a reduction in CO_2 fixation (Nemani and Running, 1989).

Nemani and Running (1989) found that a necessary hydrological equilibrium exists between climate, soil water content and maximum leaf area in water limited coniferous forests in Montana. In FOREST-BGC, a linkage between hydrologic components and carbon balance predictions of photosynthesis, respiration, and growth allocations would provide additional insight into the limitations of LAI (Nemani and Running, 1989). They were able to infer estimates of maximum leaf area that a site can

support with prior knowledge of soil and climatic conditions. Their modeled maximum LAI estimates were validated through comparing modeled maximum LAI and field estimates of LAI showing a linear correlation between field and modeled LAI (r^2=0.87). The strong relation between field and modeled LAI confirms the control water availability has on leaf area carrying capacity of forest stands (Nemani and Running, 1989). In this study, the LAI threshold value is suggested to be the point of model equilibrium between LAI, soil water content and climate.

Running and Coughlan (1988) found that based on model simulations in the mid-latitudes of west central North America, an increase in LAI is limited by hydrologic balances and partitioning, altering the subsequent photosynthesis of forest canopies. They found that there was no increase in total transpiration from an LAI of 3 to 9 because all available soil water was consumed because of low annual precipitation or there was more transpiration with higher LAI values resulting in a longer duration of canopy water stress. Therefore, there was equal total transpiration for LAI values ranging between 3 and 9. They also found that where physiological activity is substantially water limited or radiation limited, increasing LAI produced a weak positive response to photosynthesis. As photosynthesis is an important parameter in the calculation of NPP, the weak positive response to photosynthesis would have an affect on the resulting output. For example, in a FOREST-BGC modeled coniferous forest in Missoula, Montana an increase in LAI from 3, 6 and 9 resulted in an NPP of 4.1 t/ha/yr, 4.9 t/ha/yr, and 4.9 t/ha/yr (Running and Coughlan, 1988). The lack of NPP increase from 6 to 9 is likely due to the short growing season and small amount of precipitation (337mm) received in this area (Running and

Coughlan, 1988). Thus a threshold value exists here between LAI of 3 and 6, where equilibrium of LAI, SWC and climate is met.

In the Kananaskis study area of this research, similar trends occur, thus as LAI estimates increase, the resulting NPP will be limited by soil water content and climate. NPP values less than the LAI threshold were not water limited but rather LAI limited, resulting in more variable NPP estimates compared to the LAI estimates. Thus, at the LAI threshold, an equilibrium exists between SWC and climate and the amount of LAI a site can sustain. Therefore, below the LAI threshold or site equilibrium, LAI limits the amount of NPP, while above the threshold site water availability (SWC and climate) limit the amount of NPP.

4.7 Chapter Summary

In this chapter, comparisons of ground-based and remote sensing LAI estimates and the effect LAI has on modeled NPP estimates were completed. The relative comparison of the ground-based LAI estimates suggest optical techniques which incorporate clumping effects and gap fraction measured at several zenith angles, like the integrated LAI-2000 and TRAC approach, theoretically provide the most accurate LAI estimations. This approach deflated the TRAC estimate by 32-52%. The integrated approach also had the strongest relationships with the remote sensing techniques (SMA shadow fraction and vegetation indices) over any other ground-based estimate, which provided empirical evidence to support this theory, further supporting the preferred use of the integrated approach. SMA shadow fraction produced the best overall estimates of integrated LAI for the coniferous species, while NDVI produced the best estimates of the different

vegetation indices tested. For the deciduous stands (for which SMA was not conducted), SAVI had the strongest relationship with the integrated LAI. For mixedwood stands, SAVI produced the strongest relationships with all the instruments over any other vegetation indices. Species and stand structure were shown to affect LAI estimation at both ground-based and remote sensing levels.

LAI has a strong influence on the modeled NPP estimate from FOREST-BGC. Simulations showed that LAI affects NPP more than either soil water content or climate. As well, the graphical patterns observed in each of LAI and NPP estimates were similar, however, the variability between LAI and NPP was not equal. Coefficients of variations were determined for both the LAI input and the NPP output, from which a threshold LAI estimate was proposed as the point where the variability in LAI is similar to the variability of NPP. Below this threshold, the variability in LAI is greater than the variability of NPP, while the opposite is true above this threshold. This LAI threshold suggests that, initially, the increase in modeled NPP is limited by LAI, but that beyond this threshold the increase in modeled NPP is limited by soil water content and climate due to the hydrological equilibrium between climate, soil water content and leaf area.

CHAPTER V

5.0 Summary and Conclusions

5.1 Summary of Results

The ability to predict the amount of carbon in an ecosystem through NPP modeling is important for the determination of climate change effects and global carbon budgets, which has come to the forefront of much research due to anthropogenic increases in atmospheric CO_2. Process-based ecosystem models have been developed using leaf area index (LAI) as a key variable, as it can be obtained at multiple scales and over large areas using remote sensing, and it is a parameter related to energy, gas and water exchange of an ecosystem. As a result, understanding the variability in LAI from both ground-based instrumentation and from remote sensing techniques and the resulting affect this has on modeled NPP is important for making accurate estimates of carbon. In this thesis, results were obtained for the three research objectives identified. In the following sections, these results are summarized for: (i) ground-based LAI estimation, (ii) remote sensing of LAI and (iii) variability of NPP.

5.1.1 Ground-based LAI Estimation

In this research, five approaches for ground-based LAI estimation were compared including, LAI-2000, hemispherical photography, TRAC, integrated LAI-2000 and TRAC, and sapwood area/leaf area. The integrated LAI-2000 and TRAC approach provided the best theoretical basis for estimating LAI as it accounted for both the

clumping index and the gap fractions at several solar zenith angles. In this study area clumping indices were found in both coniferous and deciduous stands. For conifer stands, the integrated approach reduced LAI estimates from the TRAC by 37% and increased the LAI-2000 estimates by 19%. All the stands had lower LAI estimates for the integrated approach than the TRAC. This result suggests the importance of estimating eLAI from gap fraction at several zenith angles. However further analysis of the optical instruments in comparison with absolute LAI values should be completed. The sapwood area/leaf area estimates used from the literature may be inappropriate for this area, especially the white spruce stands, as these exceeded the optical estimates. This analysis is limited due to the lack of absolute validation of LAI, as the destructive sampling of some of these stands was not only illegal but also prohibitive in terms of monetary, location and time constraints. Thus only a relative study could be completed, however, it was stated earlier that absolute measures of LAI for the incorporation with remote sensing is difficult, impractical or impossible. This is due to the difficulties in measuring LAI over a large area that will correspond with the image pixel resolution, positional control of field measurements in relation to the exact pixel area, and field sampling that would provide an appropriate representation of forest stands. Ideally, a large sample of absolute measures of LAI from destructive sampling together with optical and allometric techniques should be used, however, with the plethora of optical LAI estimates and allometrics derived independently of the optical instruments a robust comparison was provided.

5.1.2 Remote Sensing of LAI

In the remote sensing analysis, spectral mixture analysis shadow fraction (SMA_S) ($r^2 = 0.79$) produced stronger predictive relationships for conifer LAI estimates compared to all vegetation indices tested (NDVI, WDVI, and SAVI1)($r^2 = 0.44$, 0.35, and 0.00 respectively). Of the vegetation indices, NDVI produced the strongest relationships with LAI for coniferous stands, suggesting that in the coniferous stands, which are characterized by larger tree heights and greater basal area, the effects of background are not as strong. In deciduous and mixedwood stands, the vegetation indices that account for the effects of background produced stronger relationships with LAI (SAVI r^2 increased by 0.20 from 0.41 to 0.61 compared to NDVI in deciduous). All the remote sensing techniques produced better results (higher coefficient of determination and lower RMSE) for predicting LAI with the integrated LAI-2000 and TRAC approach compared to the other predictions of the other LAI instruments (LAI-2000, hemispherical photography, allometrics, and TRAC). This further supported the argument that the integrated approach is preferred for estimating LAI.

5.1.3 Variability of NPP

Process-based NPP models have been developed using knowledge of ecological process and functions, which can be applied to broad spatial scales to determine estimates of carbon stocks. Running and Coughlan (1988) developed their process-based ecosystem model, FOREST-BGC to be driven in large part by LAI. By simulating the key model input variables, a series of controlled experiment were conducted in which these individual variables (soil water content, climate, and LAI) were analyzed, with all

other inputs held constant in each test. Of these three key variables used, LAI was the most important input based on the magnitude of change in modeled NPP as a function of changing LAI. A further analysis compared a graphic representation of mean modeled NPP and mean LAI estimates for the various LAI estimation techniques and species types. The similar patterns observed among the mean modeled NPP output and LAI inputs for the different LAI estimate techniques suggested that LAI is the driving variable in the FOREST-BGC model (Figure 4-1 and Figure 4-8). A threshold was identified, through the analysis of the coefficients of variation for both NPP and LAI, below which the variability in NPP was greater than the variability in LAI. Beyond this threshold, the opposite was true-the variability in NPP was less than the variability in LAI. The threshold value was suggested as an equilibrium point where photosynthesis is maximized and transpiration water loss is reduced so that the internal water status is maintained. The equilibrium is based on a supply-storage-demand interaction between climate, soil water content, and LAI. Below the LAI threshold, LAI limited the increase in NPP, while above the LAI threshold water availability (soil water content or climatic influences) limited the increase in NPP (Running and Coughlan, 1988). Like the LAI analysis, no absolute validation for NPP was possible due to legal, monetary, time and location constraints of the destructive sampling required. Thus absolute validation of the NPP output from the model was not possible.

5.2 Conclusions

A number of conclusions have been drawn from this research:

- The integrated LAI-2000 and TRAC approach for the estimation of LAI has been suggested as the preferred approach for estimating LAI based on the theoretical assumptions of the instruments. As well SMA and vegetation indices were shown to provide the best relationship with the integrated approach, which lends further support to the argument of this being the preferred technique.
- A clumping index is suggested in deciduous species and the assumption of a random distribution of leaves may be inappropriate.
- Spectral mixture analysis shadow fraction provided substantial improvements over vegetation indices in estimating LAI for coniferous species.
- Vegetation indices that attempt to account for the effects of soil or background in their formulation may be dependent upon the stand structural attributes (tree height, basal area, and stem density) or the species type in terms of their ability to predict LAI.
- In this montane ecoregion and at this local scale, LAI was the most important variable affecting modeled NPP from FOREST-BGC compared to soil water content or climate.
- The variability in modeled NPP was not proportional to the variability in LAI. There appears to be a LAI threshold value, where this variability is equal, above which LAI was more variable and below which NPP was more variable. It was proposed that

LAI limits the increase in NPP below the LAI threshold, and that either soil water content or climate limits the increase in NPP above this threshold.

5.3 Contributions to Research

This research has made several scientific contributions to the research community. First, by understanding the variability among the ground-based LAI estimates, researchers and other workers will be aided in the selection of ground-based LAI instruments and remote sensing image analysis methods for retrieving LAI in the field and over large areas. By understanding the variability of NPP modeled by FOREST-BGC as a function of different LAI inputs compared to other key model inputs makes a contribution towards improved NPP model use and understanding particularly in a montane forest environment where few such studies have been conducted.

5.4 Future Research

Some future research has been identified from the results of this research. To further improve the ground-based LAI comparisons an absolute LAI measure for each of the different species and stands would provide a more definitive basis for determining the best instrument or technique for estimating LAI as well for improved NPP modeling. This could be accomplished with the destructive sampling of trees within the plots or the incorporation of litter fall traps to estimate LAI without the use of equations from the literature. As well, the production of sapwood area to leaf area ratios for the Kananaskis Region would increase the applicability of these relationships to this area as they have been found to have stand-specific differences (Hungerford, 1987; Pearson et al., 1984;

Gholz et al., 1976). To further improve the remote sensing LAI estimation component of this research, a better validation data set would also be useful to determine how definitive these models are for their application on a regional scale. Also SMA endmember validation and SMA LAI estimates would be useful to complete for deciduous and mixedwood species. SMA and other vegetation indices could also be tested for relationships with other forest biophysical parameters including biomass, volume and NPP. Other remote sensing image analysis techniques including the vegetation indices in Table 2-2, and others as reviewed by Bannari et al. (1995), and Brown et al. (2000) (e.g. reduce simple ratio), as well as reflectance modeling and image texture or the application of nonlinear regression models (Fernandes et al., 2001) could be compared to provide a more robust analysis of the possible techniques used in estimating LAI. Finally, the extension of these remote sensing techniques (SMA and vegetation indices) to large areas of satellite imagery would be useful for the investigation of scale issues and the determination of better LAI predictors for larger pixel areas beyond that could be applied to regional NPP models for regional carbon estimates.

6.0 REFERENCES CITED

Adams, J.B. M.O. Smith, A. R. Gillespie. 1993. Imaging spectroscopy interpretation based on spectral mixture analysis. In: Remote Geochemical Analysis: Chapter 7 Elements and Mineralogical Composition. C.M. Peters and P. Englert, editors. LPI and Cambridge University Press, Cambridge.

Agren, G.L., R.E. McMurtrie, W.J. Parton, J. Pastor, and H. H. Shugart. 1991. State-of-the-art of Models of Production-Decomposition Linkages in Conifer and Grassland Ecosystems. Ecological Applications. 1(2): 119-138.

Altalis. 1999. Description of Elevation Data. http://www.altalis.com/1to20000dem.htm

Anger, C.D., S. Mah and S, Babey. 1994. Technological enhancements to the compact airborne spectrographic imager (CASI). In: Proceedings of the First International Conference on Airborne Remote Sensing, Strasbourg, France. Vol II, p. 205-213.

Archibald, J.H., G.D. Klappstein, and I.G.W Corns. 1996. Field Guide to Ecosites of Southwestern Alberta. Special Report 8. UBC Press, Vancouver, British Columbia. 16-12, 15-6.

Baker, J.T., and L.H. Allen. 1994. Assessment of the Impact of Rising Carbon Dioxide and Other Potential Climate Changes on Vegetation. Environmental Pollution. 83(1-2): 223-235.

Bannari, A., D. Morrin, F. Bonn, and A.R. Huete. 1995. A review of vegetation indices. Remote Sensing Reviews. 13:95-120.

Baret, F. and G.Guyot. 1991. Potentials and limits of vegetation indices for LAI and APAR assessment. Remote Sensing of Environment. 35:161-173.

Bonan, G.B. 1993. Importance of Leaf Area Index and Forest Type When Estimating Photosynthesis in Boreal Forests. Remote Sensing Environment. 43:303-314.

Brady, N.C. and R.R. Weil. 1999. The Nature and Properties of Soils. 12th Edition. Chapter 5: Soil Water: Characteristics and Behavior. Prentice-Hall Inc. Upper Saddle River, New Jersey. Pp. 171-212.

Breymeyer, A.I., D.O. Hall, J.M. Melillo, G.I. Argen. 1996. Global change: Effects on Coniferous Forests and Grasslands. Jon Wiley & Sons, Chichester.

Brown, L., J.M. Chen, S.G. Leblanc, and J. Cihlar. 2000 A shortwave infrared modification to the simple ratio for LAI retrieval in boreal forests: an image and model analysis. Remote Sensing of Environment. 71(1).

Buckley, D.S. 1999. Practical Field Methods of Estimating Canopy Cover, PAR and LAI in Michigan Oak and Pine Stands. Northern Journal of Applied Forestry. 16(1): 25-32.

CDIAC. 1999. G. Marland, T.A. Boden, R.J. Andres, A.L. Brenkert, and C.A. Johnston. http://cdiac.esd.ornl.gov/trends/emis/em_cont.htm

Canadian Forest Service (CFS). 1997. The State of Canada's Forests: learning from history. Natural Resources Canada, Canadian Forest Service, Ottawa Ontario.

Canadian Council of Forest Ministers. (CCFM). 1997. Criteria and Indicators of a Sustainable Forest Management in Canada: Technical Report. Natural Resources Canada- Canadian Forest Service. Ottawa, Ontario.

Carter, G.A. 1998. Reflectance wavebands and indices for remote estimation of photosynthesis and stomatal conductance in pine canopies. Remote Sensing of Environment. 63: 61-72.

Chen, J.M. and J. Cihlar. 1995. Plant canopy gap-size analysis theory for improving optical measurements of leaf-area index. Applied Optics. 34(27): 6211-6222.

Chen, J.M., P. M. Rich, S.T. Gower, J.M. Norman, and S. Plummer. 1997a. Leaf area index of boreal forests: Theory, techniques and measurements. Journal of Geophysical Research. 102(D24): 29,429-29,433.

Chen, J. M., P. D. Blanken, T. A. Black, M. Guilbeault and S. Chen. 1997b. Radiation regime and canopy architecture in a boreal aspen forest. Agricultural Forest Meteorology. 86:107-125.

Chen, J.M. and Kwong, M. 1997. Manual for TRAC: (Tracing Radiation and Architecture of Canopies. A New Optical Instrument for Ground Measurements of LAI and FPAR. Canadian Centre for Remote Sensing, Ottawa, Ontario.

Chen J.M. and T.A. Black. 1992. Defining leaf area index for non-flat leaves. Plant, Cell and Environment. 15: 421-429.

Chen, J.M. 1996a. Evaluation of vegetation indices and a modified simple ratio for boreal applications. Canadian Journal of Remote Sensing. 22(3): 229-242.

Chen, J.M. 1996b. Optically-based methods for measuring season variation in leaf area index in boreal conifer stands. Agricultural Forest Meteorology. 80: 135-163.

Chen, J.M., J.Cihlar, and J. Liu. 1999. Environmental Monitoring: The Boreal Ecosystems Productivity Simulator (BEPS). WWW: http://www.ccrs.nrcan.gc.ca/ccrs/tekrd/rd/apps/em/beps/bepse.html

Chen, J.M. 2002. Net Carbon Absorption/Release by Plants and Soils: Net Ecosystem Productivity (NEP). WWW:

http://www.geog.utoronto.ca/info/facweb/Chen/jxie1/BEPS%20-%20NEP.htm#estimate

Cihlar, J., L. St.-Laurent and J.A. Dyer. 1991. Relation between the Normalized Difference Vegetation Index and ecological variables. Remote Sensing of Environment. 35: 279-298.

Clevers, J.G. P.W. 1989. The Application of a Weighted Infrared-red Vegetation Index for Estimating Leaf Area Index by correcting for Soil Moisture. Remote Sensing of Environment. 29:25-37.

Cramer, W., D.W. Kicklighter, A. Bondeau, B. Moore III, G. Churkina, B. Nemry, A. Ruimy, A.L. Schloss and the participants of the Potsdam NPP Model Intercomparison. 1999. Comparing global models of terrestrial net primary productivity (NPP): overview and key results. Global Change Biology. 5(1): 1-15.

Cramer, W. and C.B. Field. 1999. Comparing global models of terrestrial net primary productivity (NPP): introduction. Global Change Biology. 5(1):iii-iv.

Crossley, D.I. 1952. The soils of Kananaskis Forest Experiment Station in the sub-alpine forest region in Alberta. Silviculture Research Notes No. 100. Forestry Branch. Canada Department of Resources and Development, Ottawa. 32pp.

CurveExpert 1.34. 1997. http://www.ebicom.net/~dhyams/cvxpt.htm

Cutini, A., G. Matteucci, G.S. Mugnozza. 1998. Estimation of leaf area index with the Li-Core LAI 2000 in deciduous forests. Forest Ecology and Management. 105:55-65.

Dean, T.J. and J.N. Long. 1986. Variation in sapwood area-leaf area relations within two stands of lodgepole pine. Forest Science. 3: 749-758.

Decagon. 1994. AccuPAR Ceptometer Operator's Manual: Light Interception, Crop, and Timber Analysis. Version 2.1. Decagon Devices Inc. Pullman Washington

Detling, J.K., W.J. Parton, and H.W. Hunt. 1979. A simulated model of *Bouteloua gracilis* dynamics in North American shortgrass prairie. Oecologia. 38:167-191.

deWit, C.T., J. Goudriaan, H.H. van Lar, F.W.T. Penning de Vries, R. Rabbinge, and H. van Keulen. 1978. Simulations of assimilation, respiration and transpiration of crops. PUDOC, Wageningen, The Netherlands.

Daughtry. C.S.T., 1990. Direct Measurements of Canopy Structure. Remote Sensing Reviews. 5(1): 45-60.

Fassnacht, K.S., S.T. Gower, J.M. Norman, and R.E. McMurtrie. 1994. A comparison of optical and direst methods for estimating foliage surface area index in forests. Agricultural and Forest Meteorology. 71:183-207.

Ford, R., S.W. Running, and R. Nemani. 1994. A Modular System for Scalable Ecological Modeling. IEEE Computational Science and Engineering. W1.1: 32-44 .

Fournier , R.A. and Mailly, D. 1999. Forestry applications of hemispherical photography: a practical manual. (for review).

Fernandes, R., H.P. White, S. Leblanc, G. Pavlic, H. McNairn, J.M. Chen and R.J. Hall. 2001. Examination of Error Propagation in Relationships between Leaf area Index and spectral Vegetation Indices from Landsat TM and ETM. Proceedings:

23rd Annual Canadian Symposium on Remote Sensing. Quebec, QC, August 20-24, 2001.

Franklin, S.E. and D.R. Peddle. 1989. Spectral Texture for Improved Class Discrimination in Complex Terrain. International Journal of Remote Sensing. 11(3): 551-556.

Frazer, G.W., Canham, C.D. and Lertzman, K.P. 1999. Gap Light Analyzer (GLA): Imaging Software to extract canopy structure and gap light transmission indices from true-colour fisheye photographs, users manual and program documentation. Simon Fraser University, Burnaby, British Columbia, and the Institute of Ecosystem Studies, Millbrook, New York.

Frazer, G.W., Lertzman, K.P. and Trofymow, J.A. 1998. Developmental trends of Canopy structure in coastal forests of British Columbia. Northwest Science. 72(2): 21-22.

Gates, D.M. 1990. Climate Change and Forests. Tree Physiology. 7: 1-5.

Gholz, H.L., F.K. Fritz, and R.H. Waring. 1976. Leaf area differences associated with old growth forest communities in western Oregon Cascades. Canadian Journal of Forest Research. 6: 49-57.

Gholz, H.L. 1982. Environmental limits on aboveground net primary production, leaf area, and biomass in vegetation zones of the Pacific Northwest. Ecology. 63(2): 469-481.

Gifford, R.M., J.L. Lutze, D. Barrett. 1996. Global atmospheric change effects on terrestrial carbon sequestration: Exploration with global C- and N-cycle model (CQUESTN). Plant and Soil. 187:369-387.

Goel, N.S. and W. Qin. 1994. Influences of Canopy Architecture on Relationships Between Various Vegetation Indices and LAI and FPAR: A computer Simulation. Remote Sensing Review. 10:309-347.

Goel, N.S. 1989. Inversion of canopy reflectance models for estimation of biophysical parameters from reflectance data. In: Theory and Application of Optical Remote Sensing. G. Asrar (ed). John Wiley and Sons, New York. p. 205-251

Government of Canada. 2001. Canada Climate Change. http://www.climatechange.gc.ca/english/index.shtml

Gower, S.T. and J.M. Norman. 1991. Rapid estimation of leaf area index in conifer and broadleaf plantations. Ecology. 72(5): 1896-1900.

Gower, S.T, Grier, C.C., Vogt, D.G. and Vogt, K.A. 1987. Allometric relations of deciduous (*Larix occidentalis*) and evergreen conifers (Pinus contorta and *Pseudostuga* menziesii) of the Cascade Mountains in Central Washington. Canadian Journal of Forest Research. 17(7): 630-634.

Gower, S.T., J.G. Vogel, J.M. Norman, C.J. Kucharik, S.J. Steele, and T.K. Stow. 1997. Carbon distribution and aboveground net primary production in aspen, jack pine and black spruce stands in Saskatchewan and Manitoba, Canada. Journal of Geophysical Research. 102(D24): 29,021-29,041.

Grier, C.C. and S.W. Running. 1977. Leaf Area of Mature Northwestern Coniferous Forests: Relation to Site Water Balance. Ecology. 58:893-899.

Guyot, G., D. Guyon, and J. Riom. 1969. Factors affecting the spectral response of forest canopies: a review. Geocarto International. 3: 3-18.

Hall, F.G., Y.E. Shimabukro, and K.F. Huemmrich. 1995. Remote sensing of forest biophysical structure using mixture decomposition and geometric reflectance models. Ecological Application. 5(4): 993-1013.

Haralick, R.K. 1979. Statistical and Structural Approaches to Texture. Proceedings of the IEEE. 67(5): 786-804.

Hendry, L.C., and H.L. Gholz. 1986. Above-ground phenology in north Florida slash pine plantation. Forest Science. 32: 779-788.

Herbert, M.T. and S.B. Jack. 1998. Leaf area index and site water balance of loblolly pine (Pinus *taeda* L.) across a precipitation gradient in East Texas. Forest Ecology and Management. 105: 273-282.

Huang, S. 1994. Ecologically Based Individual Tree Volume Estimation for Major Alberta Tree Species. Report #1: Individual Tree Volume Estimation Procedures for Alberta: Methods of Formulation and Statistical Foundations. Alberta Environmental Protection, Land and Forest Services. Forest Management Division.

Huete, A.R. 1988. A Soil-Adjusted Vegetation Index (SAVI). Remote Sensing of Environment. 25: 295-309.

Hughes, J.W., T.J. Fahey, and B. Browne. 1987. A better seed and litter trap. Canadian Journal of Forest Research. 17(12): 1623-1624.

Hungerford, R.D., R.R. Nemani, S.W. Running, J.C. Coughlan. 1989. MTCLIM: A Mountain Microclimate Simulation Model. United States Department of Agriculture. Forest Service. Intermountain Research Station. Research Paper INT- 414

Hungerford, R.D. 1987. Estimation of foliage area in dense Montana lodgepole pine stands. Canadian Journal of Forest Research. 17:320-324.

Hunt, E.R., F.C. Martin, and S.W. Running. 1991. Simulating the effects of climatic variation on stem carbon accumulation of a ponderosa pine stand: comparison with annual growth increment data. Tree Physiology. 9: 161-171.

IPPC (Intergovernmental Panel on Climate Change). 2001. Summary for Policy Makers of Working Group 1 of the Third Assessment Report. Cambridge University Press, Cambridge.

IGBP Terrestrial Carbon Working Group. 1998. The terrestrial carbon cycle: implications for the Kyoto Protocol. Science. 280: 1393-1394.

Izrael, Y.A. 1991. Climate Change Impact Studies: The IPCC Working Group II Report. In Climate Change: Science, Impacts and Policy. Proceedings of the Second World Climate Conference. Edited by J. Jager and H.L. Ferguson. World meteorological Organization. pp 83-86.

Jensen, J. 1996. Introductory digital image processing: a remote sensing perspective. Englewood Cliffs, NJ, Prentice-Hall.

Johnson, R.L. 2000. Airborne Remote Sensing of Forest Leaf Area Index in Mountainous Terrain. Unpublished Master's Thesis, Department of Geography, University of Lethbridge, Lethbridge, Alberta.

Johnson, D., L. Kershaw, A. MacKinnon, and J. Pojar. 1995. Plants of the Western Boreal Forest and Aspen Parkland. Lone Pine Publishing, Edmonton, Alberta

Jordan, C.F. 1969. Derivation of Leaf Area Index from quality of light on the forest floor. Ecology. 50(4): 663-666.

Kananaskis Country Environmental Education Library (KCEED). 1995. Lusk Creek Book # 13.

Kaufmann, M.R. and C.A. Troendle. 1981. The Relationship of Leaf Area and Foliage Biomass to Sapwood Conducting Area in Four Subalpine Forest Tree Species. Forest Science. 27(3): 477-482.

Keeling, C.D., T.P. Whorf, M. Wahlen, and J. van der Plicht. 1995. Interannual extremes in the rate of rise of atmospheric carbon dioxide since 1980. Nature. 375: 666-670.

Keeling, C.D., J.F.S. Chin, and T.P. Whorf. 1996. Increased activity of northern vegetation inferred from atmospheric CO2 measurements. Nature. 382: 146 – 149.

Keeling, C.D. and T.P. Whorf and the Carbon Dioxide Research Group. 2001. Atmospheric carbon dioxide record from Mauna Loa. Scripps Institution of Oceanography (SIO), University of California, La Jolla, California USA 92093-0244. http://cdiac.esd.ornl.gov/trends/co2/sio-mlo.htm

Kimmins, J.P. 1997. Forest Ecology: A Foundation for Sustainable Management 2nd Edition. Prentice Hall, Upper Saddle River, New Jersey.

Kirby, C.L. 1973. The Kananaskis Forest Experimental Station, Alberta (History, Physical Features, and Forest Inventory. Northern Forest Research Centre Information Report NOR-X-51, Canadian Forest Service.

Kucharik, C. J., J. M. Norman, L. M. Murdock, and S.T. Gower. 1997. Characterizing Canopy Nonrandomness with a Multiband Vegetation Imager (MVI). Journal of Geophysical Research. 102: 29,455-29,473.

Lambers, H., F.S. Chapin, T.L. Pons. 1998. Plant Physiological Ecology. Springer-Verlag. New York.

Lauenroth, W.K. , C.D. Canham, A.P. Kinzig, K.A., Poiani, W.M. Kemp, and S.W. Running. 1998. Simulation Modeling in Ecosystem Science. In Successes, Limitations, and Frontiers in Ecosystem Science. By M.L. Pace and P.M. Groffman. pp. 401-415.

Lavigne, M.B., J.E Luther, S.E. Franklin, and E.R. Hunt, Jr. 1996. Comparing branch biomass prediction equations for *Abies balsamea*. Canadian Journal of Forest Research. 26:611-616.

Leblanc, S. G. and J.M. Chen. 1998. LAI measurements in deciduous and coniferous forests with two optical instruments. Proceedings: Scaling and Modeling in Forestry: Applications in Remote Sensing and GIS, International Workshop March 19-21, 1998. University of Montreal, Montreal, Quebec. pp. 119-125

Li-cor Inc. 1992. LAI-2000 Plant Canopy Analyzer: Operating Manual. Li-cor Inc, Lincoln Nebraska.

Li, X and A.H. Strahler. 1985. Geometric-optical modeling of a conifer forest canopy. IEEE Transactions on Geoscience and Remote Sensing. GE-23 (5): 705-720.

Li , X and A.H. Strahler. 1986. Geometric-optical bi-directional reflectance modeling of a conifer forest canopy. IEEE Transactions on Geoscience and Remote Sensing. GE-24 (6): 906-919.

Li, X and A.H. Strahler. 1992. Geometric-optical bi-directional reflectance modeling of the discrete crown vegetation canopy: effects of crown shape and mutual shadowing. IEEE transactions on Geoscience and Remote Sensing. 30: 276-296.

Lillesand, T.M. and R.W. Kiefer. 1994. Remote Sensing and Image Interpretation. John Wiley and Sons, New York, NY.

Liu, J., J.M. Chen, J.Cihlar, and W.M. Park. 1997. A Process-Based Boreal Ecosystem Productivity Simulator Using Remote Sensing Inputs. Remote Sensing Environment. 62: 158-175.

Long, J.N. and F.W. Smith. 1988. Leaf area-sapwood area relations of lodgepole pine as influenced by stand density and site index. Canadian Journal of Forest Research. 18: 247-250.

Marshall, J.D. and R.H. Waring, 1986. Comparison of methods of estimating leaf area index in old-growth Douglas fir. Ecology. 67(4): 975-979.

Melillo, J.M., A.D. McGuire, D.W., Kicklighter, B. Moore, C.J. Vorosmarty, and A.L. Schloss. 1993. Global climate change and terrestrial net primary production. Nature. 363: 234-240.

Mencuccini, M. and J. Grace. 1995. Climate influences the leaf area/sapwood are ratio in Scots pine. Tree Physiology. 15: 1-10.

Meyer, P., K.I. Itten, T. Kellenberger, S. Sandmeier, R. Sandmeier. 1993. Radiometric corrections of topographically induced effects on LANDSAT TM data in an alpine environment. Journal of Photogrammetry and Remote Sensing. 48(4): 17-28.

Miller, J.B. 1967. A formula for average foliage density. Australian Journal Botany. 15: 141-144.

Miller, J., P. White, J. Chen, D. Peddle, G. McDermid, R. Fournier, P. Shepherd, I. Rubinstein, J. Freemantle, R. Soffer and E. LeDrew, 1997. Seasonal Change in

Understorey Reflectance of Boreal Forests and Influence on Canopy Vegetation Indices. Journal of Geophysical Research. Special Issue: BOREAS. 102(D24): 29,475-29,482.

Noble, A.D. and Schumann, A.W. 1992. The Indirect Measurements of Leaf Area Index (LAI) Using a Hand Held Ceptometer. ICFR Bulletin 31/92. http://www.icfrnet.unp.ac.za/bulletin/31-92/index.htm

Norman, J.M. and G.S. Campbell. 1989. Canopy Structure. In: R.W. Pearcy, J. Ehleringer, H.A. Mooney, and P.W. Rundel. Plant Physiological Ecology: Field Methods and Instrumentation. Chapman and Hall. London. pp 301-326.

Nemani, R.R. and S.W. Running. 1989. Testing a theoretical climate-soil-leaf area hydrologic equilibrium of forests using satellite data and ecosystem simulation. Agricultural and Forest Meteorology. 44: 245-260.

Nemani, R.R., S.W.Running, L.E.Band, and D.L.Peterson. 1993. Regional hydro-ecological simulation system: an illustration of the integration of ecosystem modeling with a GIS. Pp296-304. IN: Environmental Modeling with GIS. M.F.Goodchild, B.O.Parks and L.T.Steyart eds. Oxford University Press.

Pearson, J.A., Fahey, T.J., and D.H. Knight. 1983. Biomass and leaf area in contrasting lodgepole pine forests. Canadian Journal of Forest Research. 14: 259-265.

Peddle, D.R. 1995. Knowledge formulation for supervised evidential classification. Photogrammetric Engineering and Remote Sensing. 61:409-417.

Peddle, D.R. and S.E. Franklin. 1991. Image Texture Processing and Data integration for Surface Pattern Discrimination. Photogrammetric Engineering and Remote Sensing. 57(4): 413-420.

Peddle, D.R., F.G. Hall, and E.F. LeDrew. 1999a. Spectral mixture analysis and geometric optical reflectance modeling of boreal forest biophysical structure. Remote Sensing of Environment. 67(3): 288-297.

Peddle, D.R., D.P. Davidson, R.L. Johnson and R.J. Hall. 1999b. Airborne Image Texture and Mixture Analysis of a Forest Scale Continuum: A Comparison with NDVI Biophysical Estimates, Kananaskis Alberta. In the Proceedings of the Fourth International Airborne Remote Sensing Conference and Exhibition/21st Canadian Symposium on remote Sensing, Ottawa, Ontario, Canada, 21-24 June 1999.

Peddle, D.R. and R.L. Johnson, 2000. Spectral Mixture Analysis of Airborne Remote Sensing Imagery for Improved Prediction of Leaf Area Index in Mountainous Terrain, Kananaskis Alberta. Canadian Journal of Remote Sensing. 26(3): 176-187.

Peddle, D.R. 1998. Field spectroradiometer data acquisition and processing for spectral mixture analysis in forestry and agriculture. In, Proceedings, First International Conference on Geospatial Information in Agriculture and Forestry. ERIM International;. Vol. II., Lake Buena Vista, Florida, U.S.A. June 1-3. pp. 645-652

Peddle, D.R., S.P. Brunke, and F.G. Hall. 2001. A comparison of spectral mixture analysis and ten vegetation indices for estimating boreal forest biophysical information from airborne data. Canadian Journal of Remote Sensing. 27(6): 627-635.

Peddle, D.R. 1997. Remote sensing boreal forest terrain: sub-pixel scale mixture analysis of landcover and biophysical parameters at forest stand and regional scales.

Unpublished Ph.D. Thesis. Department of Geography. University of Waterloo, Waterloo, Ontario.

Peterson, D., M. Spanner, S.W. Running and K. Tueber. 1987. Relationship of Thematic Mapper Simulator data to leaf area index of temperate coniferous forests. Remote Sensing of Environment. 22: 323-341.

Pinty, B. and M.M. Verstrate. 1992. GEMI: a Non-Linear Index to Monitor Global Vegetation from Satellites. Vegetation. 10(1): 15-20.

Pierce, L.L., S.W. Running and J. Walker. 1994. Regional-Scale Relationships of Leaf Area Index to Specific Leaf Area and Leaf Nitrogen Content. Ecological Applications. 4(2): 313-321.

Pierce, L.L., and S.W. Running. 1988. Rapid estimation of coniferous forest leaf area index using portable integrating radiometer. Ecology. 69(6): 1762-1767.

Prescott, C.E., J.P. Corbin, D. Parkinson. 1989. Biomass, productivity, and nutrient-use efficiency of aboveground vegetation in four Rocky Mountain coniferous forests. Canadian Journal of Forest Research. 19: 309-317.

Qi, J., A. Cheekbone, A.R. Huete, Y.H. Kerr and S. Sorooshian. 1994. A modified soil adjusted vegetation index. Remote Sensing of Environment. 48: 119-126.

Raven, P.H., R.F. Evert, and S.E. Eichhorn. 1992. Biology of Plants Fifth Edition. Worth Publishers, New York, New York

Richardson, A.J. and C.L. Wiegand. 1977. Distinguishing Vegetation from Soil Background Information. Photogrammetric Engineering and Remote Sensing. 43(12): 1541-1552.

Rizzo, B. and E. Wiken. 1992. Assessing the sensitivity of Canada's Ecosystems to Climatic Change. Climate Change. 21: 37-55.

Ross, J. 1981. The Radiation Regime and Architecture of Plant Stands. Dr. W. Junk Publishers. The Hague, The Netherlands

Roughgarden, G., S.W. Running, and P.A. Matson. 1991. What does remote sensing do for ecology. Ecology. 72(6): 1923-1933.

Roujean, J.L, and F.M. Breon. 1995. Estimating PAR Absorbed by Vegetation from Bi-directional Reflectance Measurements. Remote Sensing of Environment. 51: 375-384.

Rouse, J.W, R.H. Hass, J.A. Schell, and D.W. Deering. 1973. Monitoring Vegetation Systems in the Great Plains with ERTS-1. Proceedings, 3rd Earth Resource Technology Satellite Symposium, NASA SP-351, December 10-14. I: 309-317.

Running, S.W., D.L. Peterson, M.A. Spanner and K.B. Teuber. 1986. Remote sensing of coniferous forest leaf area. Ecology. 67(1): 273-276.

Running, S.W., R. Nemani, D. Peterson, L. Band, D. Potts, L. Pierce, M. Spanner. 1989. Mapping regional forest evapotranspiration and photosynthesis by coupling satellite data with ecosystem simulation. Ecology. 70(4): 1090-1101.

Running, S.W. 1990. A modified integrated NDVI for improving estimates of terrestrial net primary production. SPIE Vol.1300: Remote Sensing of the Biosphere. Editor James Smith, Bellingham, Washington. pg 15- 24.

Running, S.W. and J.C. Coughlan. 1988. A General Model of Forest Ecosystem Processes for Regional Applications: 1. Hydrologic Balance, Canopy Gas Exchange and Primary Production Processes. Ecological Modeling. 42: 125-154.

Running, S.W. 1990. Estimating terrestrial Primary Productivity by combining remote sensing and ecosystem simulation. In Ecological Studies by H.A. Mooney. Springer-Verlag, New York.

Running, S.W. and S.T. Gower. 1991. FOREST-BGC, A general model of forest ecosystem processes for regional applications. II Dynamic carbon allocation and nitrogen budgets. Tree Physiology. 9: 147-160.

Running, S.W. and R.Nemani. (1991). Regional hydrologic and carbon balance responses of forests resulting from global climate change. Climatic Change. 19: 349-368.

Running, S.W. and E.R. Hunt. 1993. Generalization of a Forest Ecosystem Process Model for Other Biomes, BIOME-BGC and an Application for Global Scale Models. In Scaling Physiological Processes: Leaf to Globe ed. James, Ehleringer. Academic Press. pp 141- 158.

Running, S.W. 1993. Modeling terrestrial carbon cycles at varying temporal and spatial resolutions. NATO ASI Series vol. 115: The Global Carbon Cycle ed. M. Iteimann. Springer-Verlag Berlin. pp 201-217.

Running, S.W. and K.S. Milner. 1993. Extrapolating forest ecosystem processes from tree to landscape scales. In Modeling Sustainable Forest Ecosystems ed. D. Lemaster. Washington, D.C. American Forest. pp 1-15

Running, S.W. 1994. Testing FOREST-BGC Ecosystem Process Simulations Across a Climatic Gradient in Oregon. Ecological Applications. 4(2): 238-247.

Sall, J and A. Lehman. 1996. JMP Start Statistics. A Guide to Statistics and Data Analysis Using JMP and JMP IN Software. Duxbury Press, Belmont.

Sellers , P.J. and D. Schimel. 1993. Remote sensing of the land biosphere and biogeochemistry in the EOS era: science priorities, methods and implementation. Global and Planetary Change. 7: 279-297.

Sheppard, D.L. 1996. Modeling the Spatial Characteristics of Hydrometeorology in the Upper Oldman River Basin, Alberta. Masters Thesis, University of Lethbridge, Lethbridge, Alberta

Schroeder, P.E., B. McCandish, R.H. Waring and D.A. Perry. 1982. The relationship of maximum canopy leaf area to forest growth in eastern Washington. Northwest Science. 56: 121-130.

Smith, R.L. 1990. Ecology and Field Biology Fourth Edition. HarperCollins. New York. PP 20.

Snell, J.A.K., and J.K. Brown. 1978. Comparison of tree biomass indicators – DBH and sapwood area. Forest Science. 24(4): 455-457.

Steel, R.G.D. and J.H. Torrie. 1980. Principles and Procedures of Statistics: A Biometrical Approach. McGraw-Hill Book Company, New York.

Strahler, A.H. and D.L.B. Jupp. 1990. Geometric optical modeling of forest as remotely sensed scenes composed of three-dimensional, discrete objects. In: Photon-Vegetation Interactions: Applications in Optical Remote Sensing and Plant Ecology (R. Myneni and J. Ross, Eds.), Springer-verlag, Heidelberg, 162-190

Teillet, P.M., B. Guidon and D.G. Goodenough. 1982. On the slope-aspect correction of multispectral scanner data. Canadian Journal of Remote Sensing. 8(2): 84-106.

Voss, J.M. and H.L. Allen. 1988. Leaf Area, Stemwood Growth, and Nutrition Relationships in Loblolly Pine. Forest Science. 34(3): 547-563.

Waring, R.H. and W.H. Schlesinger. 1985. Forest Ecosystems Concepts and Management. Academic Press Inc, San Diego

Waring, R.H., P.E. Schroeder, and R. Oren. 1982. Application of the pipe model theory to predict canopy leaf area. Canadian Journal of Forest Research. 12: 556-560.

Waring, R.H. 1985. Imbalanced forest ecosystems: assessments and consequences. Forest Ecology and Management. 12: 93-112.

Waring, R.H. and Running, S.W. 1998. Forest Ecosystems: Analysis at Multiple Scales. Second Edition. Academic Press. San Diego, California.

Welles, J.M., 1990. Some Indirect Methods of Estimating Canopy Structure. Remote Sensing Reviews. 5(1): 31-43.

Wessman, C., J. Aber, D. Peterson, and J. Melillo. 1986. Remote sensing of canopy chemistry and nitrogen cycling in temperate forest ecosystem. Nature. 335:

White, J, S. Running, R. Nemani, R. Keane, and K. Ryan. 1997. Measurement and remote sensing of LAI in Rocky Mountain montane ecosystems. Canadian Journal of Forest Research. 27: 1714-1727.

Woodcock, C.E., J.B. Collins, V.D. Jackbhazy, X. Li, S.A. Macomber, and Y. Wu. 1997. Inversion of the Li-Strahler canopy reflectance model for mapping forest structure. IEEE Transactions on Geoscience and Remote Sensing. 35(2): 405-414.

Wulder, M., S. Franklin, and M. Lavigne. 1996. High Spatial Resolution Optical Image Texture for Improved Estimation of Forest Stand Leaf Area Index. Canadian Journal of Remote Sensing. 22(4): 441-449.

Wulder, M., E. LeDrew, S. Franklin, and M. Lavigne. 1998. Aerial Image Texture Information in the Estimation of Northern Deciduous and Mixed Wood Forest Leaf Area Index (LAI). Remote Sensing Environment. 64: 64-76.

Wulder, M.A. 1998. Optical remote sensing techniques for the assessment of forest inventory and biophysical parameters. Progress in Physical Geography. 4(2): 449-476.

Appendix A – Actual and Predicted Sapwood Area Estimates From Tree Basal Area.

Actual and predicted estimates of sapwood area from the validation data set. Predicted estimates were determined through linear regression models and saturation growth model for diameter at breast height (DBH) with sapwood area estimates for Douglas-Fir, lodgepole pine, white spruce and a composite deciduous species.

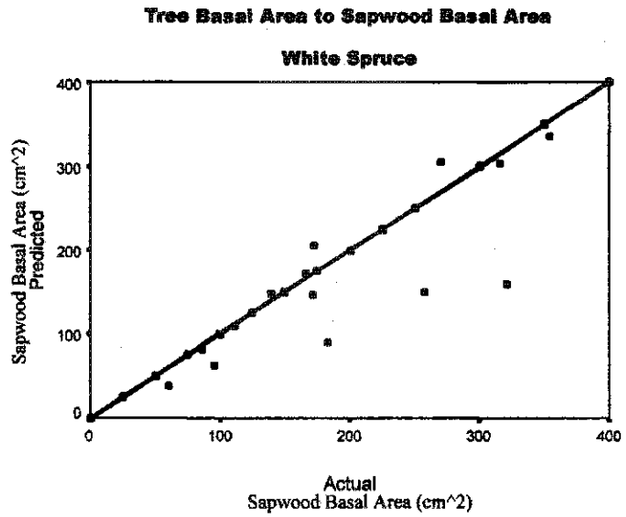
Tree Basal Area to Sapwood Basal Area
White Spruce
Sapwood Basal Area (cm^2) Predicted
Actual Sapwood Basal Area (cm^2)
0
100
200
300
400

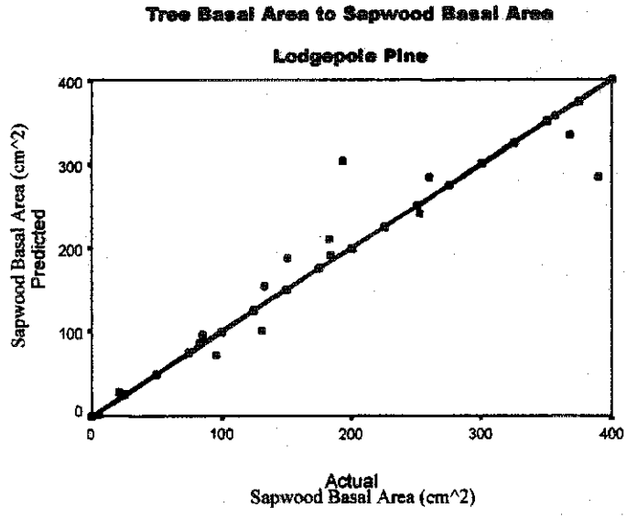
Tree Basal Area to Sapwood Basal Area
Lodgepole Pine
Sapwood Basal Area (cm^2) Predicted
Actual Sapwood Basal Area (cm^2)
0
100
200
300
400

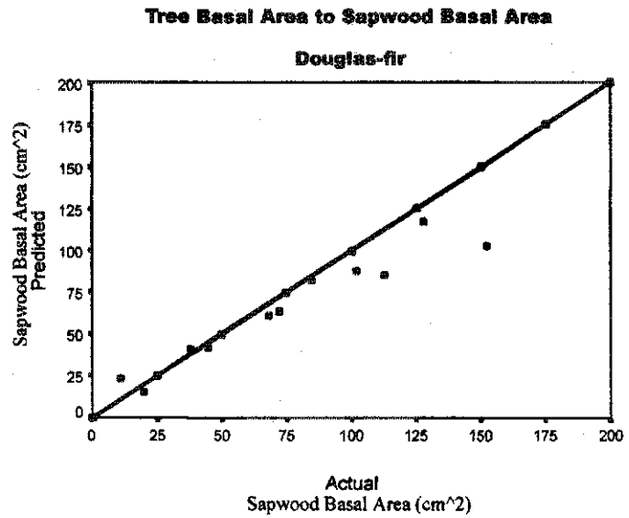
Tree Basal Area to Sapwood Basal Area
Douglas-fir
Sapwood Basal Area (cm^2) Predicted
Actual Sapwood Basal Area (cm^2)
0
25
50
75
100
125
150
175
200

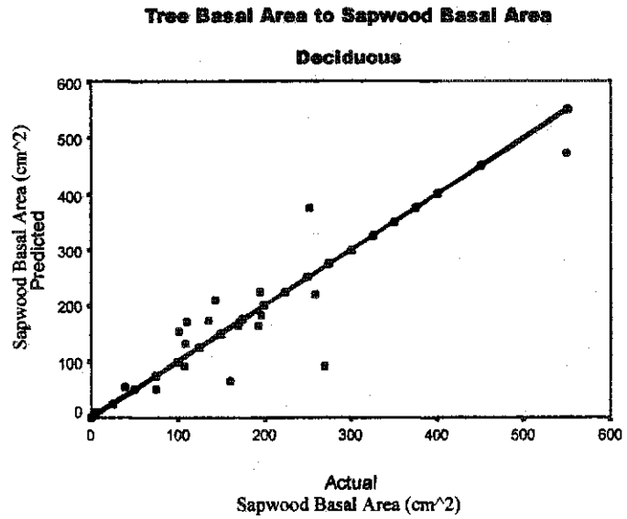
Tree Basal Area to Sapwood Basal Area
Deciduous
Sapwood Basal Area (cm^2) Predicted
Actual Sapwood Basal Area (cm^2)
0
100
200
300
400
500
600

Appendix B – Residual Plots for Regression Models for Remote Sensing Techniques and LAI

Regression standardized residuals plots for linear regression models for spectral mixture analysis shadow fraction and vegetation indices with the ground-based LAI estimation techniques, including hemispherical photography, LAI-2000, TRAC, integrated approach and sapwood area/leaf area.

Regression Standardized Residuals for the Integrated LAI and Remote Sensing Techniques for Coniferous Stands

Integrated and NDVI

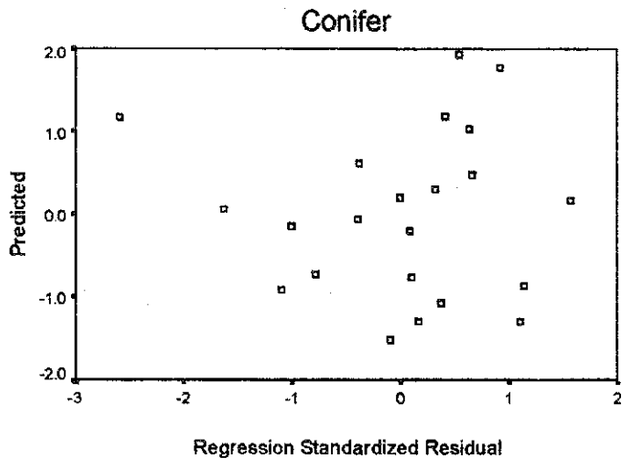

Integrated and SMA_S

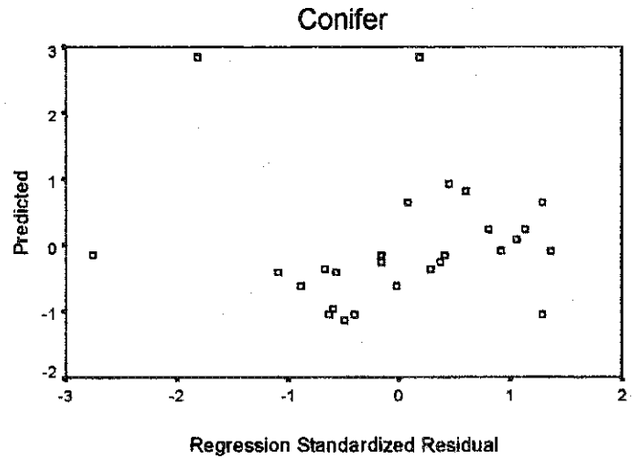

Integrated and WDVI

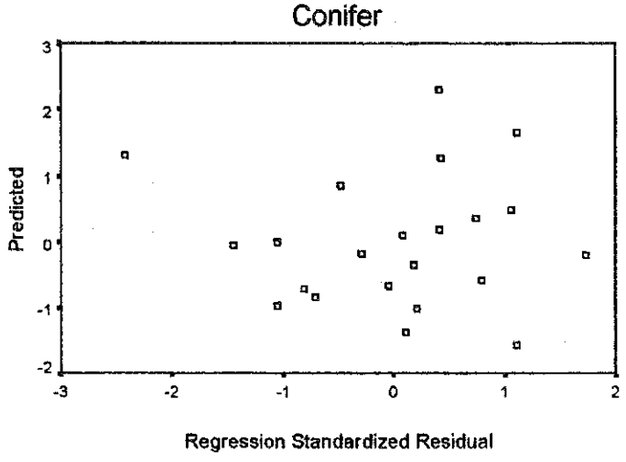

Integrated and SAVI1

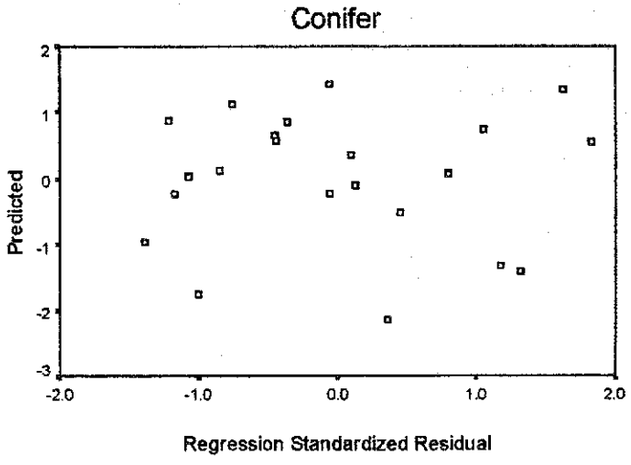

Regression Standardized Residuals for the LAI-2000 and Remote Sensing Techniques for Coniferous Stands

LAI-2000 and NDVI

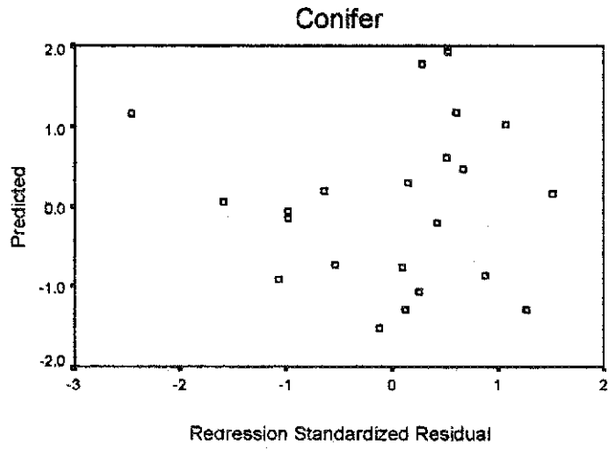

LAI-2000 and SMA_S

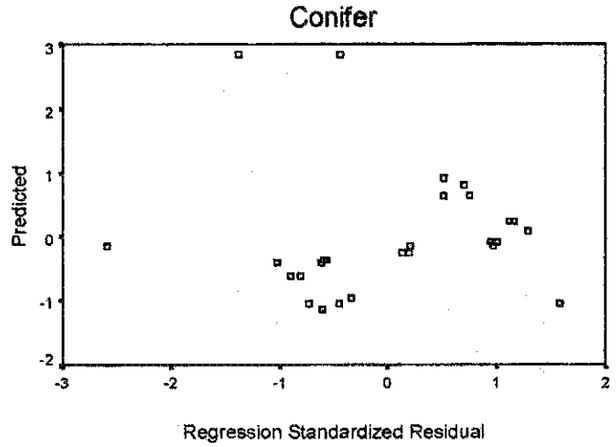

LAI-2000 and WDVI

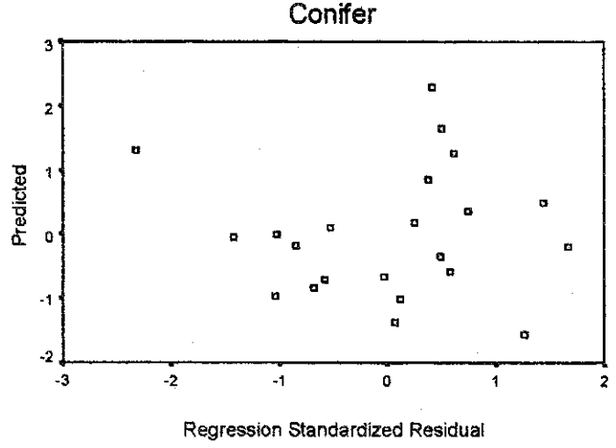

LAI-2000 and SAVI1

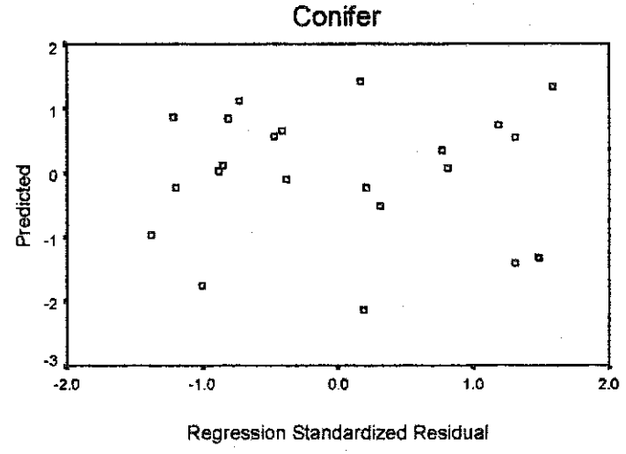

Regression Standardized Residuals for the Hemi and Remote Sensing Techniques for Coniferous Stands

Hemi and NDVI

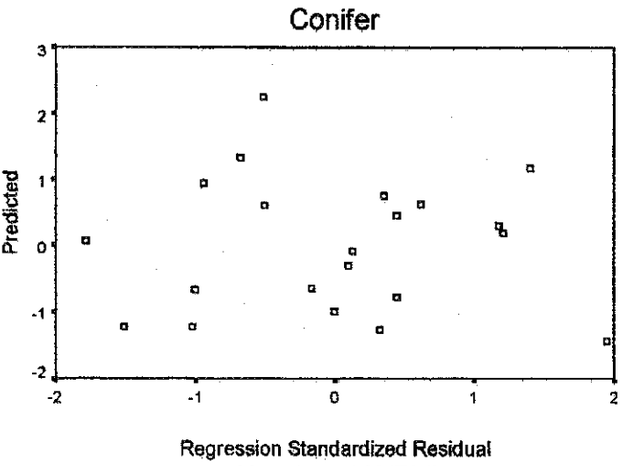

Hemi and SMA_S

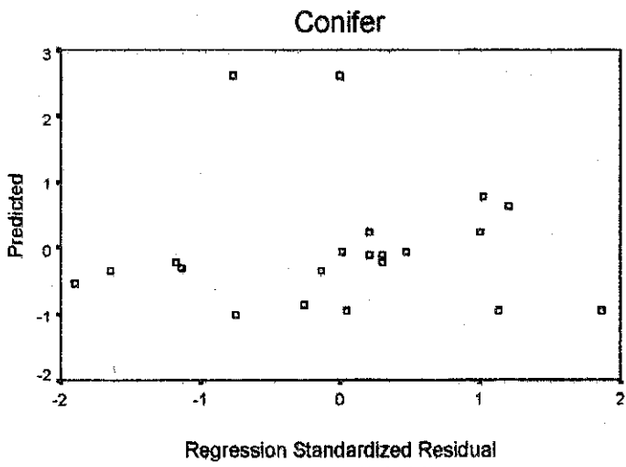

Hemi and WDVI

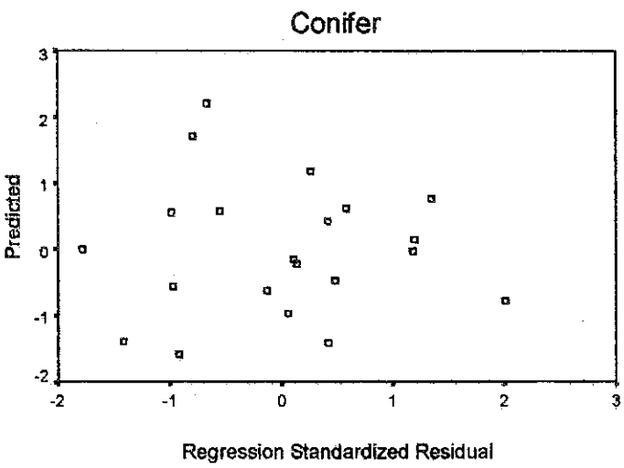

Hemi and SAVI1

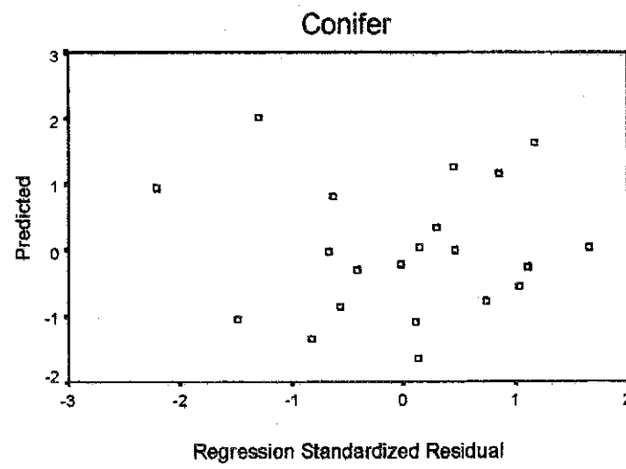

Regression Standardized Residuals for the TRAC and Remote Sensing Techniques for Coniferous Stands

TRAC and NDVI

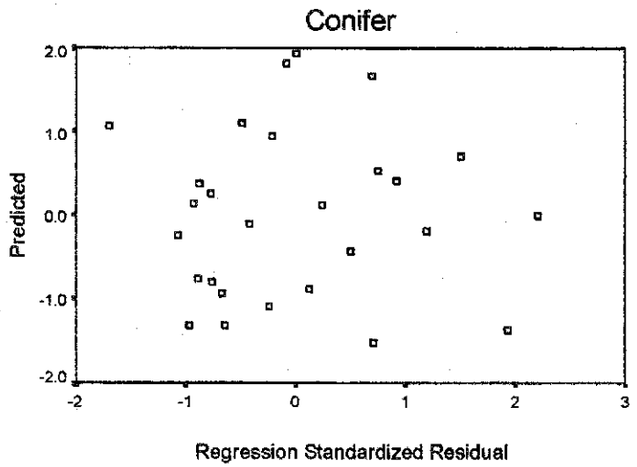

TRAC and SMA_S

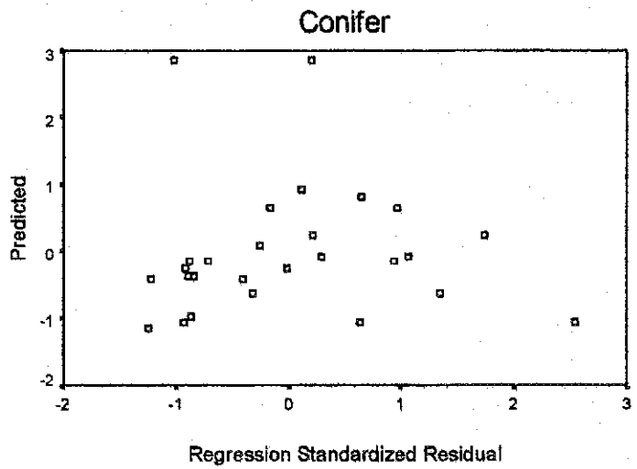

TRAC and WDVI

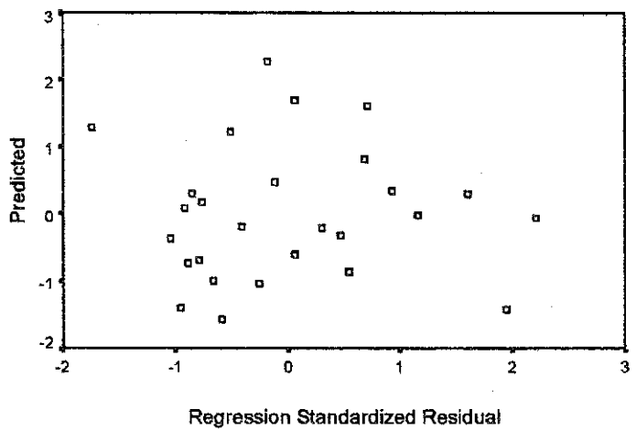

TRAC and SAVI1

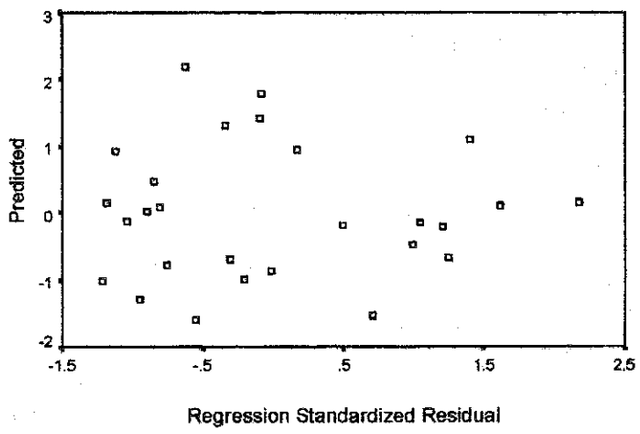

Regression Standardized Residuals for the Sapwood Area and Remote Sensing Techniques for Coniferous Stands

Sapwood Area and NDVI

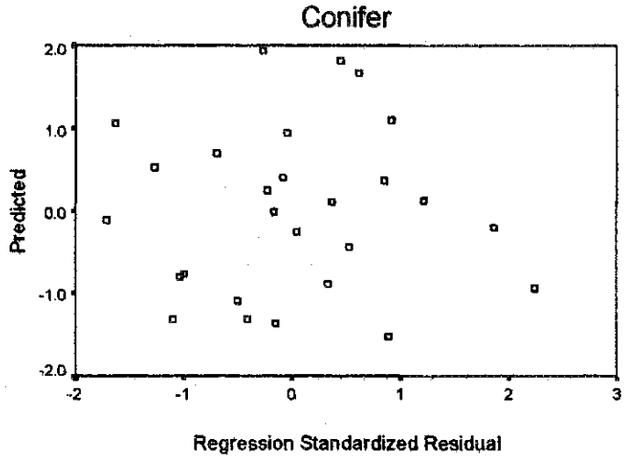

Sapwood Area and SMA_S

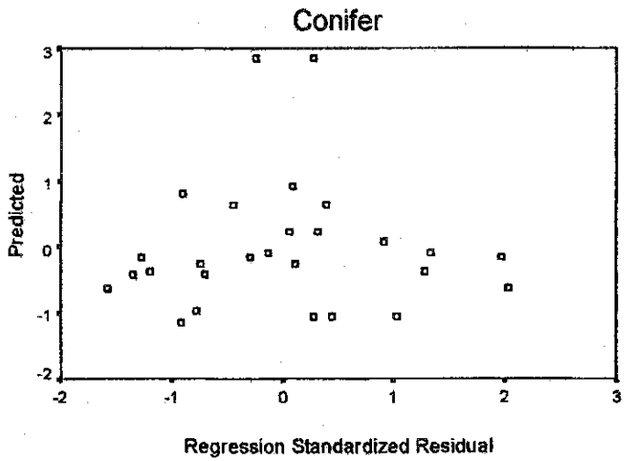

Sapwood Area and WDVI

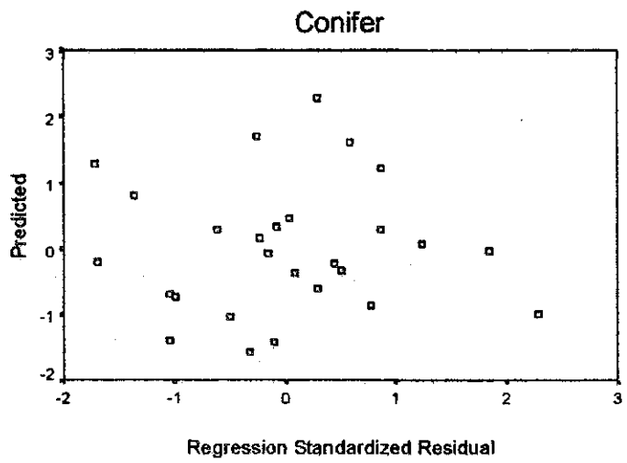

Sapwood Area and SAVI1

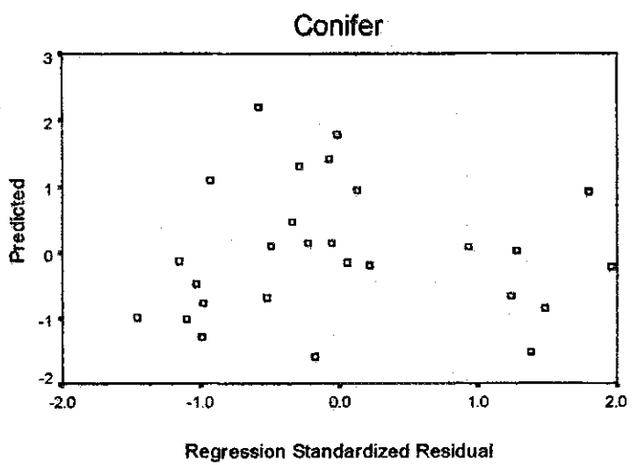

Regression Standardized Residuals for the Integrated LAI and Remote Sensing Techniques for Deciduous Stands

Integrated and NDVI

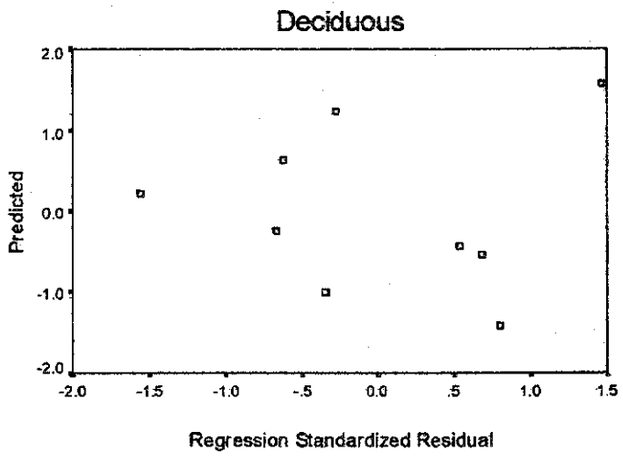

Integrated and WDVI

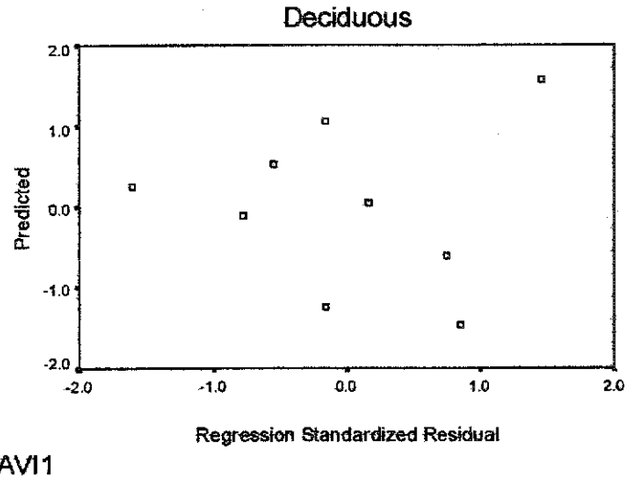

Integrated and SAVI1

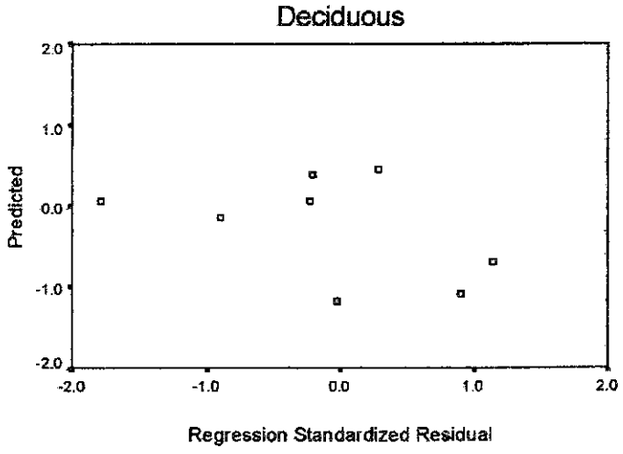

Regression Standardized Residuals for the LAI-2000 and Remote Sensing Techniques for Deciduous Stands

LAI-2000 and NDVI

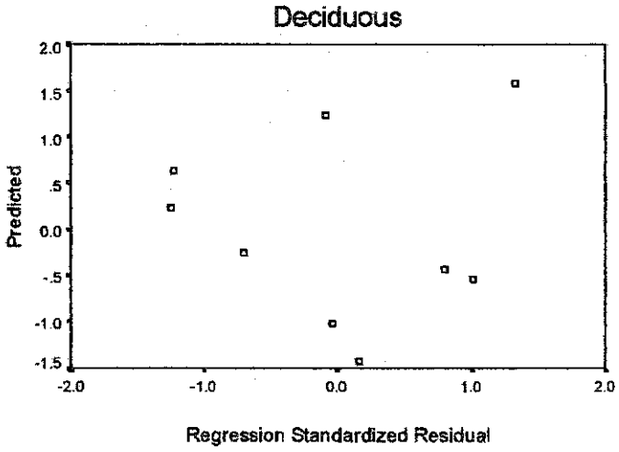

LAI-2000 and WDVI

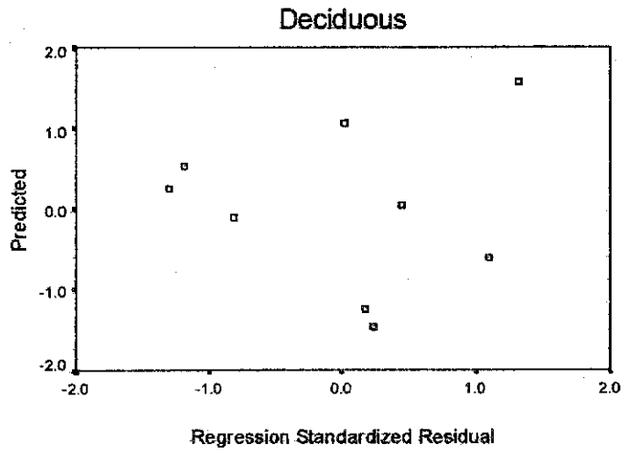

LAI-2000 and SAVI1

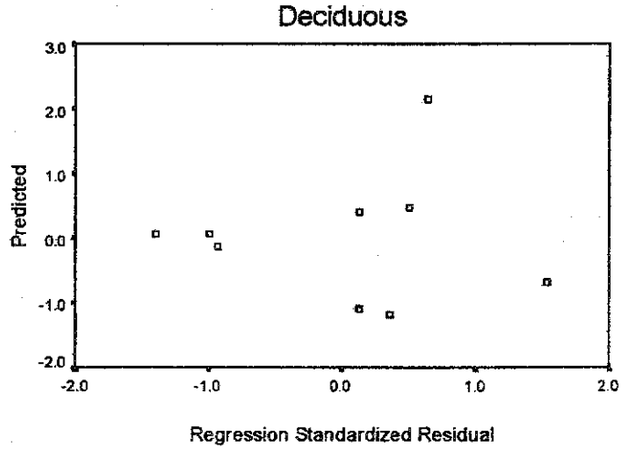

Regression Standardized Residuals for the Hemispherical Photography and Remote Sensing Techniques for Deciduous Stands

Hemi and NDVI

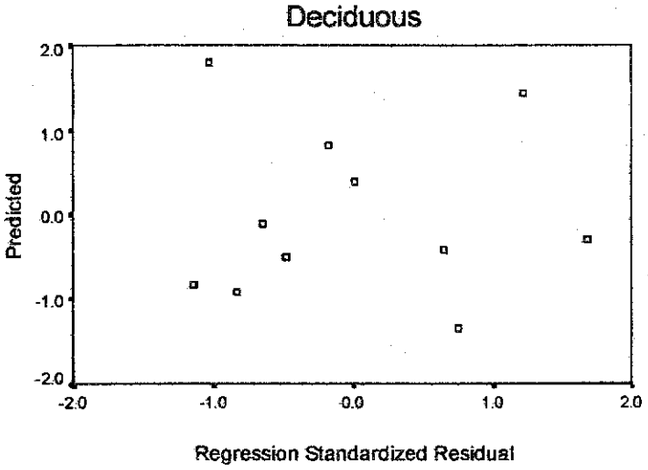

Hemi and WDVI

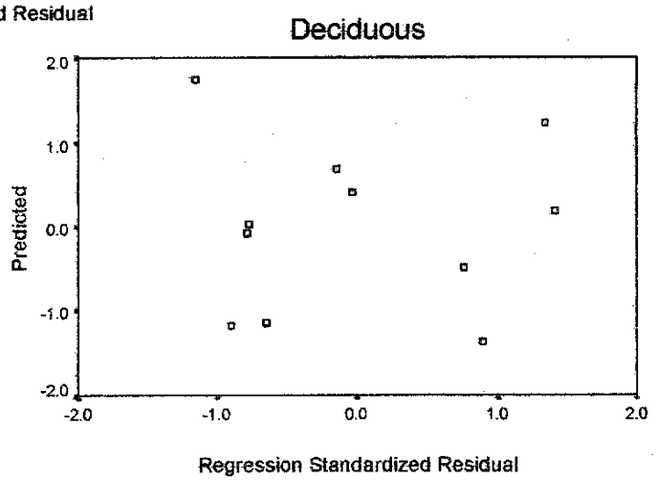

Hemi and SAVI1

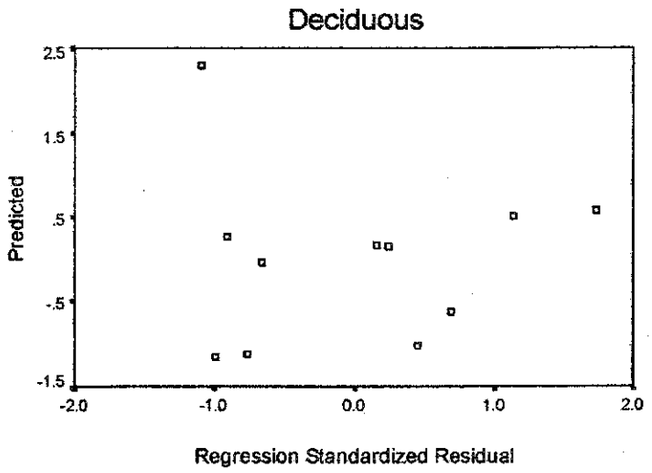

Regression Standardized Residuals for the TRAC and Remote Sensing Techniques for Deciduous Stands

TRAC and NDVI

Deciduous

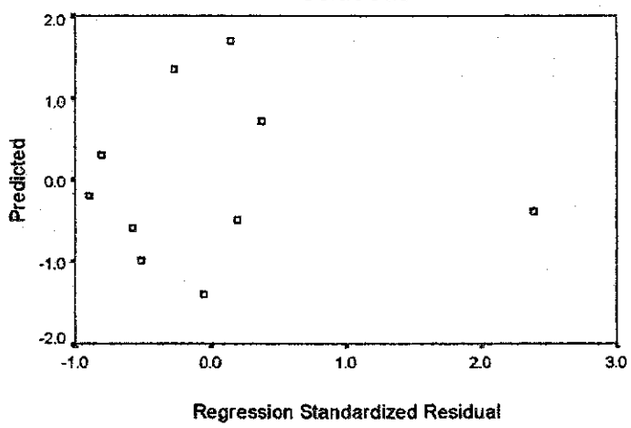

TRAC and WDVI

Deciduous

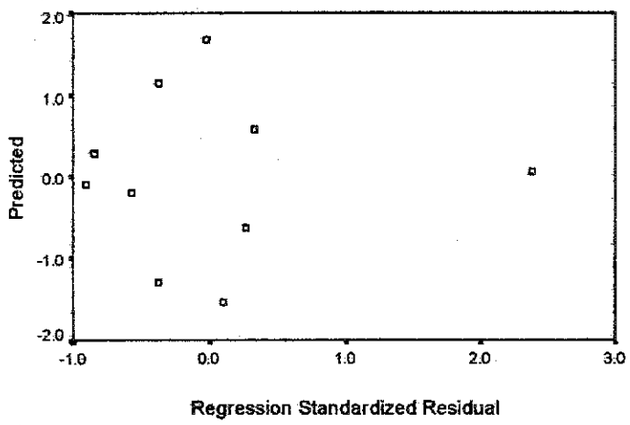

TRAC and SAVI

Deciduous

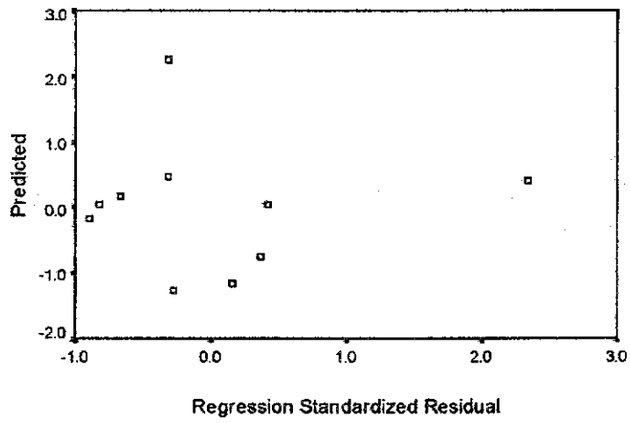

Regression Standardized Residuals for the Sapwood area/leaf area and Remote Sensing Techniques for Deciduous Stands

Sapwood Area and NDVI

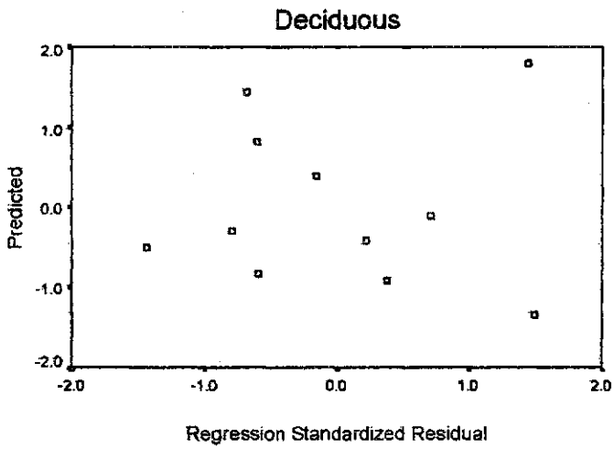

Sapwood Area and WDVI

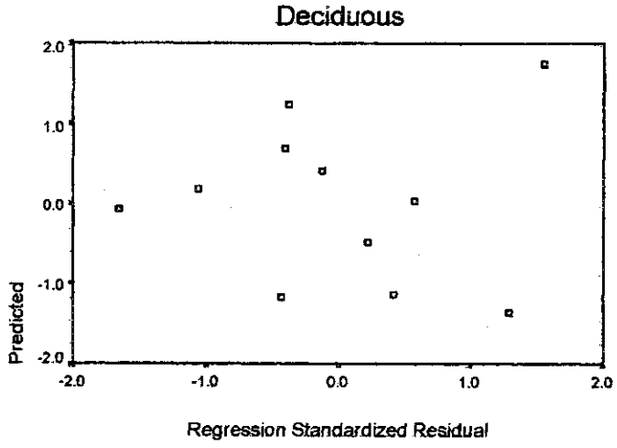

Sapwood Area and SAVI1

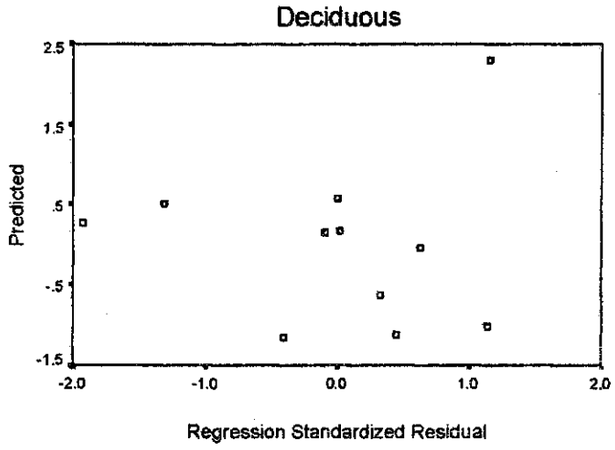

Regression Standardized Residuals for the Integrated and Remote Sensing Techniques for Mixedwood Stands

Integrated and NDVI

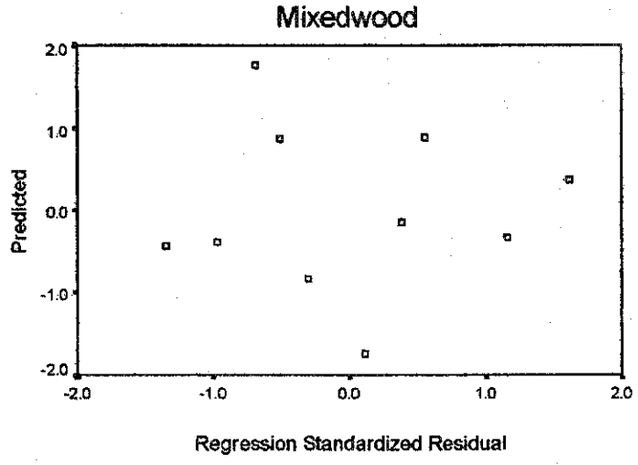

Integrated and WDVI

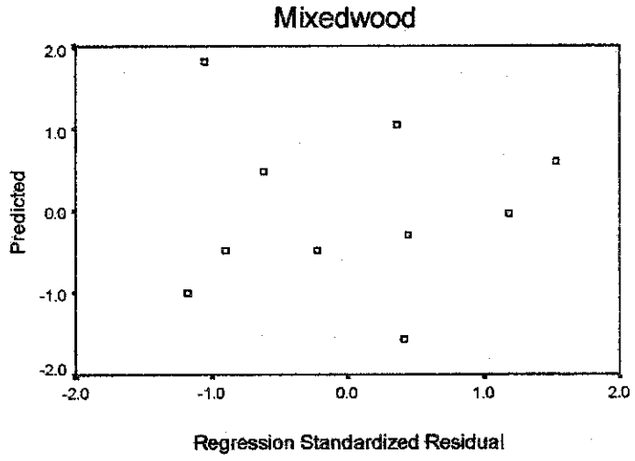

Integrated and SAVI1

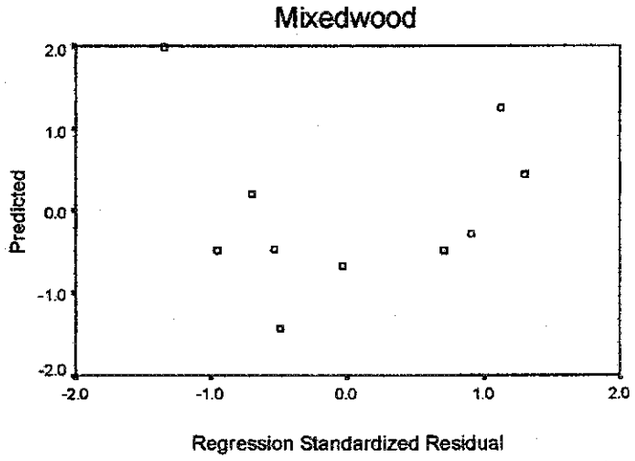

Regression Standardized Residuals for the LAI-2000 and Remote Sensing Techniques for Mixedwood Stands

LAI-2000 and NDVI

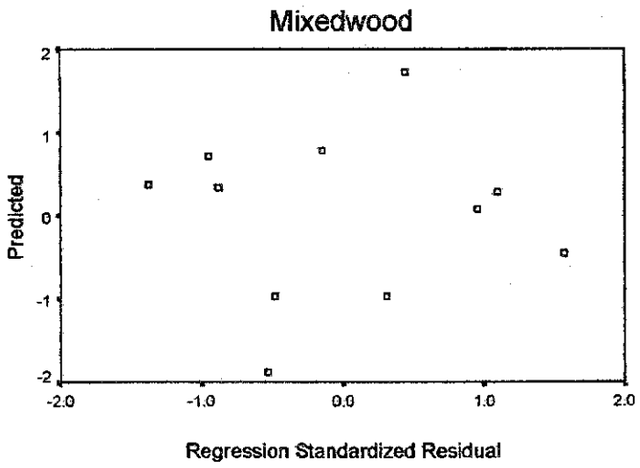

LAI-2000 and WDVI

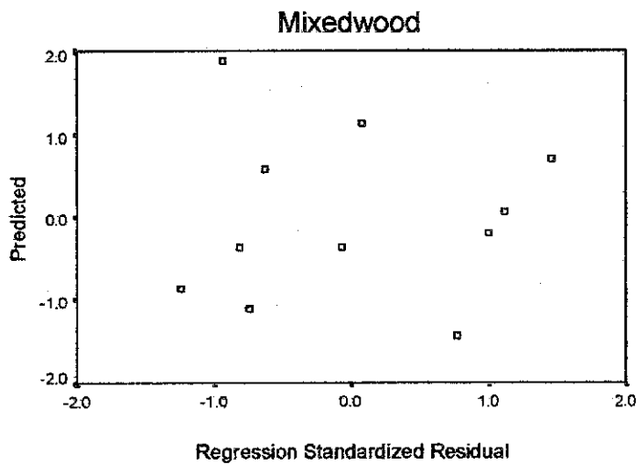

LAI-2000 and SAVI1

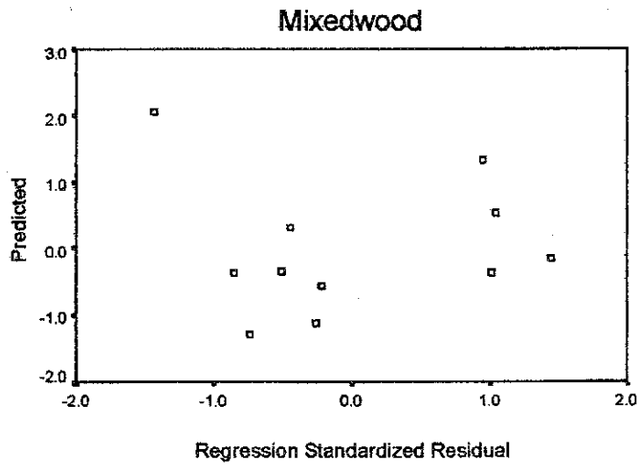

Regression Standardized Residuals for the Hemispherical Photography and Remote Sensing Techniques for Mixedwood Stands

Hemi and NDVI

Mixedwood

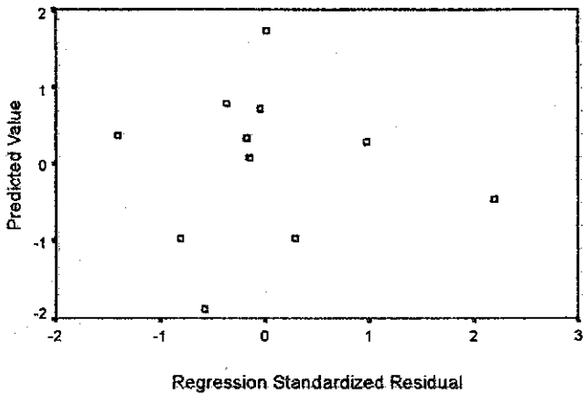

Hemi and WDVI

Mixedwood

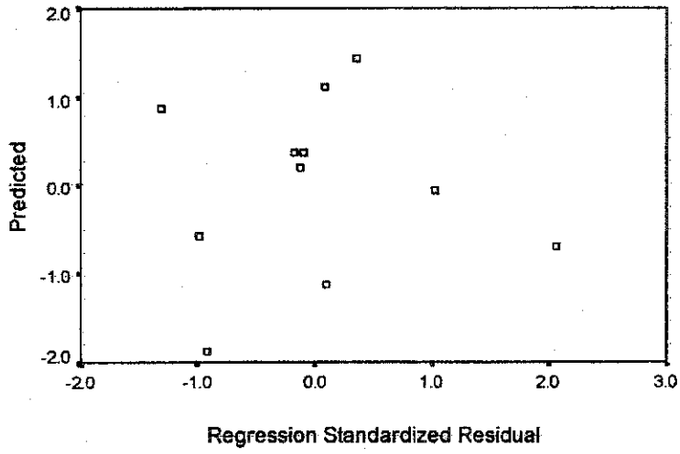

Hemi and SAVI

Mixedwood

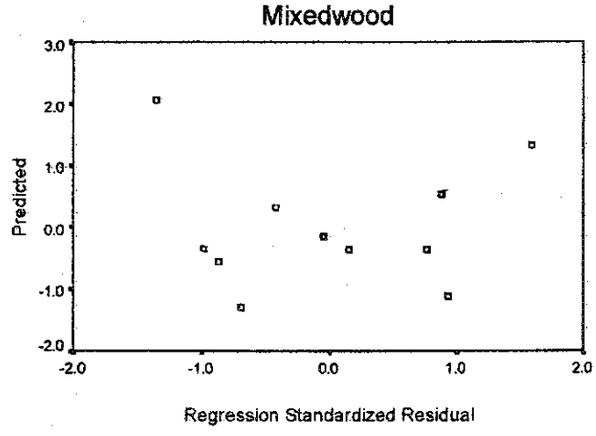

Regression Standardized Residuals for the TRAC and Remote Sensing Techniques for Mixedwood Stands

TRAC and NDVI

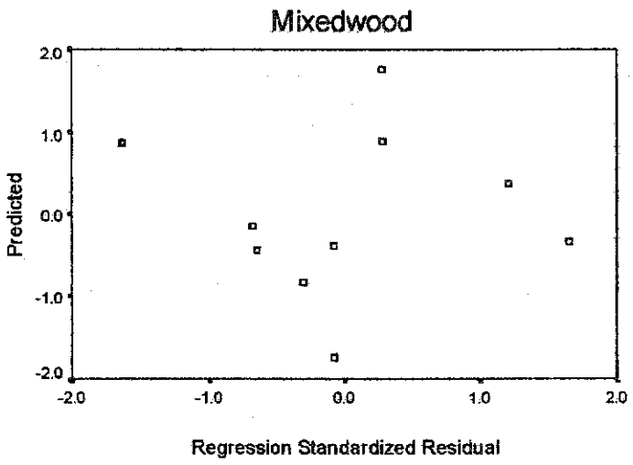

TRAC and WDVI

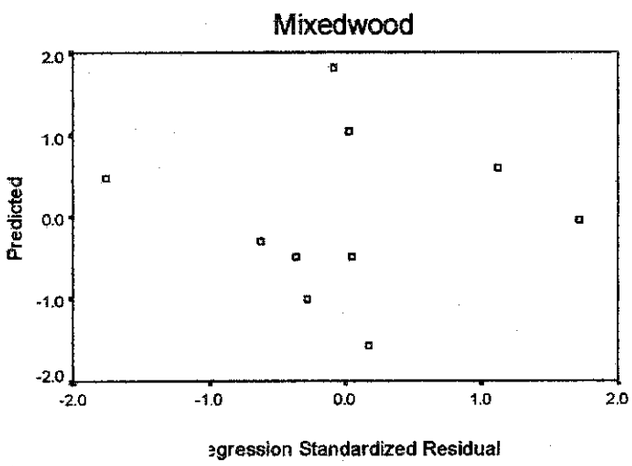

TRAC and SAVI1

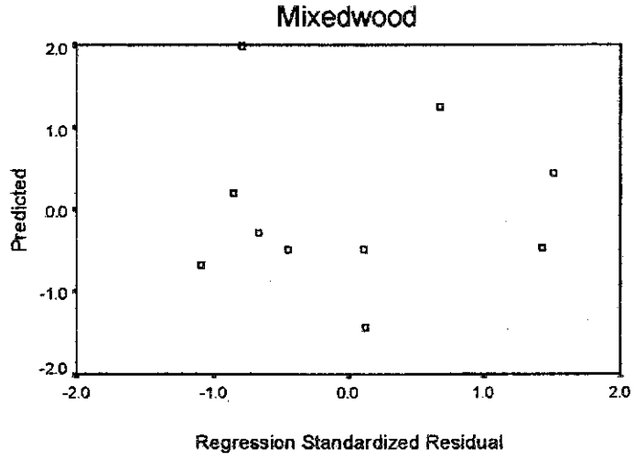

Regression Standardized Residuals for the Sapwood Area/Leaf Area and Remote Sensing Techniques for Mixedwood Stands

Sapwood Area and NDVI

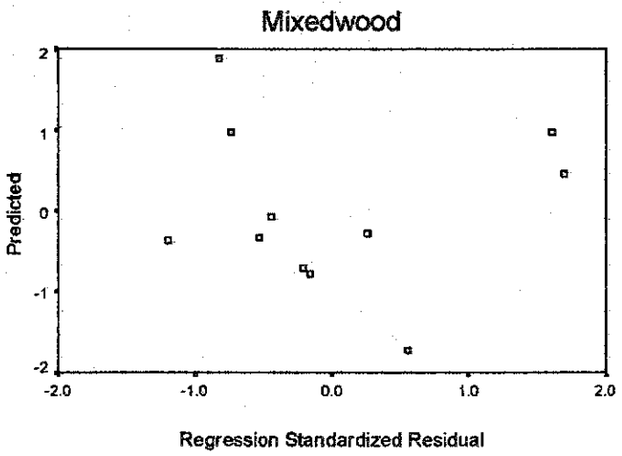

Sapwood Area and WDVI

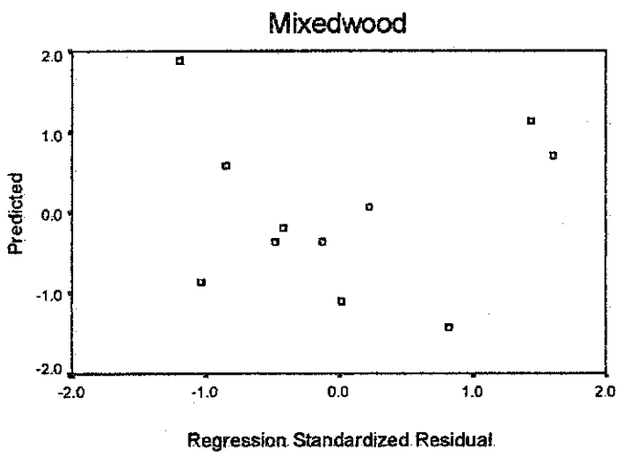

Sapwood Area and SAVI1

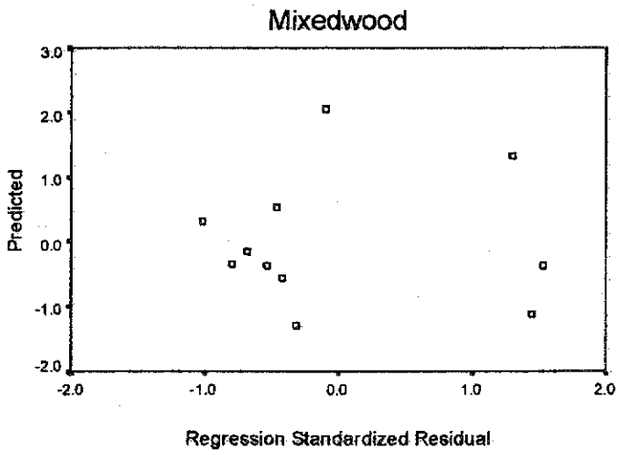

Appendix C – Regression Equations for Remote Sensing Techniques and LAI

Equations for the regression models built for vegetation indices or SMA and ground-based LAI.

Table C-1 Model equations using each LAI estimation technique and vegetation indices for conifer species.

Instrument	NDVI equation	WDVI equation	SAVI equation	SMA_S equation
TRAC	17.97x -9.42	13.32x + 4.07	7.56x – 8.22	6.64x + 0.41
LAI-2000	19.80x -13.41	13.01x + 1.49	0.22x + 1.83	11.75x – 5.08
Hemi	0.09x + 1.65	1.65x + 1.68	-7.37x + 4.41	0.72x + 1.39
Integrated	23.48x -15.96	15.48x + 1.71	0.41x + 2.06	14.35x – 6.33
Sapwood area	16.40x - 8.20	13.94x + 4.06	-10.43x + 8.39	17.00x – 5.61

Table C-2 Model equations using each LAI estimation technique and vegetation indices for deciduous species.

Instrument	NDVI equation	WDVI equation	SAVI equation
TRAC	-3.51x + 6.04	-3.96x + 3.78	-4.91x + 5.94
LAI-2000	-13.61x + 13.03	-5.57x + 2.65	-5.31x + 4.80
Hemi	-5.01x + 5.78	-2.14x + 1.98	-1.35x + 2.40
Integrated	-12.49x +12.03	-5.03x + 2.50	-4.85x + 4.47
Sapwood area	-25.88x +24.37	-8.77x + 4.32	-7.41x + 7.14

Table C-3 Model equations using each LAI estimation technique and vegetation indices for mixedwood species.

Instrument	NDVI equation	WDVI equation	SAVI equation
TRAC	-12.68x + 14.60	-14.60x + 5.37	-8.85x + 7.78
LAI-2000	0.79x + 1.73	-2.88x + 2.57	-5.57x + 4.58
Hemi	-9.85x + 2.75	-3.78x + 2.94	-7.41x + 5.54
Integrated	5.51x - 2.67	0.70x + 1.75	-4.94x + 3.77
Sapwood area	-5.61x + 8.17	-13.30x + 4.62	-22.06x + 12.39